Graduate Theses and Dissertations

Graduate School

5-1-2014

Selected Topics in Foundation Design, Quality Assurance, and Remediation

Danny Winters
University of South Florida, dwinters@usf.edu

Follow this and additional works at: https://scholarcommons.usf.edu/etd

Part of the Engineering Commons

Selected Topics in Foundation Design, Quality Assurance, and Remediation

by

Danny Winters

A dissertation submitted in partial fulfillment
of the requirements for the degree of
Doctor of Philosophy
Department of Civil and Environmental Engineering
College of Engineering
University of South Florida

Co-Major Professor: Austin Gray Mullins, Ph.D.
Co-Major Professor: Rajan Sen, Ph.D.
Daniel Hess, Ph.D.
Sarah Kruse, Ph.D.
Michael J. Stokes, Ph.D.

Date of Approval:
February 18, 2014

Keywords: Drilled Shaft, Driven Piles, Thermal Integrity
Post Grout, Fiber-Reinforced Polymers

Copyright © 2014, Danny Winters

ACKNOWLEDGMENTS

I would like to thank my family for all the support throughout my education. Without your support none of this could happen. I would also like to thank Dr. Gray Mullins and Dr. Rajan Sen for the incredible opportunity provided to me as a research associate and their constant encouragement and teachings. Finally, I would like to thank all the students who have come through our research program.

TABLE OF CONTENTS

iii

LIST OF TABLES

iv

LIST OF FIGURES

ABSTRACT

There are over 602,000 bridges in the United States, of which 12.5% are classified as functionally obsolete and 11.2% are structurally deficient. The functionally obsolete bridges will require expansion or replacement to increase the service capacity of the bridge. The structurally deficient bridges will either need remediation of the load carrying elements which are damaged or deteriorated or will need to be replaced completely. Replacement of the bridges means new construction; new construction means better design and quality assurance to meet the 100+ year service life requirement in place now. Rehabilitation of bridges will require better design and quality assurance to increase the current service life of the structure. This dissertation presents new design, testing, and repair methods developed to extend the life of new and existing bridges through pressure grouting, thermal integrity testing of drilled shafts, and the bond enhancement of fiber reinforced polymer (FRP) repair materials bonded to concrete with vacuum bagging and pressure bagging, respectively.

Pressure grouting of drilled shaft tips has been used for over five decades to improve the end bearing capacity, but no rational design procedure had ever been published until this study. The research outlined in this dissertation analyzed nine grouted shafts and compared them to standard design procedures to determine the improvement in end bearing. Improvements ranged from 60% to 709% increase in end bearing capacity. From these improvements, a design procedure was developed for pressure grouted drilled shafts.

Post construction inspection of drilled shafts relies largely on non-visual techniques dealing with measured concrete quantities, acoustic wave speed or frequency, gamma radiation

attenuation and now the internal temperature of the curing concrete. Thermal Integrity Profiling (TIP), developed at USF, utilizes the heat of hydration of curing concrete to evaluate the concrete cover, foundation shape, cage alignment, and concrete mix design performance. This research developed standard test equipment and procedures for thermal integrity testing.

Comparing the results of the different types of integrity tests is difficult due to the varied nature of the different tests. The dissertation looked at various shafts constructed across the nation which were tested with thermal and at least one other integrity test method. When compared to acoustic and gamma radiation test results, TIP agreed with 4 of 6 cases for acoustic and 2 of 5 cases using gamma radiation. In the one case were both sonic caliper and inclination data were available, TIP showed good agreement.

Vacuum bagging and pressure bagging are techniques for improving the FRP-concrete bond in the repair of partially submerged piles. Prototype vacuum bagging and pressure bagging systems were developed and bond improvement assessed from results of pullout tests on full size piles repaired under simulated tidal exposures in the laboratory. Pressure bagging gave better bond and was found to be simpler because it did not require an airtight seal. A field demonstration project was conducted in which pressure bagging was used in combination with two different glass FRP systems to repair two corroding piles supporting the Friendship Trails Bridge across Tampa Bay. Inspection of the post-cured wrap showed no evidence of air voids.

CHAPTER 1 INTRODUCTION

The American Society of Civil Engineers (ASCE) grades the United States infrastructure every four years, which includes water and environment, transportation, public facilities and energy. Each area is given a letter grade based on the capacity, condition, funding, future need, operation and maintenance, public safety, and resilience. The overall condition of America's infrastructure was given a D+ in 2013 (ASCE, 2013). Within transportation, bridges were given a C+.

Of the 602,880 bridges in America, about 11% of bridges are classified as structurally deficient (FHWA, 2014). Structurally deficient bridges require significant maintenance, rehabilitation, or replacement and are inspected at least every year since critical load-carrying elements were found to be in poor condition due to deterioration or damage (ASCE, 2013). Figure 1.1 shows the structurally deficient bridges per county across the United States.
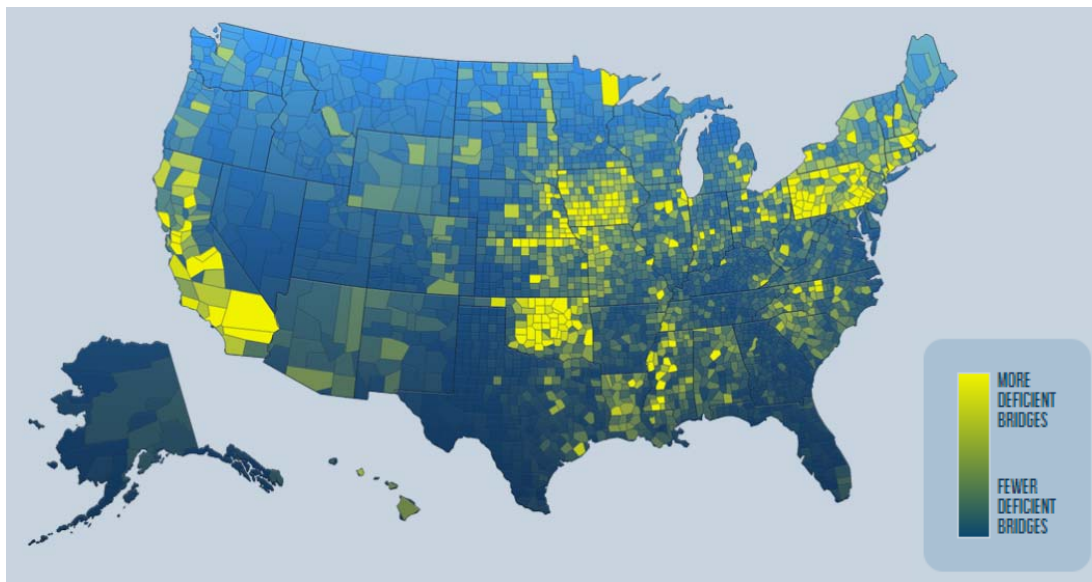
Figure 1.1 Structurally deficient bridges per county (ASCE, 2013).

1

ASCE estimates the average age of these bridges to be 42 years and the Federal Highway Administration (FHWA) estimates over 30% of the bridges have exceeded their 50 year design life. This requires the nation to invest an estimated $20.5 billion annually in maintenance, repair, rehabilitation, or replacement of these structures but currently only $12.8 billion is being spent (ASCE, 2013). Today, current design standards require new structures to last 100+ years to help alleviate future maintenance, repair, and rehabilitation costs. Therein, engineers are developing better designs, construction standards and quality assurance test methods for bridges, as well as investigating new techniques for rehabilitation.

1.1 Organization of Dissertation

This dissertation presents new design, testing, and repair methods developed to extend the life of new and existing bridges; it is a compilation of four separate articles selected from 22 published by the author within different venues (all publications are listed in the reference list of this chapter). As such, each chapter retains the format standard of the original publication. The topics are specific to foundation elements where Chapters 2 through 4 address applications for drilled shafts and Chapter 5 deals with repair of corrosion damaged concrete piles.

Chapter 2 presents design procedures and investigates how to improve the load carrying capacity of drilled shaft foundations. Drilled shafts are cast-in-place concrete elements that develop load carrying capacity via side shear and end bearing. The displacement at which side shear and end bearing develop is drastically different causing engineers to adjust the amount of load carrying ability accordingly. Figure 1.2 shows the degree of side shear and end bearing that can be developed in cohesionless soils (sands) as a function of shaft diameter (Reese and O'Neill, 1988). Combining the two plots further accentuates this incompatibility (Figure 1.3). Side shear develops fully (~100%) within a settlement of 0.5%D (where D is shaft diameter)

2

while at that same displacement end bearing develops only 25%. To develop full end bearing, the shaft is required to displace 4.25%D or more. As a result of the strain incompatibility, design of drilled shafts typical does not include (or significantly reduces) end bearing within the load carrying capacity. By pressure grouting the bottom of the shaft, full development of the end bearing occurs within the same range of settlement associated with side shear, and the potential of higher end bearing values within loose soils can be provided. A design method for the application of pressure grouting is presented.

Quality assurance is paramount in extending the life spans of new structures and as such, new test methods are constantly evolving. Chapters 3 and 4 focus on quality assurance techniques for drilled shaft construction. As drilled shafts are cast-in-place below the ground surface, the construction process is typically unable to provide visual inspection and can unwittingly result in section losses (Figure 1.4). Therefore, various quality assurance test methods are used to verify the pre and post-concreting condition. These methods typically use ultrasonic wave speed, gamma radiation counts, or reflective wave/impedance calculations to infer the concrete quality within the shaft. Short-comings associated with these technologies are that the entire cross section of the shaft section cannot be tested and that reflected waves cannot test long shafts. The need for determining the quality of the drilled shaft concrete for all lengths and sections led to the development of thermal integrity profiling (TIP). TIP uses the temperature generated by the curing concrete to evaluate the integrity of the shaft. Chapter 3 discusses the test method for TIP and Chapter 4 presents case studies.

With the focus of chapters 2 through 4 on new construction, Chapter 5 focuses on extending the life of existing structures using fiber-reinforced polymers (FRP). The number of structurally deficient bridges in the US is intuitively linked to age, but can also be attributed to

3

the construction techniques at that time. Figure 1.5 shows the number of these bridges relative to age. Advancements in FRP are making repairs of such structures more cost effective. However, the FRP bond to the substrate is critical in ensuring long-term durability of the repaired structure. Vertical and overhead flat surface structures prove to be problematic in ensuring a uniform bond due to effects of gravity and that these materials are typically glued into place like wallpaper. Therefore, during the adhesive curing timeframe, the material may become dislodged. Figure 1.6 shows thermal imaging of a FRP-concrete repair on a square pile subjected to harsh marine environment (Mullins et al., 2007). The image shows good bond near the corners of the pile and poor bond near the center. To obtain uniform bond across a flat surface or any surface, vacuum bagging and pressure bagging systems were investigated and are discussed in Chapter 5.
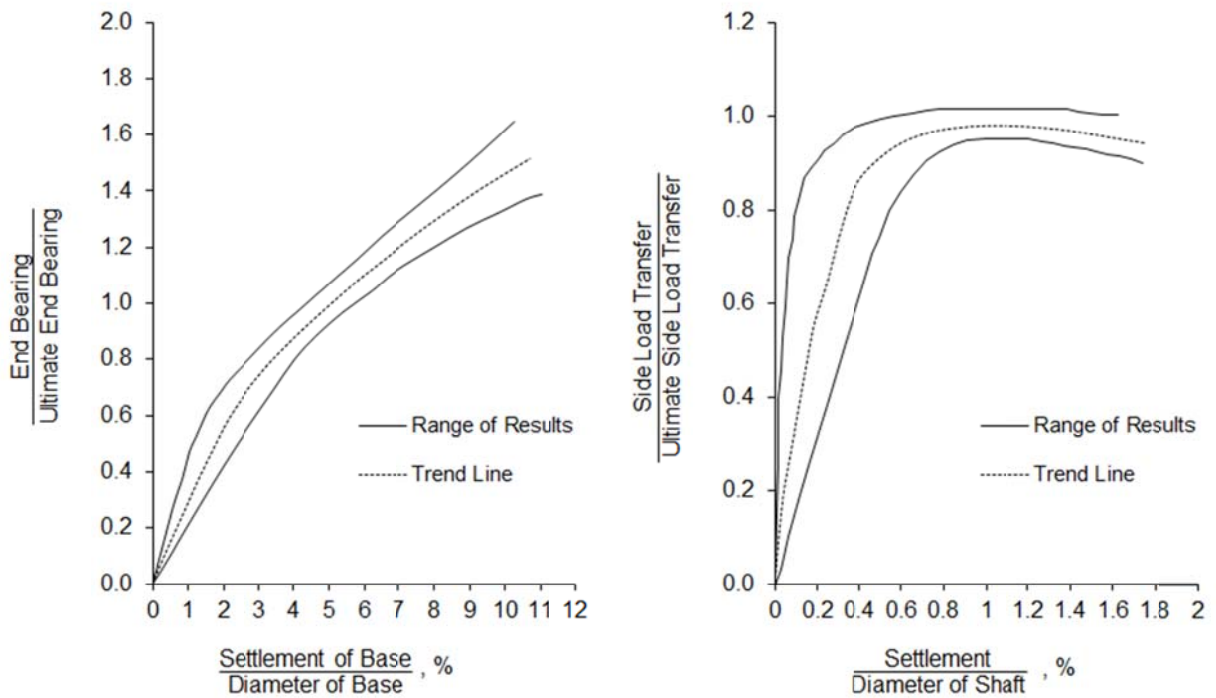
Figure 1.2 Normalized load transfer in side shear (left) and end bearing (right) versus settlement in cohesionless soils for drilled shafts (after Reese and O'Neill, 1988).
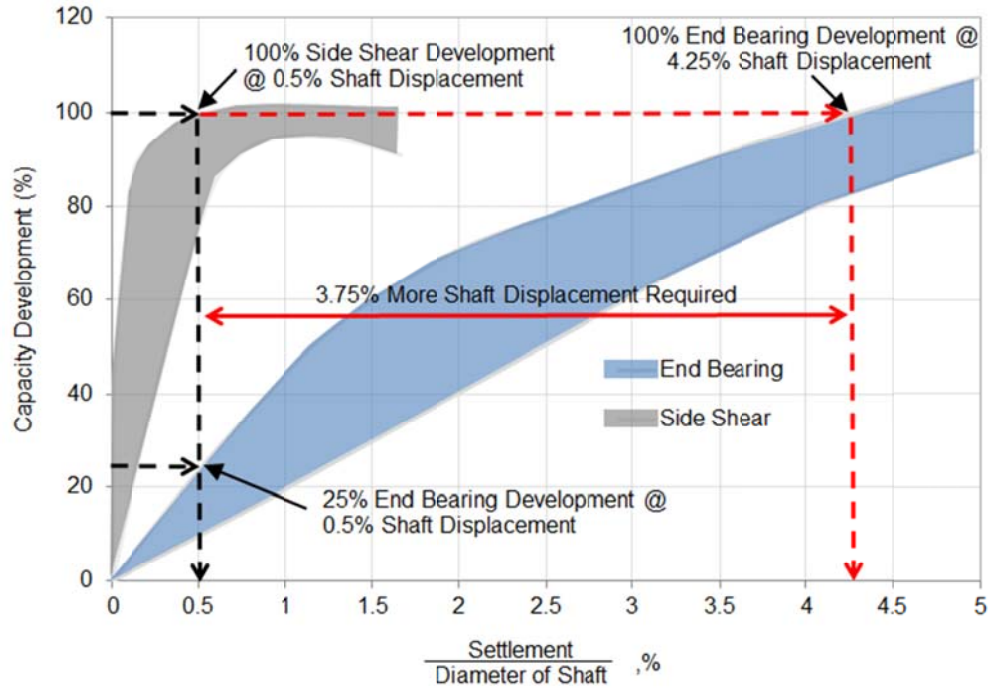
Figure 1.3 Combined load transfer plots for side shear and end bearing.

Figure 1.4 Underground flaws in drilled shafts that required excavation to identify.
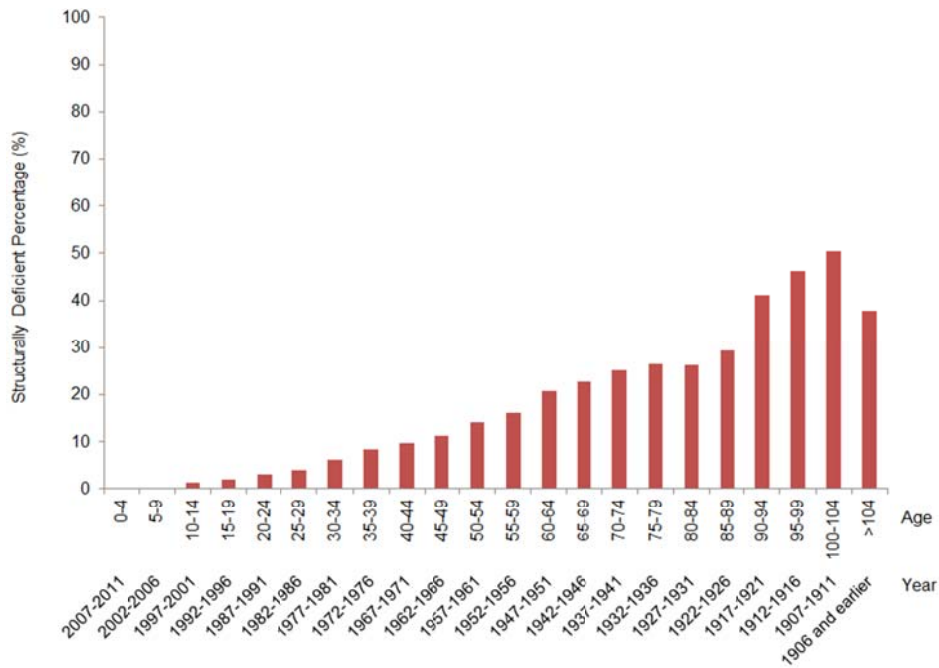
Figure 1.5 Percentage of structurally deficient bridges in the United States.
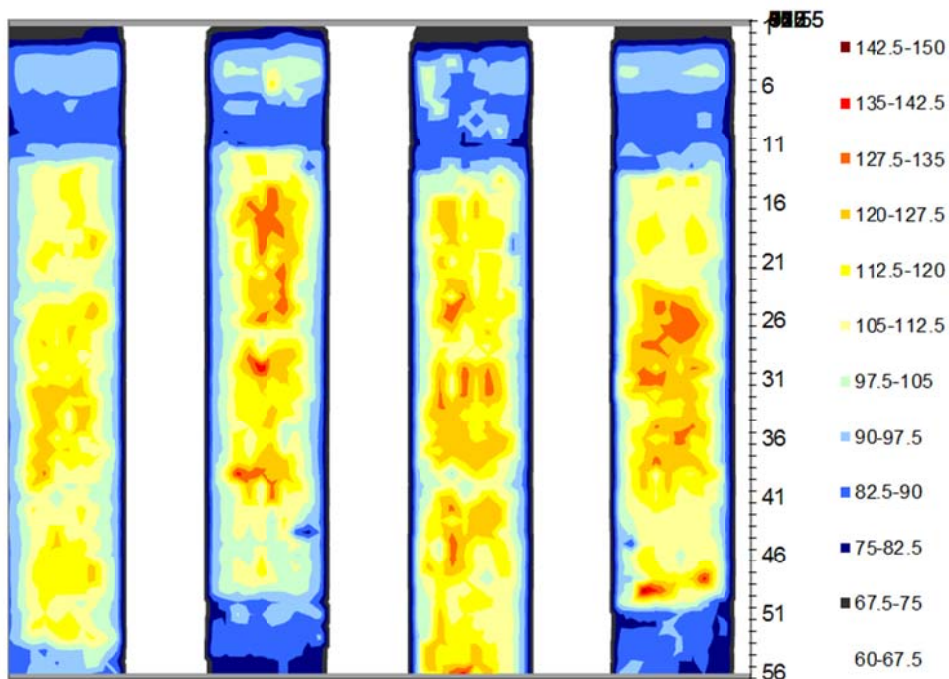
Figure 1.6 Thermal bond image of FRP repaired pile.

الﻣﻨﺎرة للاستشارات

www.manaraa.com

In closing, Chapter 6 summarizes the findings of the individual studies and makes

recommendations for future work in the respective areas.

1.2 References

Aguilar, J., Winters, D., Sen. R., Mullins, G. and Stokes, M. (2010). "FRP-CP System for Pile Repair in Tidal Waters". Transportation Research Record 2150, pp. 111-118.

Aguilar, J., Winters, D., Sen. R., Mullins, G. and Stokes, M. (2009). "Improvement in FRP-Concrete Bond by External Pressure". Transportation Research Record, No. 2131, pp. 145-154.

ASCE (2013). "2013 Report Card for America's Infrastructure." Retrieved January 22, 2014, from http://www.infrastructurereportcard.org/a/#e/sd-fo-bridges-state.

FHWA (2014). "Structure Type by Year Built." Retrieved January 22, 2014, from http://www.fhwa.dot.gov/bridge/structyr.cfm

Johnson, K., Mullins, G., and Winters, D. (2007). "Concrete Termperature Reduction via Voided Drilled Shafts" ASCE Geo-Denver: Contemporary Issues in Deep Foundations, pp. 1-12.

Mullins, G., Sen, R., Suh, K. and Winters, D. (2006). "A Demonstration of Underwater FRP Repair" Concrete International, Vol. 28, No. 1, pp. 70-73.

Mullins, G., Sen, R., Suh, K and Winters, D. (2005). "Underwater Fiber-Reinforced Polymers Repair of Prestressed Piles in the Allen Creek Bridge". ASCE, Journal of Composites for Construction, Vol. 9, Issue 2, pp. 136-146.

Mullins, G., Sen, R., Suh, K., and Winters, D. (2004) "Underwater FRP Repair of the Friendship Trails Bridge" Concrete International, American Concrete Institute, Farmington Hills, MI.

Mullins, G. and Winters, D. (2012), "Rapid Hydration of Mineral Slurries," Foundation Drilling, ADSC, The International Association of Foundation Drilling, Irving, TX. Vol. XXXIII, Mar-Apr pp. 25-34.

Mullins, G. and Winters, D. (2011) "Infrared Thermal Integrity Testing, Quality Assurance Test Method To Detect Drilled Shaft Defects." WSDOT Project WA-RD 770.1, 175 pp.

Mullins, G., Winters, D, and Dapp, S., (2008). "Closure to Predicting End Bearing Capacity of Post Grouted Drilled Shafts in Cohesionless Soils" ASCE Journal of Geotechnical and GeoEnvironmental Engineering, Vol. 134, No. 3, p. 413.

Mullins, G., Winters, D., and Dapp, S. (2006). "Predicting End Bearing Capacity of Post Grouted Drilled Shafts in Cohesionless Soils" ASCE Journal of Geotechnical and GeoEnvironmental Engineering, Vol. 132, No. 4. pp. 478-487.

Reese, L.C. and O'Neill, M.W. (1988) "Drilled Shafts: Construction and Design." FHWA, Publication No. HI-88-042.

Sen, R., Mullins, G., Suh, K.S. and Winters, D. (2007). "Performance of FRP in Reducing Corrosion in Prestressed Elements". Proceedings of the 17th International Offshore and Polar Engineering Conference, Lisbon, Portugal, July 1-6, Vol. 4, pp. 3504-3507.

Sen, R., Mullins, G., Suh, K. S. and Winters, D. (2005). "FRP Application in Underwater Repair of Corroded Piles". ACI SP 230, Vol. 2, pp. 1139-56.

Stokes, M., Mullins, G., Ealy, C., and Winters, D. (2008). "Statnamic Damping Coefficient: A Numerical Modeling Approach," Journal of Geotechnical and GeoEnvironmental Engineering, Vol. 134, No. 9, pp.1290-1298.

Suh, K.S., Mullins, G., Sen, R. and Winters, D. (2010). "Effective Repair for Corrosion Control Using FRP". ASCE, Journal of Composites for Construction, Vol. 14, No. 4, pp. 388-396.

Suh, K.S., Sen, R, Mullins, G. and Winters, D. (2008). "Corrosion Monitoring of FRP Repaired Piles in Tidal Waters". ACI SP-252, pp. 137-156.

Suh, K.S., Mullins, G. Sen, R. and Winters, D. (2007). "Corrosion Monitoring of FRP Wrapped Piles", Proceedings, Third International Conference on Durability of Fibre Reinforced Polymer Composites for Construction, Quebec City, Canada, pp. 407-414.

Suh, K., Mullins, G., Sen, R. and Winters, D (2007). "Effectiveness of Fiber-Reinforced Polymer in Reducing Corrosion in Marine Environment". ACI Structural Journal, Vol. 104, No. 1, 76-83.

Winters, D. (2014). "Comparative Study of Thermal Integrity Profiling with Other Non-Destructive Integrity Test Methods for Drilled Shafts," 2014 Geo-Congress: Geo-Characterization and Modeling for Sustainability February 23-26, 2014 Atlanta, Georgia.

Winters, D. and Mullins, G. (2012). "Thermal Integrity Profiling of Concrete Deep Foundations," Proceedings Geo-Construction Conference / ADSC Expo 2012, San Antonio, TX, pp. 155-165.

Winters, D., Mullins, G., Sen, R., Schrader, A. and Stokes, M. (2008). "Bond Enhancement for FRP Pile Repair in Tidal Waters". ASCE, Journal of Composites for Construction, Vol. 12, No. 3, pp. 334-343.

Winters, D., Mullins, G., Stokes, M. and Sen, R. (2009). "Development of Pressure / Vacuum Bagging for FRP Repair". Proceedings, Fifth International Conference on Construction in the 21st Century (CITC-V), Istanbul, Turkey, May, CDROM.

CHAPTER 2 PREDICTING END BEARING CAPACITY OF POST-GROUTED DRILLED SHAFT IN COHESIONLESS SOILS[1]

Although pressure grouting beneath the tips of drilled shafts had been used successfully worldwide for close to four decades, it has remained relatively unused in the United States in part due to the absence of a rational design procedure. Previous international usage relied predominantly upon experience and unpublished proprietary approaches. More recently, research aimed at quantifying the improvement that could be derived from post grouting drilled shaft tips has resulted in a design methodology. This chapter briefly discusses the post grouting process and outlines the full scale test programs used to identify parameters affecting post grouting performance. Correlations developed between applied grout pressure and end bearing improvement are presented along with a numerical example illustrating the design procedure.

2.1 Introduction

The unit ultimate end bearing of drilled shafts tipped in cohesionless soil can be on the order of twenty times the unit ultimate side shear. However, this enormous capacity is rendered virtually unusable due to multiple mechanisms associated with construction techniques and soil mechanics. The two primary construction-related mechanisms that hamper end bearing development include: (1) soil relaxation beneath the shaft tip due to excavation and (2) debris remaining after clean out. Furthermore, even under ideal shaft construction conditions, ultimate side shear is developed in only a fraction of the displacement required to develop the ultimate

---

[1] This chapter was published in ASCE Journal of Geotechnical and GeoEnvironmental Engineering (Mullins, et al. 2006). Permission is included in Appendix A.

end bearing. The side shear fully develops at a displacement between 0.5 to 1.0% of the shaft diameter (D); whereas, the end bearing is fully mobilized at displacements of 10 to 15%D (Bruce 1986; Mullins, et al. 2000). Therefore, the end bearing requires 10 to 30 times more displacement than side shear in order to mobilize the same percentage of its ultimate value. As a result, engineers typically must discount or significantly reduce the end bearing contribution to the capacity of drilled shafts to accommodate service/displacement limits.

In 1999, a four year study was initiated to quantify the effects of pressure grouting beneath the base of drilled shafts and show its potential to mitigate the above mechanisms plaguing end bearing capacity. This method was expected to be applicable to projects with deep cohesionless deposits where the soil strata would require excessively long drilled shaft lengths without considerable end bearing contribution and in urban areas where vibrations associated with pile driving are not well tolerated. This chapter briefly discusses the results from this study and introduces a new design procedure for predicting end bearing capacity in post-grouted drilled shafts tipped in cohesionless soils.

2.2 Background

In the early 1960's, efforts to improve the end bearing of drilled shafts began in Europe using high pressure grout injected beneath the shaft tip (Bolognesi and Moretto 1973; Gouvenot and Gabiax 1975; Sliwinski and Flemming 1984). Thereafter, numerous case studies have been documented stating its effectiveness. This end bearing modification technique, also called post-grouting or base grouting, has been used worldwide, yet literature on its use lacks a rational design approach. As a consequence, there has been little use in the United States. As this chapter focuses on the design of the end bearing capacity, a thorough overview of post grouting processes can be found elsewhere (Bruce 1986; Mullins, et al. 2000).

10

In general, the post grouting technique involves casting drilled shafts with a grout delivery system incorporated into the reinforcing cage capable of placing high pressure grout at the base of the shaft (after the shaft concrete has cured). This both densifies the in situ soils and compresses any debris left by the drilling process. Moreover, by preloading the soil beneath the tip, end bearing capacity can be developed within service/displacement limits. In previous studies, it was suggested that pressure-grouted shafts tipped in loose to medium dense sand provided the most benefit, but improvement was observed in all soil types cited. Specifically, end bearing could be improved in sands and clays with ultimate capacities as much as two to three times conventional ungrouted shafts (Bruce 1986). The same sources purported end bearing improvement to be dependent on the volume of grout injected. However, the improvement was shown to be more directly related to grout pressure by the authors and forms the basis of the new design method.

During base grouting, the grout pressure produces a bi-directional force at the shaft tip, wherein the development of the end bearing is resisted by the skin friction of the shaft. Hence, longer shafts or shafts that develop more side shear can resist higher grout pressure. Previous studies that cited both the applied grout pressure and shaft length (or depth) show an increasing trend of grout pressure with depth (Figure 2.1). This is in keeping with the understanding that the maximum grout pressure is dependent on the available side shear on which the grout pressure can react.

In concept, the anticipated grout pressure for a given site can be generalized with respect to the shaft length, diameter and the average unit side shear (Figure 2.2). As the grout pressure is a function of tip area, unit side shear, and shaft length, the expression for anticipated grout pressure can be simplified as follows:

11
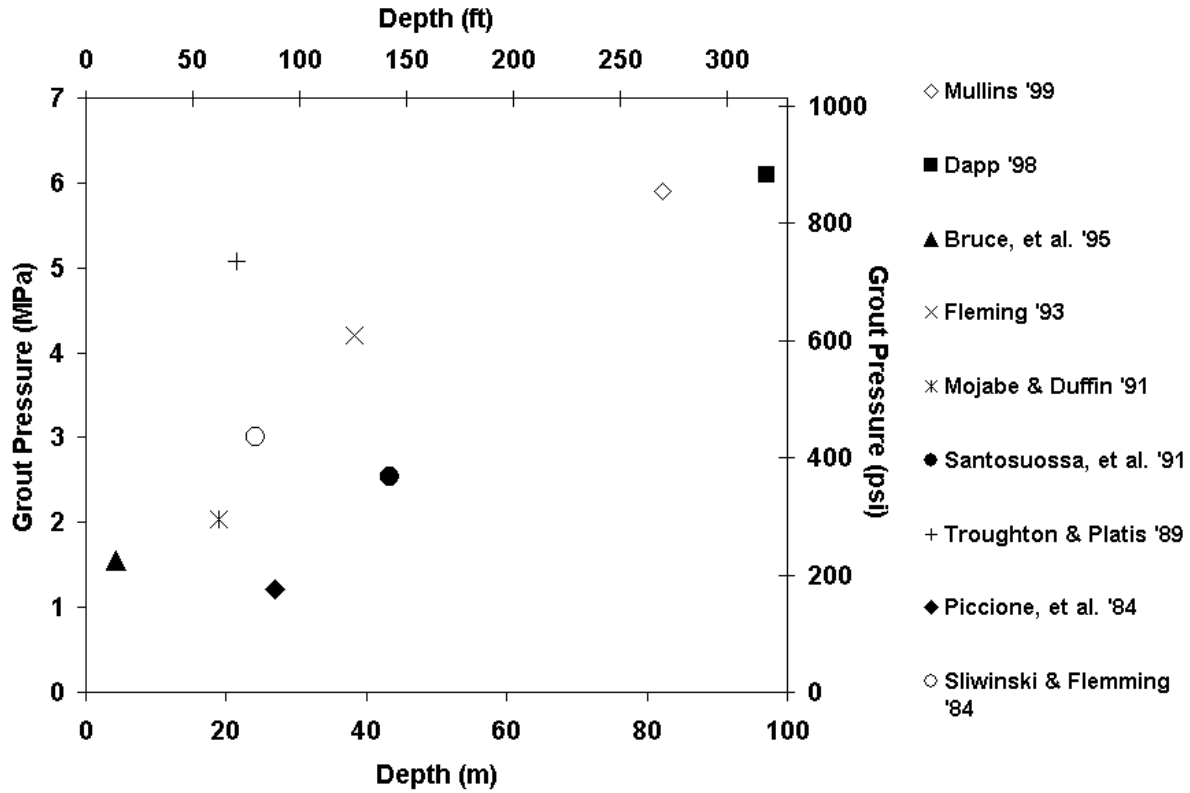
Figure 2.1 Published grout pressure versus depth prior to this research program.

$$GP_{max} = \frac{Side\ Shear\ Force}{Tip\ Area} \tag{1}$$

$$GP_{max} = \frac{q_s \pi D L}{\left(\frac{\pi D^2}{4}\right)} \tag{2}$$

$$GP_{max} = 4 q_s \frac{L}{D} \tag{3}$$

where GP_{max} represents the maximum predicted grout pressure, q_s the unit side shear, and L/D the shaft length to diameter ratio.

12

From a more practical perspective, several ranges are also identified in Figure 2.2 that denote applicable limits on grout pressure. The lines denoting unit side shear values present upper bounds on grout pressure for shafts constructed in soils with average unit side shear values of 0.05, 0.1, and 0.2 MPa (0.5, 1.0 and 2.0 tsf). For all soils and L/D ratios, an upper limit on grout pressure is typically applied that considers the construction limitations of the grout pump, grout tubes, or the working life of the neat cement grout. Although pressures as high as 11 MPa (1600 psi) are attainable, a 6.9 MPa (1000 psi) upper limit is more realistic without having to use specialized equipment.
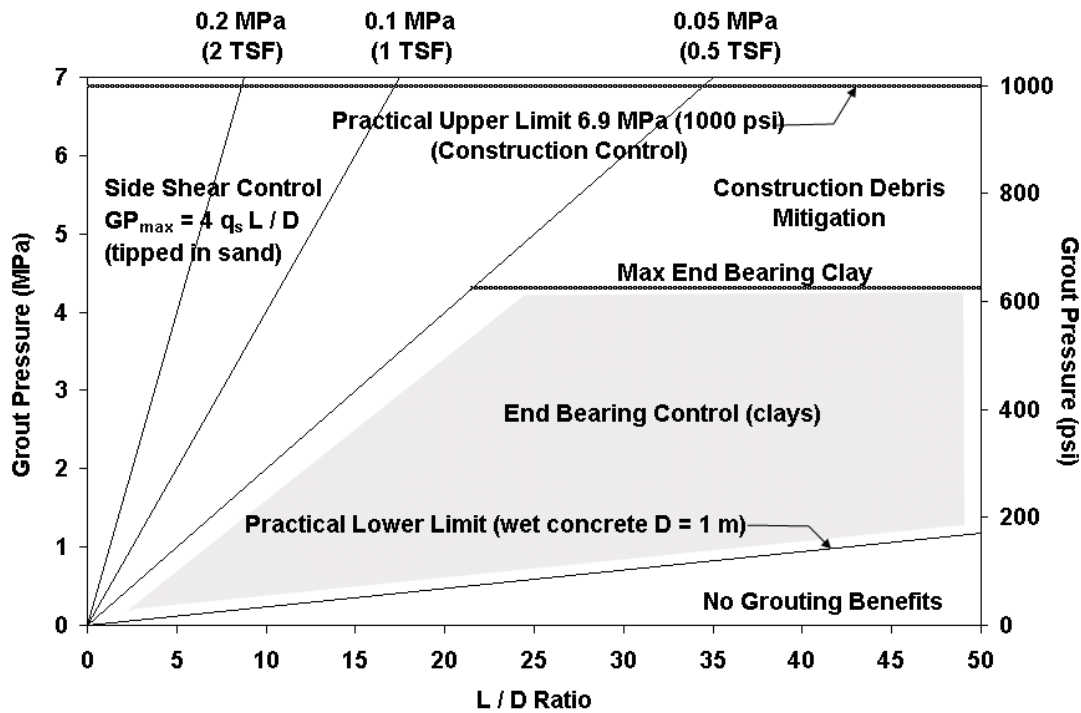
Figure 2.2 Concept graph of pressure versus depth.

An example lower limit is also presented that represents the hydrostatic pressure of wet concrete for a 1 meter diameter shaft. Assigning a grout pressure at or below this level does not provide a benefit worthy of the effort. Although in some instances the process of merely

13

flushing grout through the tubes and grouting cell has shown grout volume taken into soft areas or unexpected voids, far more can be derived from a pressure grouting protocol that takes full benefit from an optimized design.

2.3 End Bearing Development

Reese and O'Neill (1988) showed that the end bearing capacity of conventional ungrouted shafts could be expressed as a function of shaft diameter and the permissible settlement (Figure 2.3). Therein, the ultimate design capacity based on 5% displacement was given by:

$$q_b = 0.057N \tag{4}$$

where q_b is the ultimate unit end bearing capacity (in MPa), and N is the uncorrected Standard Penetration Test (SPT) blow count.

At displacements less than 5%D, a reduced capacity should be assigned using a tip capacity multiplier (TCM < 1) based on the above relationship and the permissible displacement; at larger displacements beyond 5%D even more end bearing can be developed (TCM > 1). Equation 5 provides a convenient curve fit for the TCM trend shown in Figure 2.3.

$$TCM = \frac{\%D}{0.4(\%D) + 3.0} \tag{5}$$

TCM values greater than 1.0 corroborate Bruce's (1986) statement that shafts tipped in sand could continue to develop capacity up to 15%D. Unfortunately, large displacements such as these are rarely permissible due to service limits. For example, a 1.2 m (4 ft) diameter shaft would have to displace 61 mm (2.4 in) in order to achieve ultimate capacity; whereas the side shear would develop in 6 - 12 mm (0.24 - 0.48 in), shown in Figure 2.4. At full side shear

14

development, only about a third of the design end bearing has been developed. As an alternate, post grouting beneath the shaft tip provides a method to avail higher usable end bearing at more reasonable displacements.
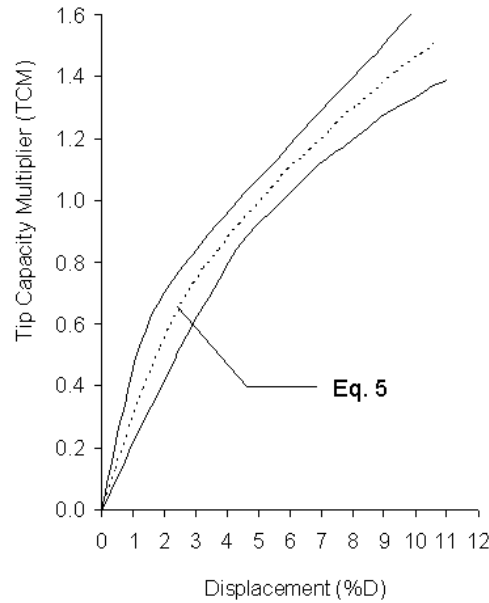
Figure 2.3 Usable end bearing as a function of permissible displacement (adapted from Reese and O'Neill, 1988).
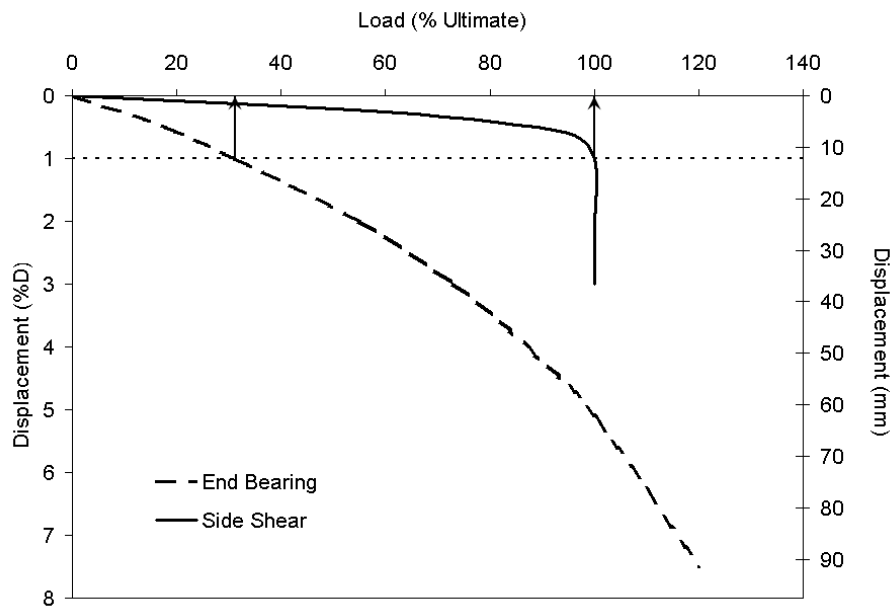
Figure 2.4 Typical displacement mismatch between end bearing and side shear.

15

2.4 Effects of Side Shear Capacity on Grout Pressure

The grout pressure required to affect end bearing improvement in cohesionless soil is dependent on the available side shear. As such, uplift of the shaft is possible as the force from the applied grout pressure over the area of the toe approaches the ultimate side shear capacity. At this point, the grout pressure has both displaced/compressed the soil beneath the toe and strained the side shear in uplift. Depending on whether the grout pressure is maintained or released during the curing of the grout, two stress states may exist. Figure 2.5 and Figure 2.6 conceptually show the load history of the side shear and soil beneath the toe during the grouting and structural loading phases for maintained and released grout pressure, respectively. Four points are highlighted on each graph showing pertinent phases: Point (1), the initial unstressed state; Point (2), the maximum applied grout pressure; Point (3), the grout cured, prior to structural loading; and Point (4), after structural loading assuming a 1%D settlement. Although the mechanism by which the load is transferred into the soil is significantly different for the two approaches, the net effect is virtually identical with regards to load carrying capabilities.

When the grout pressure is maintained or locked-in during curing (Figure 2.5), the toe load required to hold the shaft in negative side shear increases slightly as applied structural loads overcome the negative side shear (small displacements). In effect, the side shear load required to hold the soil beneath the toe in compression is replaced by the structural loading until the negative side shear is completely overcome. After which, additional load can be developed by positive side shear and a further increase in end bearing. The load carrying mechanism from precompressing the toe soils is analogous to pretensioning bolts used for tensile loading. Therein, bolts are commonly pretensioned during installation to over 90% of the usable capacity. This causes a clamping force that equals the sum of the bolt group pretensioning. The tensile

16

load in the bolts remain the same throughout the life of the connection but are ultimately resisted by a combination of structural loads and clamping forces. If the structural load exceeds the initial clamping force, plate separation occurs and the remaining 10% of the bolt capacity can be mobilized as needed up to the ultimate load. Table 2.1 shows the similarities between post grouted shaft tips and a bolted tension connection (bolt analogy explained in italics).

When the grout pressure is released before curing or unlocked (Figure 2.6), the soil beneath the toe is loaded normally during grouting allowing large pre-compressing displacements to occur followed by a relatively stiff unloading. The side shear is stressed upwards and returned to its unstressed state. Upon application of structural loading, the side shear develops normally (acting upward) while the end bearing is reloaded along a much stiffer path where the displacement required to fully develop the end bearing is commensurate with that of the side shear.

Minimal differences have been observed in the resultant capacity from these two mechanisms (Frederick 2001; Mullins and Winters 2004). In reality, some relaxation occurs in the soil beneath the toe even when the pressure is locked-in. Consequently, the actual response in these cases reflects a combination of both scenarios.

The design method presented herein stems from a database of twenty-six grouted and ungrouted test shafts tipped in sand, silt, and clay at eight different sites which incorporated both locked-in and unlocked approaches. Five of these sites had shafts tipped in sand, silty sand, shelly sand, or slightly cemented sand. This chapter focuses on the improvement in cohesionless soils. Therefore, discussion of the sites in cohesive soils are not presented within this chapter.

17
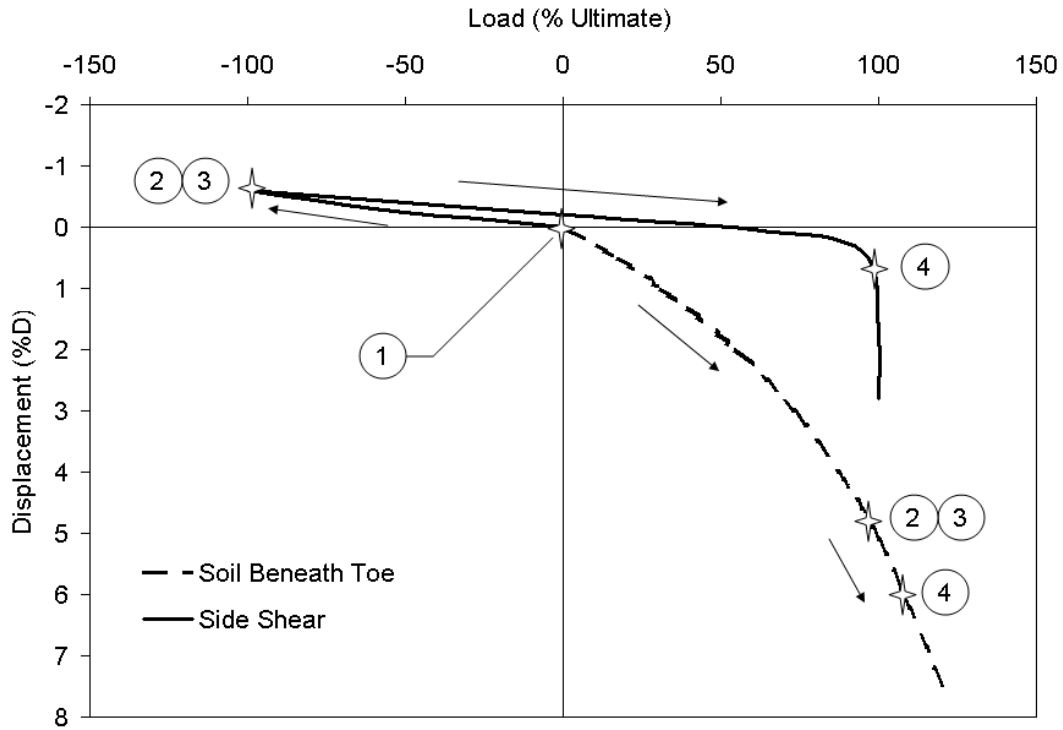
Figure 2.5 Conceptual load / displacement history for locked-in grout pressure.
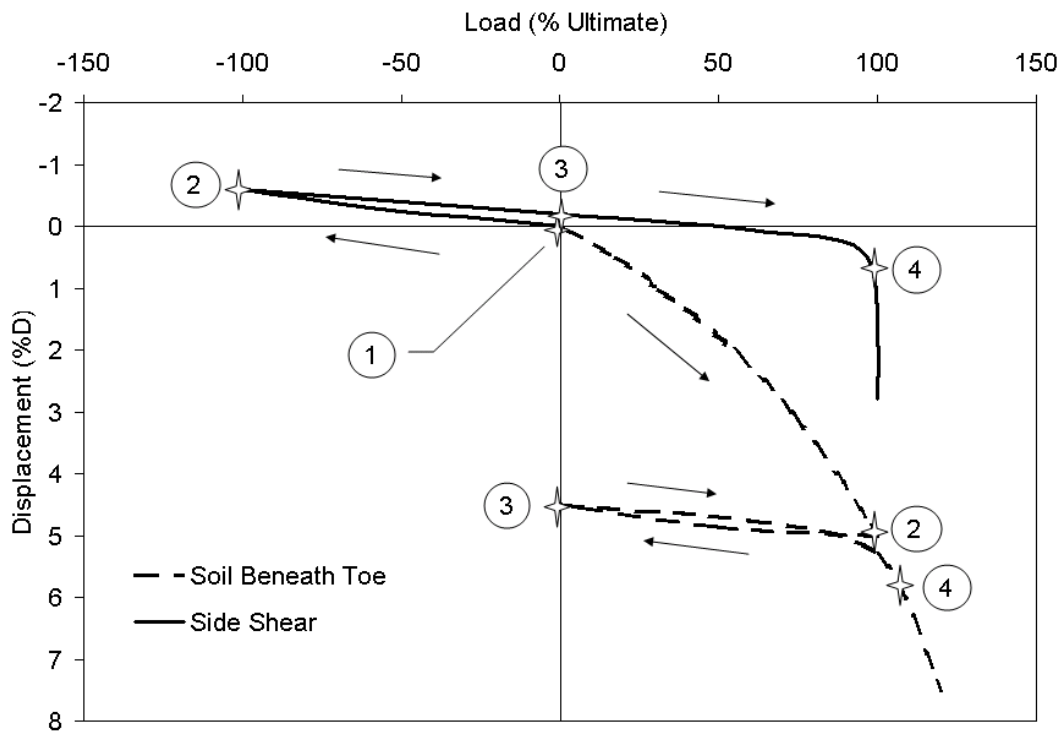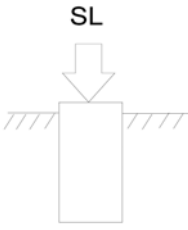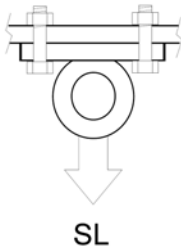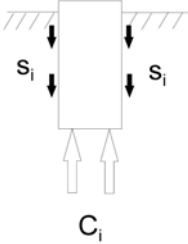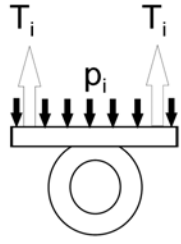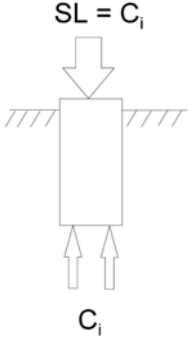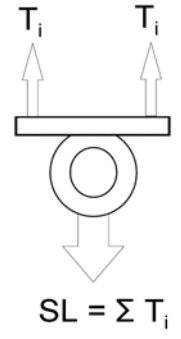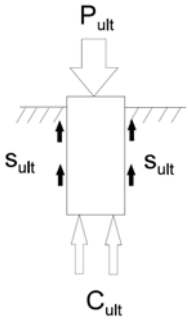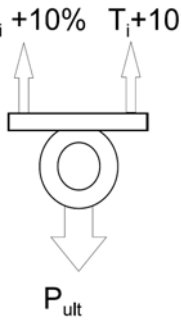
Figure 2.6 Conceptual load / displacement history for unlocked grout pressure.

www.manaraa.com

Table 2.1 Comparison of bolt pretensioning to shaft tip precompression.

Drilled Shaft	Bolt Analogy	Description
SL	SL	Normal application of structural loads (SL).
s_i s_i C_i	T_i T_i p_i	After grouting the initial precompression force (C_i) in the soil beneath the toe holds the uplifted shaft in an initial negative side shear (s_i), Point (2) above.

Similarly, pretensioning the bolts to code-specified minimum values (T_i*) creates an initial clamping pressure (*p_i*).* |
| SL = C_i C_i | T_i T_i SL = $\Sigma\ T_i$ | As structural loads are progressively applied, the initial negative side shear is relaxed until the structural load equals the precompression load, C_i and the side shear returns to an unstressed state (between Points (3) and (4) above).

Similary, the clamping pressure beneath the tension plate decreases to zero as the structural load approaches the sum of the bolt pretensioning forces. |
| P_{ult} s_{ult} s_{ult} C_{ult} | T_i +10% T_i+10% P_{ult} | Additional structural loading can be withstood up to the point where the side shear has fully developed in positive side shear and the end bearing increases slightly in response to the additional displacement, Point (4) above.

In contrast, application of more load creates separation between the bolted plates and additional capacity can only be derived from the reserve bolt capacity (~10%). |

19

2.5 Full-Scale Field Study

The research program consisted of both model-scale and full-scale testing. Model-scale testing was carried out within a frustum confining vessel and explored parameters affecting post-grouting performance and cavity expansion where the shafts could be easily exhumed (Dapp 2002; Frederick 2001; Mullins, et al. 2001; Mullins and Winters 2004). The objective of the field studies were three-fold: (1) to quantify the improvement that could be developed by pressure grouting the tip of the shaft,(2) to develop design recommendations for the use of pressure grouting drilled shaft tips, and (3) to establish criteria / guidelines for effective grouting. Although, the majority of sites included a control shaft (conventional, with no post grouting), the response of the grouted shafts was also compared to end bearing design capacity predictions from soil boring logs (i.e. AASHTO 1999).

Two different grout distribution systems were used throughout the study, the flat jack and the sleeve port (also known as tube-a-manchette). Each system has associated advantages, but both provided similar end bearing improvement. A full discussion of these systems can be found elsewhere (Dapp 2002 and Mullins, et al. 2001). The ensuing sections outline the site conditions and load test results for each of the sites where shafts were tipped in sandy soils.

2.5.1 Sites I & II: Clearwater, FL

A total of 8 shafts were constructed and tested within two adjacent sites located in Clearwater, Florida. These shafts each had a diameter of 0.61 m (2.0 ft) and were 4.57 m (15 ft) in length. Five shafts, including one control shaft, were tested in Site I (loose to medium dense shelly sand); while 3 shafts, including one control shaft, were tested in Site II (loose silty sand). Soil exploration involved mini-cone (2.5 cm2) and full-size (10 cm2) cone penetration soundings as well as standard penetration testing. The mini-cone was used to quickly delineate site

20

variability, the 10 cm2 cone was used at each shaft location, and the SPT borings were conducted between the shaft locations. Excavation was conducted using polymer slurry for stabilization. Full details can be found elsewhere (Mullins, et al. 2000; Mullins, et al. 2001; Dapp and Mullins 2002). Figure 2.7 and Figure 2.8 show the soil profiles for Site I and II, respectively. Likewise, Figure 2.9 and Figure 2.10 show the load-displacement responses for each test shaft for the two sites as well as the applied grout pressure load and AASHTO predicted end bearing values. In each graph the capacities at displacements of 1, 2, and 5%D are indicated for future reference (also provided in Table 2.2).
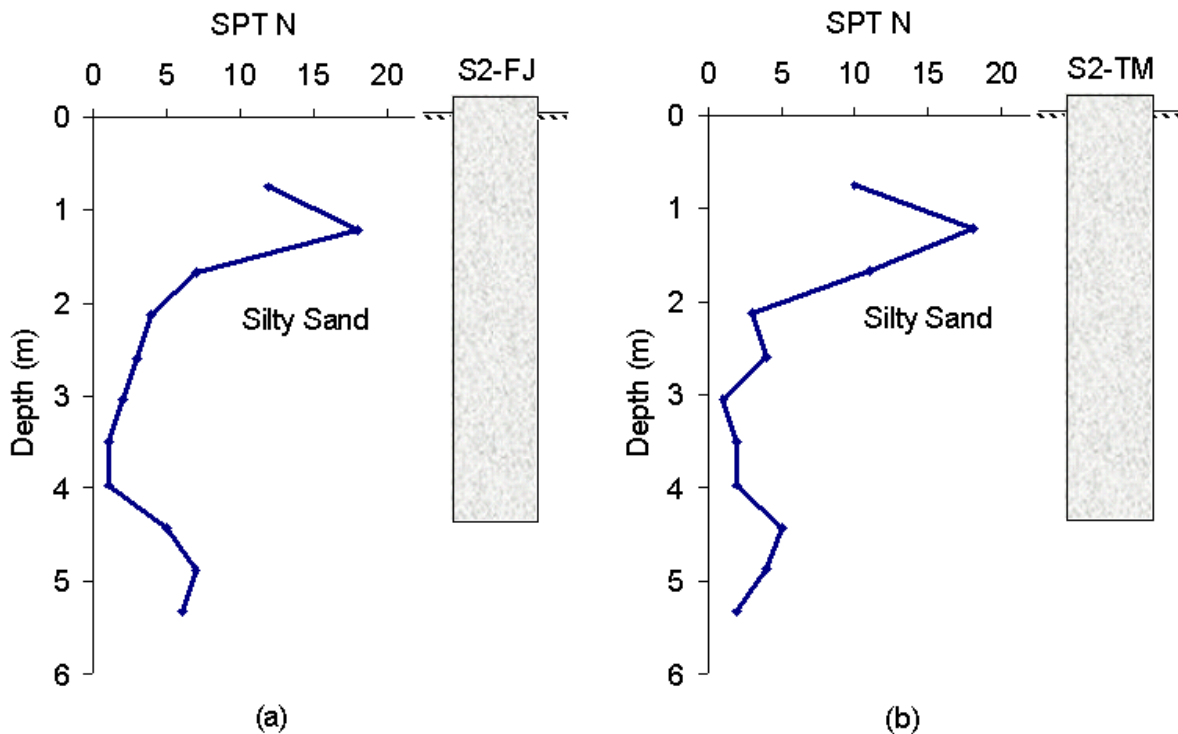
Figure 2.7 Soil boring logs for Site I (a) Flat-Jack and (b) Sleeve-Port test shafts.
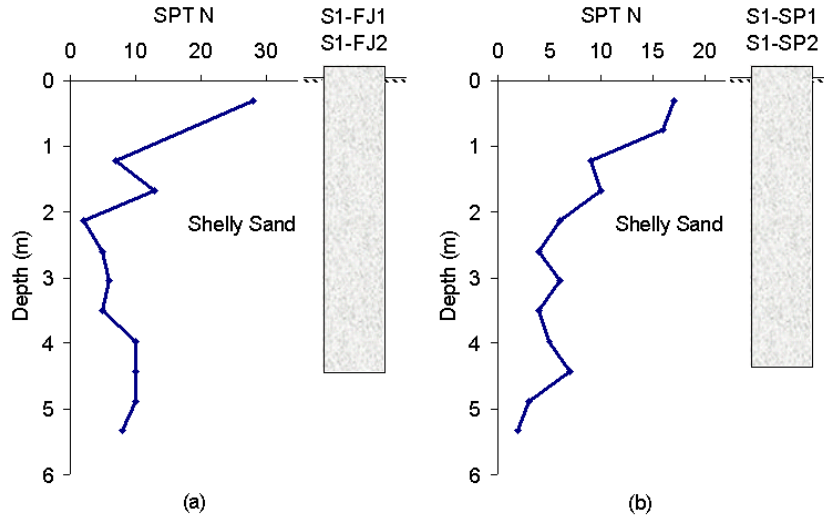
Figure 2.8 Site II soil boring logs for test shafts (a) S2-FJ and (b) S2-TM.
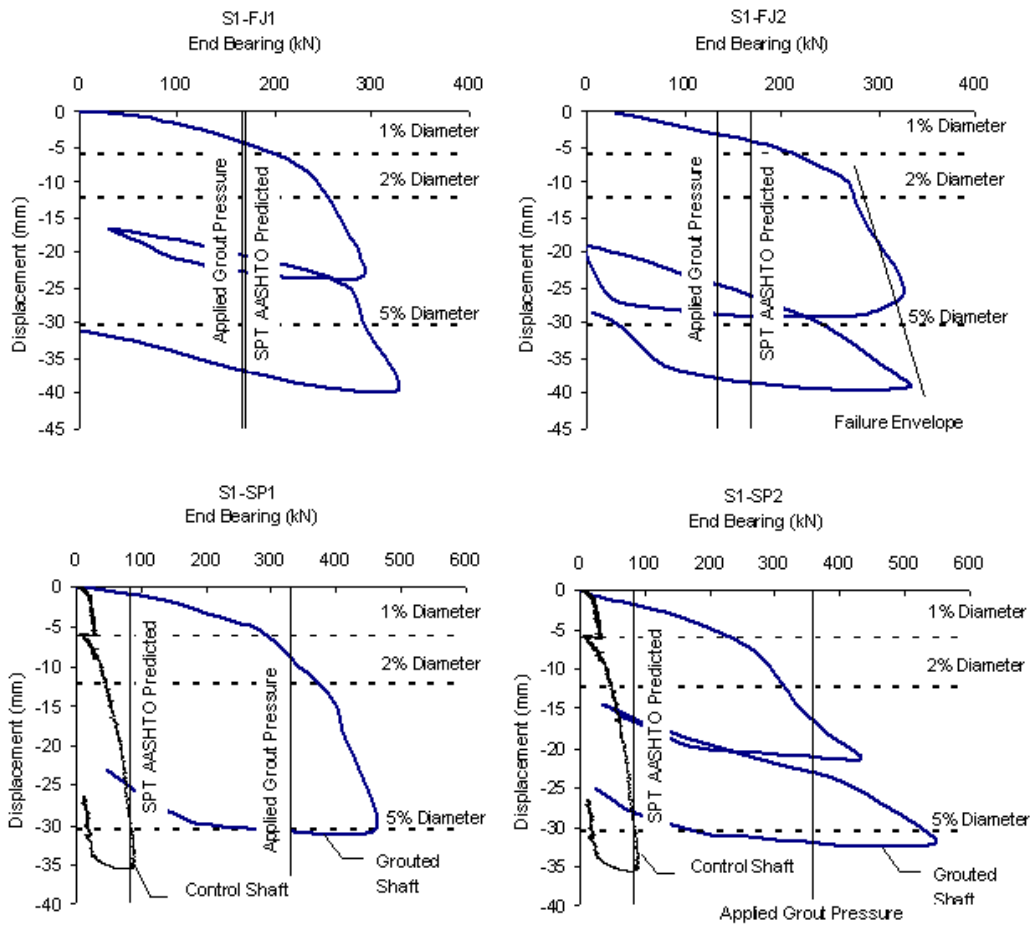
Figure 2.9 Load test results for Site I.

22
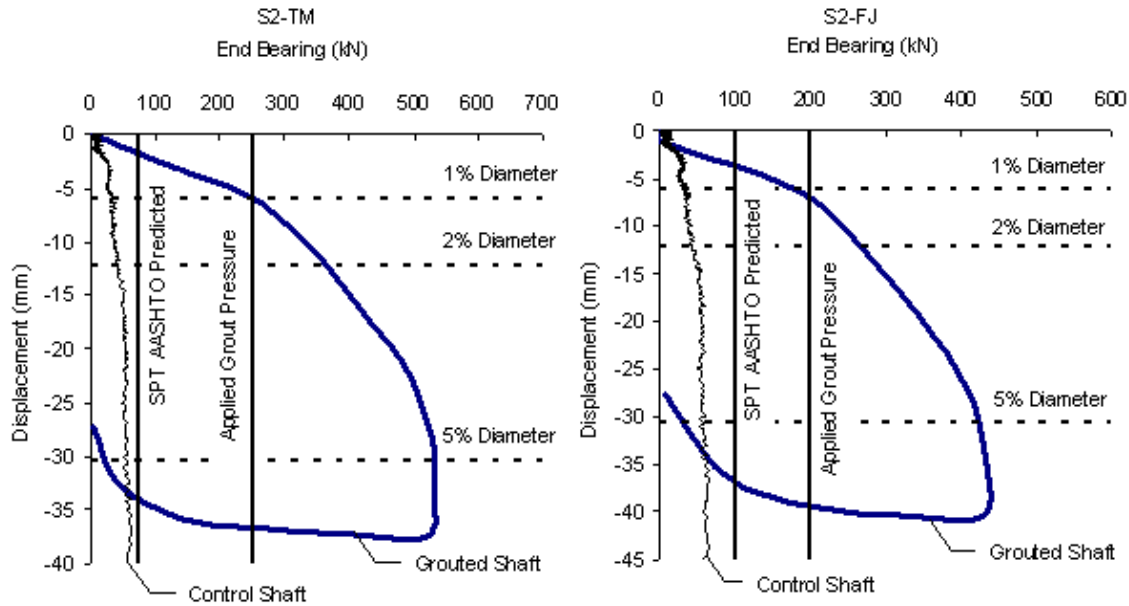
Figure 2.10 Load test results for Site II.

2.5.2 Site III: Palm Beach, FL

Three test shafts, grouted and ungrouted, were constructed and tested in slightly cemented coquina sand located at the Royal Park Bridge crossing the Intracoastal waterway in Palm Beach, Florida. One of these shafts, LT-3, is a 1.22 m (4.0 ft) diameter, 34.80 m (114.2 ft) long grouted shaft. A combination of temporary and permanent casing was used with sea water drill slurry. Figure 2.11 shows the SPT soil boring and the end bearing results for LT-3. Additional information for Site III can be found in Dapp and Mullins (2002).

2.5.3 Site IV: West Palm Beach, FL

Two test shafts, grouted and ungrouted, were constructed and load tested as part of the PGA Blvd Grade Separation Bridge Project in West Palm Beach, FL. The load test program for this site revolved around the relative end bearing performance of two 0.91 m (3 ft) diameter, 18.3 m (60 ft) long test shafts constructed in loose to medium dense shelly sand. Test shaft LT-1 served as the ungrouted control while LT-2 was grouted. Each shaft was constructed with

23

mineral slurry. A SPT boring was performed at the centerline of each test shaft. The SPT soil

boring and end bearing results for LT-2 are shown in Figure 2.12.
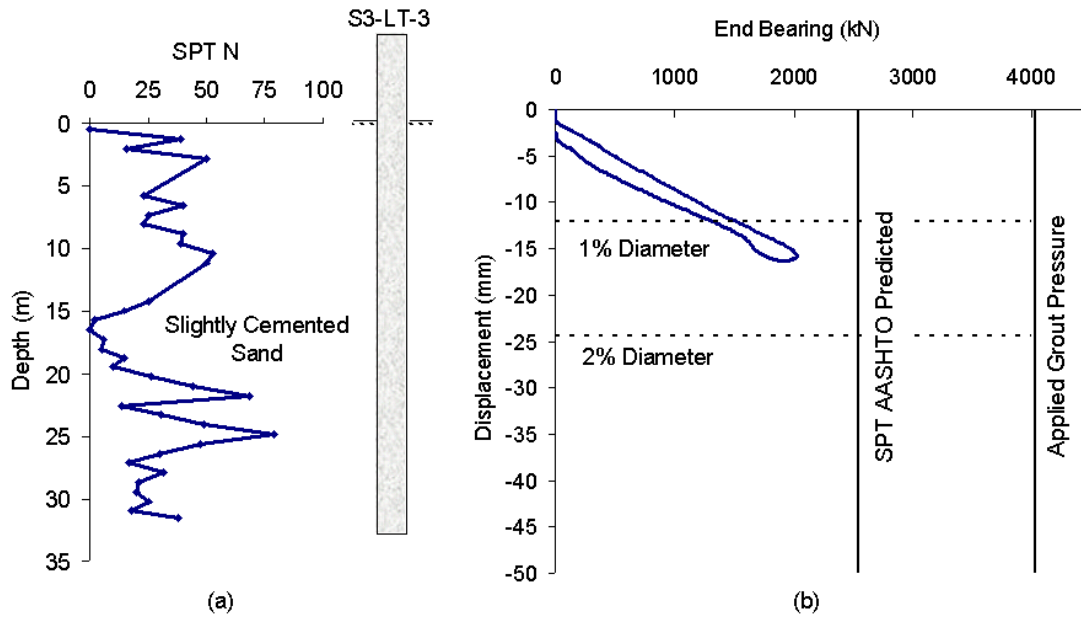
Figure 2.11 Site III (a) soil boring log and (b) end bearing load test results for test shaft LT-3.
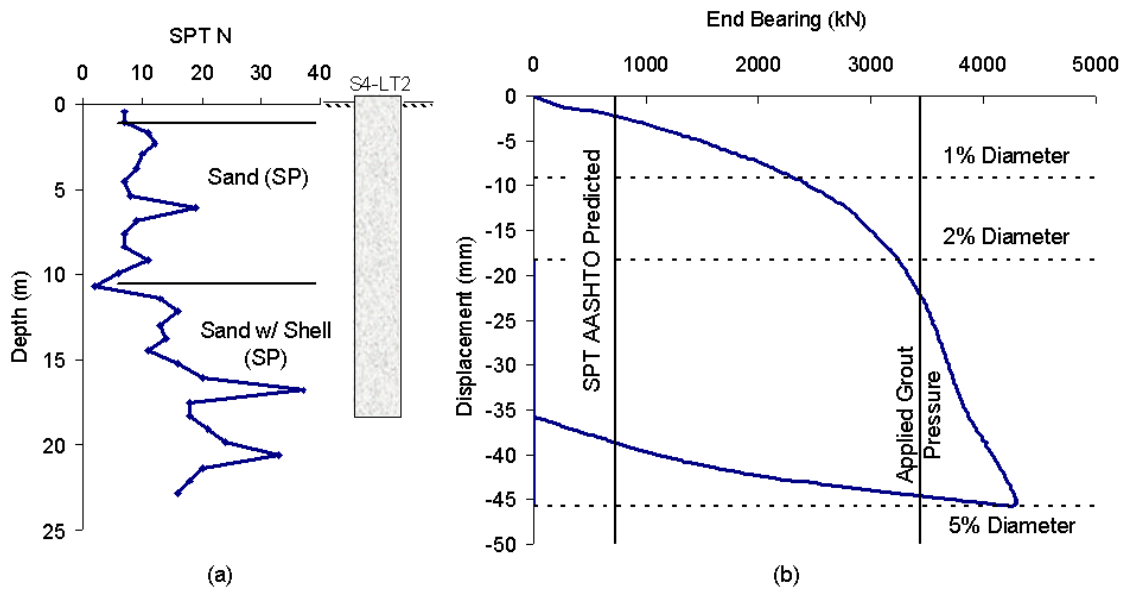
Figure 2.12 Site IV (a) soil boring log and (b) end bearing load test results for test shaft LT-2.

2.5.4 Site V: Houston, TX

Testing at Site V (dense sand) was a collaboration between the University of Houston (UH) and the University of South Florida (USF) to demonstrate to the Texas Department of Tranportation the effectiveness of post grouting drilled shafts in soils native to the Houston region. A total of four 1.22 m (4.0 ft) diameter drilled shafts were constructed. A target load of 17.8 MN (2000 tons) was used in determining the shaft lengths. Two shafts were tipped in sandy soil while the other two shafts were tipped in clayey soil. Each pair of test shafts included a control shaft and a grouted shaft. The subsurface investigation of the test site was performed using three primary methods of exploration: Standard Penetration Tests, SPT; Texas Cone Penetration Tests, TCP; and Cone Penetration Tests, CPT. All shafts were constructed using mineral slurry. Figure 2.13 shows the SPT soil boring and load test results for test shaft S-2 (tipped in sand and grouted). A full geological and load test discussion for this site can be found in Mullins and O'Neill (2003).
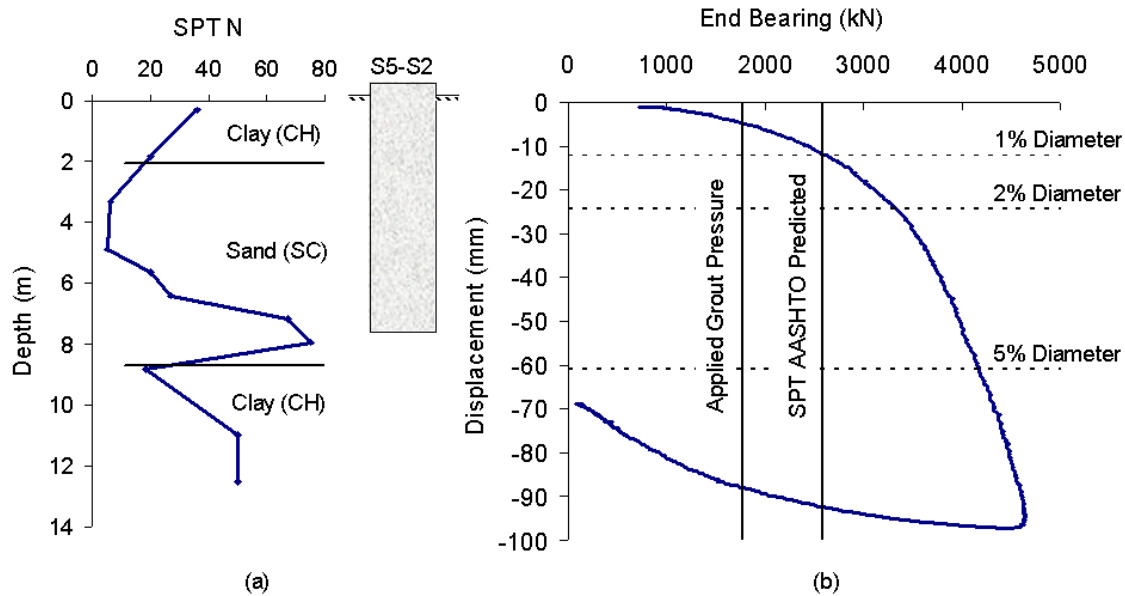
Figure 2.13 Site V (a) soil boring log and (b) end bearing load test results for test shaft S-2.

25

2.6 End Bearing Results

Many design methodologies exist for the calculation of drilled shaft tip capacities in sandy soils. For example, AASHTO (1999) presents four methods from which this determination can be made. These methods vary in the required parameters but use either SPT N values, the relative density state, and/or the depth of embedment expressed as a multiple of the diameter to calculate the end bearing capacity. An important aspect of this capacity determination is the displacement at which the capacity will be developed. Some methods clearly state this criterion as a percentage of the shaft diameter or as some service limit displacement (e.g. 5% of D, or 1"). while other methods do not.

This research project used the Reese and O'Neill (1988) method (Eq. 4) to predict the ultimate end bearing capacity from SPT values as well as load test data. Table 2.2 provides details from each of the full-scale grouted test shafts expressed as a multiple of the Reese and O'Neill predicted capacity. The end bearing improvement is given in terms of the tip capacity multiplier, TCM, for the measured end bearing at 1, 2, and 5%D displacements. As the end bearing improvement is dependent on the applied grout pressure, the grout pressure is also listed both dimensionally (in kPa) and non-dimensionally (as the Grout Pressure Index). The Grout Pressure Index (GPI) is defined as a non-dimensional ratio of the applied grout pressure to the ungrouted end bearing at a displacement of 5%D (Eq. 4). The applied grout pressure was taken as the maximum sustained grout pressure and not a short duration pressure spike.

2.7 Design of Post-Grouted Tip Capacity

To quantify the improvement with respect to standard design practice, a predictive approach was established on the basis of the TCM and the GPI. The TCM was defined as a function of displacement and grout pressure. By plotting the results from Table 2.2 (Figure

26

2.14), a surface can be defined that incorporates both the effects of grout pressure and permissible displacement (Figure 2.15). Dashed lines in Figure 2.15 show lines of constant TCM while solid lines show lines of constant displacement and grout pressure.

Table 2.2 Full-scale field study results.

Shaft I.D.	$q_{p\ Ultimate}$* (kPa)	Grouted Capacity TCM			Applied Grout Pressure (kPa)	GPI
		1%D	2%D	5%D		
S1-FJ1	574	1.22	1.50	1.79	586	1.02
S1-FJ2	574	1.21	1.67	1.91	462	0.80
S1-SP1	287	3.48	4.44	5.51	1138	3.96
S1-SP2	287	3.09	4.06	6.18	1220	4.25
S2-FJ	344	1.69	2.58	4.18	683	1.98
S2-TM	258	3.33	4.72	7.09	862	3.34
S3-LT3	2178	0.60	N/A**	N/A**	3447	1.58
S4-LT2	630	3.15	4.40	5.84	5240	4.68
S5-S2	3969	1.05	1.30	1.63	1517	0.69

*Reese and O'Neill (1988) (Eq. 4).
**Unable to fully mobilize test shaft during testing (see Figure 2.11).

27
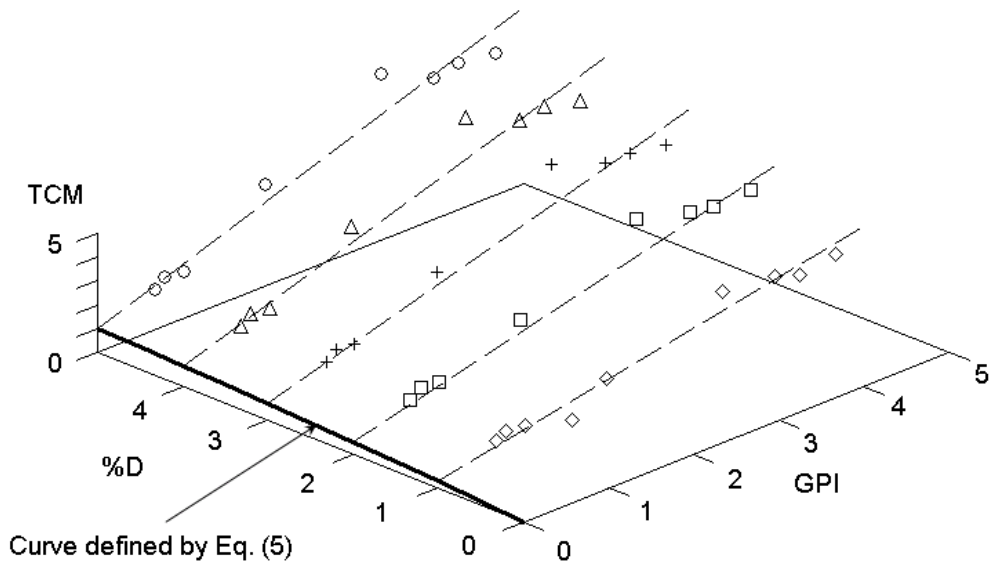
Figure 2.14 Full-scale field study results.
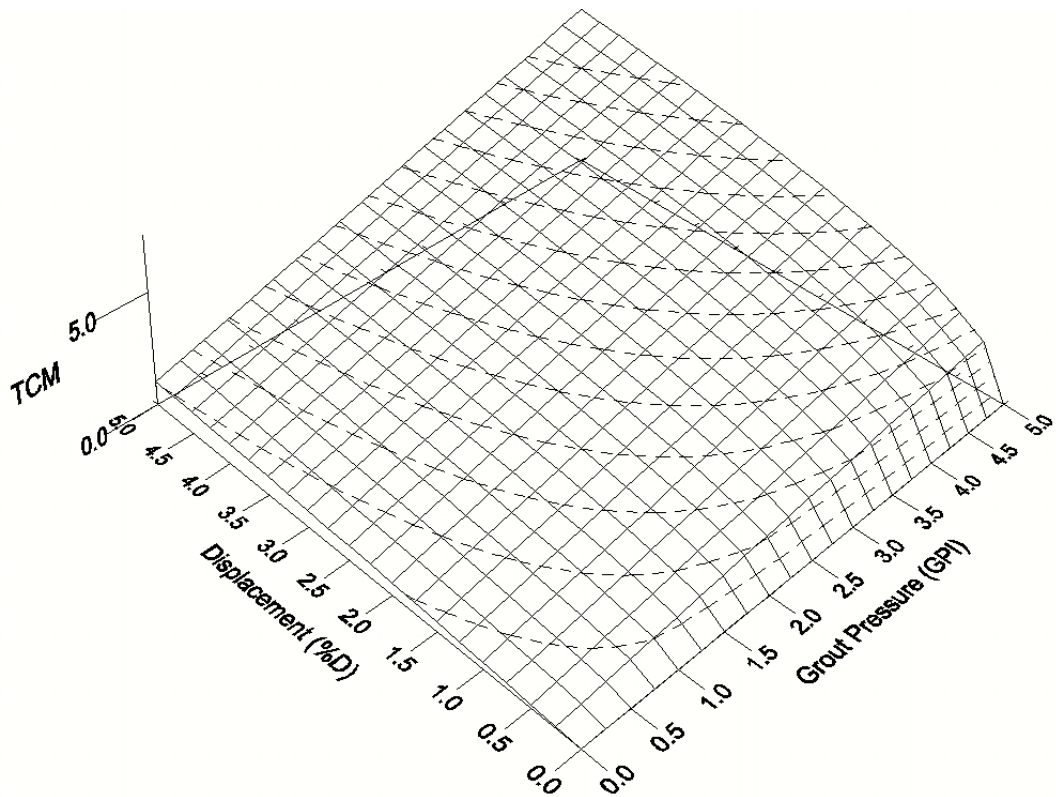
Figure 2.15 Surface defined by TCMs derived from load test data dependent on grout pressure and displacement.

The plane defined by the displacement and TCM axes intersects the surface forming a hyperbolic relationship identical to the centerline trend that Reese and O'Neill published in 1988 shown in Figs. 2.3 and 2.14. Therein, when the GPI = 0 no improvement is expected and it therefore predicts the same capacity as an ungrouted shaft. Likewise, when the permissible displacement approaches zero, so does the predicted mobilized capacity. A more usable form of this surface is given in Figure 2.16 which shows the TCM contours. Given the GPI and displacement, the TCM can be estimated using Figure 2.16 or with the following empirical relationship:

$$TCM = 0.713(GPI)(\%D^{0.364}) + \frac{\%D}{0.4(\%D) + 3.0} \qquad (6)$$
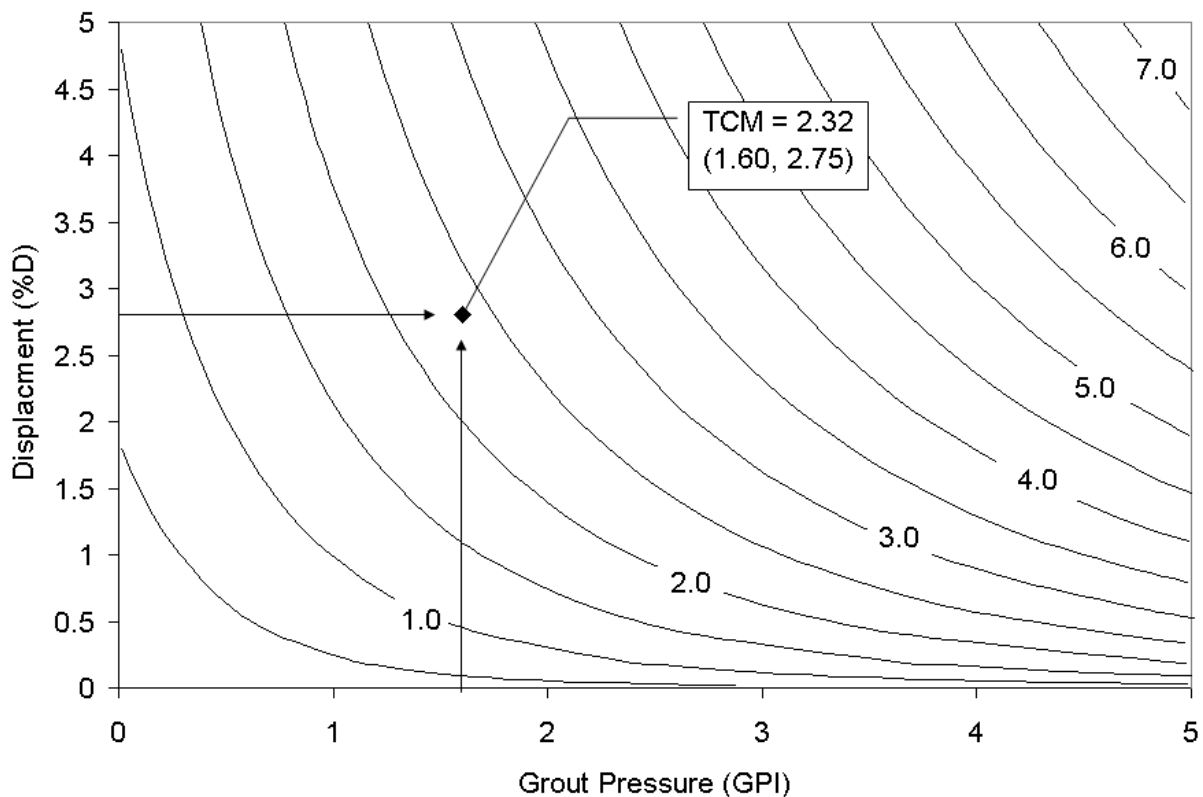
Figure 2.16 TCM contours easily adapted for design applications.

29

The surface defined by Figure 2.15 is non-linear with respect to %D but linear with respect to variations in GPI. As the GPI and the TCM are both ratios based on the ungrouted end bearing, both the TCM and GPI increase or decrease similarly dependent on the ungrouted end bearing selected. Therefore, the TCM is only mildly affect by the method of determining the ungrouted end bearing. At high GPI values and low %D values, the TCM is insensitive to the ungrouted prediction method. As GPI approaches zero, the grouted end bearing approaches the ungrouted capacity and therefore is subject to the conservatism or un-conservatism associated with whatever method was used to estimate the ungrouted capacity.

2.8 Design Procedure

For a given shaft diameter and embedment length, the method for estimating the unit end bearing of grouted shafts involves the following steps:

1.   Calculate the ungrouted end bearing capacity at 5%D displacement, $q_{p\ Ultimate}$.

2.   Calculate the ultimate side shear resistance, F_s, for the total length of embedded shaft.

3.   Divide the ultimate side shear resistance by the cross-sectional area, A, of the shaft to determine the maximum anticipated grout pressure, GP_{max}.

$$GP_{max} = \frac{F_s}{A} \tag{7}$$

4.   Calculate the Grout Pressure Index, GPI, as the ratio of the maximum anticipated grout pressure (Step 3) to the ungrouted unit tip resistance (Step 1).

$$GPI_{max} = \frac{GP_{max}}{q_{p\_Ultimate}} \tag{8}$$

5.   Establish the maximum permissible service displacement as a ratio of the shaft diameter, *%D*.

30

6. Determine the Tip Capacity Multiplier given the Grout Pressure Index (Step 4) and the permissible displacement (Step 5) using Figure 2.16 or Eq. (6).

7. Estimate the grouted unit tip resistance as the product of the Tip Capacity Multiplier (Step 6) and the ultimate ungrouted end bearing capacity (Step 1).

$$q_{grouted} = (TCM)(q_{p\_Ultimate}) \tag{9}$$

For example, a 0.91 m (3 ft) diameter drilled shaft with an ultimate side shear resistance of 1780 kN (200 tons) will have a grouted end bearing capacity of 3.97 MPa (41.8 tsf). This is with a permissible shaft displacement of 25 mm (1 in) and a ungrouted end bearing capacity of 1.71 MPa (18 tsf) using Eq. 4 (N = 30).

2.9 Summary and Conclusions

A rational method of predicting the end bearing capacity of post grouted shafts tipped in cohesionless soils has been developed based on the performance of full scale grouted shaft load tests. The new approach incorporates input parameters such as the service displacement criteria, the attainable grout pressure, and the estimated conventional ungrouted shaft end bearing. Unlike conventional shaft construction and the associated quality assurance methodologies, each and every shaft is tested via the grouting process. Inherently, the grouting then provides quantitative data on the skin friction and end bearing capacity of each shaft. Therefore, grouting verifies a lower limit of total shaft capacity that equals two times the grout pressure acting over the entire tip area. The actual capacity, which is predicted using Eq. 9, is somewhat higher due to an increase in the mobilized end bearing during downward structural loading and the ~30% increase in side shear from downward instead of upward movement (O'Neill 2002).

As the attainable GPI relies on the side shear capacity on which the grout pressure can react, the aspect ratio (embedment length / diameter) of the drilled shafts should be carefully

31

considered in order to provide the most cost efficient design. Note that potentially stringent lateral loading conditions may govern the foundation design, and may further define the shaft geometry that best supplies the capacities required (both axial and lateral). The methodology presented herein only addresses axial capacity.

The use of grouted shafts has long reaching implications with regards to the state of drilled shaft construction and design. This stems from the unparalleled quality assurance that accompanies the process. Shaft lengths can be reduced and an associated cost savings realized. Further, by statically grout testing each shaft, an increased resistance factor (or lower safety factor) may likely result for shafts constructed in this fashion. Such an increase in the resistance factor can lead to additional economy.

2.10 References

AASHTO, LRFD Bridge Design Specifications, SI (1st Edition). (1999), American Association of State Highway and Transportation Officials, Washington, D.C.

Bolognesi, A. J. L. and Moretto, O. (1973) "Stage Grouting Preloading of Large Piles on Sand" Proceedings of 8th ICSMFE, Moscow.

Bruce, D.A. (1986), "Enhancing the Performance of Large Diameter Piles by Grouting," Parts 1 and 2, Ground Engineering, May and July, respectively.

Bruce, D. A., Nufer, P. J., and Triplett, R. E. (1995) " Enhancement of Caisson Capacity by Micro-Fine Cement Grouting - a recent case history" ASCE Special Publication 57, Verification of Geotechnical Grouting.

Dapp, S. D. (2002). "Pressure Grouting of Drilled Shafts in Sands." Ph.D. Dissertation, University of South Florida, Tampa, Florida.

Dapp, S. and Mullins, G. (2002). "Pressure-Grouting Drilled Shaft Tips: Full-Scale Research Investigation for Silty and Shelly Sands." Deep Foundations 2002: An International Perspective on Theory, Design, Construction, and Performance, ASCE Geo Institute, GSP No. 116, Vol. I, pp. 335-350.

Dapp, S.D. (1998). "Interviews with engineers during load testing on the My Thuan Bridge." Mekong Delta, Vietnam.

Flemming, W. G. K. (1993) "The Improvement of Pile Performance by Base Grouting" Proceedings of the Institution of Civil Engineers, London.jm

Frederick, E. M. (2001). "Pressure Grouting Drilled Shaft Tips: Laboratory Scale Study in a Frustum Confining Vessel." Master's Thesis, University of South Florida, Tampa.

Gouvenot, D. and Gabiax, F. D. (1975), "A New Foundation Technique using Piles Sealed by Concrete Under High Pressure," Proceedings, Seventh Annual Offshore Technical Conference.

Mojabe, M.S. and Duffin, M. J. (1991) "Large Diameter, Rock Socket, Base Grouted Piles in Bristol" Proceedings of the 4th International Conference on Piling and Deep Foundations, Stresa, Italy, April

Mullins, G. (1999). "Interviews with engineers during load testing on the Taipei Financial Center." Taipei, Taiwan.

Mullins, G., Dapp, S., Frederick, E., and Wagner, R. (2001). "Pressure Grouting Drilled Shaft Tips - Phase I Final Report." Final Report submitted Florida Department of Transportation, December.

Mullins, G., Dapp, S., and Lai, P. (2000). "New Technological and Design Developments in Deep Foundations, Pressure-Grouting Drilled Shaft Tips in Sands." American Society of Civil Engineers, Denver, Colorado.

Mullins, G. and O'Neill, M. (2003). "Pressure Grouting Drilled Shaft Tips - A Full-Scale Load Test Program." Research Report, University of South Florida, Tampa, Florida, May.

Mullins, G. and Winters, D. (2004). "Post Grouting Drilled Shaft Tips - Phase II Final Report." Final Report submitted Florida Department of Transportation, June.

Mullins, G., Winters, D., and Dapp, S. (2006). "Predicting End Bearing Capacity of Post Grouted Drilled Shafts in Cohesionless Soils" ASCE Journal of Geotechnical and GeoEnvironmental Engineering, Vol. 132, No. 4. pp. 478-487.

O'Neill, M.W. (2002). Discussion of "Side Resistance in Piles and Drilled Shafts," Journal of Geotechnical and Geoenvironmental Engineering, Vol.127, No. 1, pp. 3-16.

Piccione, M., Carletti, G., and Diamanti, L. (1984) "The Piled Foundations of the Al Gazira Hotel in Cairo" Proceedings of the International Conference on Advances in Piling and Ground Treatment for Foundations, Institution of Civil Engineers, London, UK.

Reese, L.C. and O'Neill, M.W. (1988) "Drilled Shafts: Construction and Design." FHWA, Publication No. HI-88-042.

Santosuossa, M., Rizzi, G., and Diamanti, L. (1991) "Construction of Pile Foundation of the Postal Citadel in the Direction Center of Naples" Proceedings of the 4th International Conference on Piling and Deep Foundations, Stresa, Italy, April.

Sliwinski, Z. J., and Flemming, W. G. K. (1984) "The Integrity and Performance of Bored Piles" Proceedings of the International Conference on Advances in Piling and Ground Treatment for Foundations, Institution of Civil Engineers, London, UK.

Troughton, V. M. and Platis, A. (1989) "The Effects of Changes in Effective Stress on a Base Grouted Pile in Sand" Proceedings of the International Conference on Piling and Deep Foundations, London, UK, May.

34

CHAPTER 3 THERMAL INTEGRITY PROFILING OF CONCRETE DEEP FOUNDATIONS[2]

Post construction inspection of deep cast-in-place concrete foundations relies largely on non-visual techniques dealing with measured concrete quantities, acoustic wave speed or frequency, gamma radiation attenuation and now the internal temperature of the curing concrete. The latter has been shown to provide information about the concrete cover, foundation shape, cage alignment, and concrete mix design performance. This chapter discusses the thermal concept, test methods, analysis, and a brief case study comparing thermal results with other test methods.

3.1 Introduction

Curing cementitious materials within concrete react exothermically during hydration to produce large amounts of heat energy. This energy has historical been cause for concern with regards to mass concrete effects and thermal induced cracking where the differential temperature within the concrete must be less than 35 to 40ºF depending on the specification. More recently, further concerns over delayed ettringite formation have resulted in more stringent restrictions in the peak core temperature that will be accepted, e.g. less than 180ºF (FDOT, 2010). This energy is actually quite remarkable and now useful; as a point of reference, a typical 9 CY concrete truck contains the same energy as 400-500 lbs of trinitrotoluene, TNT, depending on the cement content. Clearly the difference is the time frame over which the energy is released (days vs. split

---

[2] This chapter was published in Proceedings Geo-Construction Conference / ADSC Expo 2012 (Winters and Mullins, 2012). Permission is included in Appendix A.

second). Thermal integrity profiling is a technique used to evaluate the soundness of concrete on the basis of measurements of internal temperature stemming from the hydration energy.

3.2 Background

Methods to assess the integrity of drilled shafts and similarly constructed concrete foundations have been developed to combat the blind nature of the construction process. Above ground concrete structures have the luxury of visual inspection coupled with routine cylinder breaks. In such cases, anomalous findings such as those shown in Figure 3.1 are easily detected and the cause dealt with appropriately (Mullins and Ashmawy, 2005). Below ground, very little of a shaft is usually visible short of the upper region that might be exposed for footing construction.

Figure 3.1 Soft concrete visually identified (left); full anomalous extent removed (right).

36

In cases where concreting logs indicate an incorrect placement volume (less than theoretical), simple surface excavation might reveal the problem, lead to full exhumation, or installation of a nearby supplemental shaft. Visual inspection alone does not verify concrete quality, it just helps identify problems. Figure 3.2 shows shafts exposed to find visually intact and visually deficient cases. Unfortunately, the visually intact shaft required a supplement shaft due to poor concrete quality (discussed later).

Figure 3.2 Visually intact shaft (left); visually deficient shaft (right).

The most common non-destructive test methods of assessing shaft integrity use: acoustic waves sent between access tubes to check the concrete between tubes (Figure 3.3 white lines); or gamma radiation reduction to check the density of the material immediately surrounding the access tubes (zone shown as blue circles). Alternate single-tube acoustic methods have similar coverage to the gamma radiation method.

Figure 3.3 Testing coverage from acoustic (lines) and gamma radiation (circles) methods.

The outer most concrete forms the bond between the reinforcing cage and the bearing strata, provides a durable cover to protect the steel from corrosion, and contributes the most to the structural moment of inertia of the section. In each case, the most important concrete in the shaft goes largely untested. The thermal test method detects loss of section or cement content both inside and outside the reinforcing cage.

3.3 Thermal Integrity Principles

Like acoustic and gamma radiation methods, thermal integrity profiling identifies abnormalities relative to the rest of the shaft. In general, regions that are measured to be cooler imply less concrete (necks or inclusions) and those that measure warmer than the rest of the shaft indicate more concrete or bulges (Mullins, 2010). A normal temperature distribution in a shaft

38

and the surrounding soil is shown in Figure 3.4. The warmest temperatures occur at the shaft center, coolest concrete is at the edges, and elevated temperature extends into the surrounding soil. The location of the access tubes (shown as blue disks) coincides with the steepest part of the temperature versus shaft radius relationship. This makes the measured temperature sensitive to cage eccentricity.
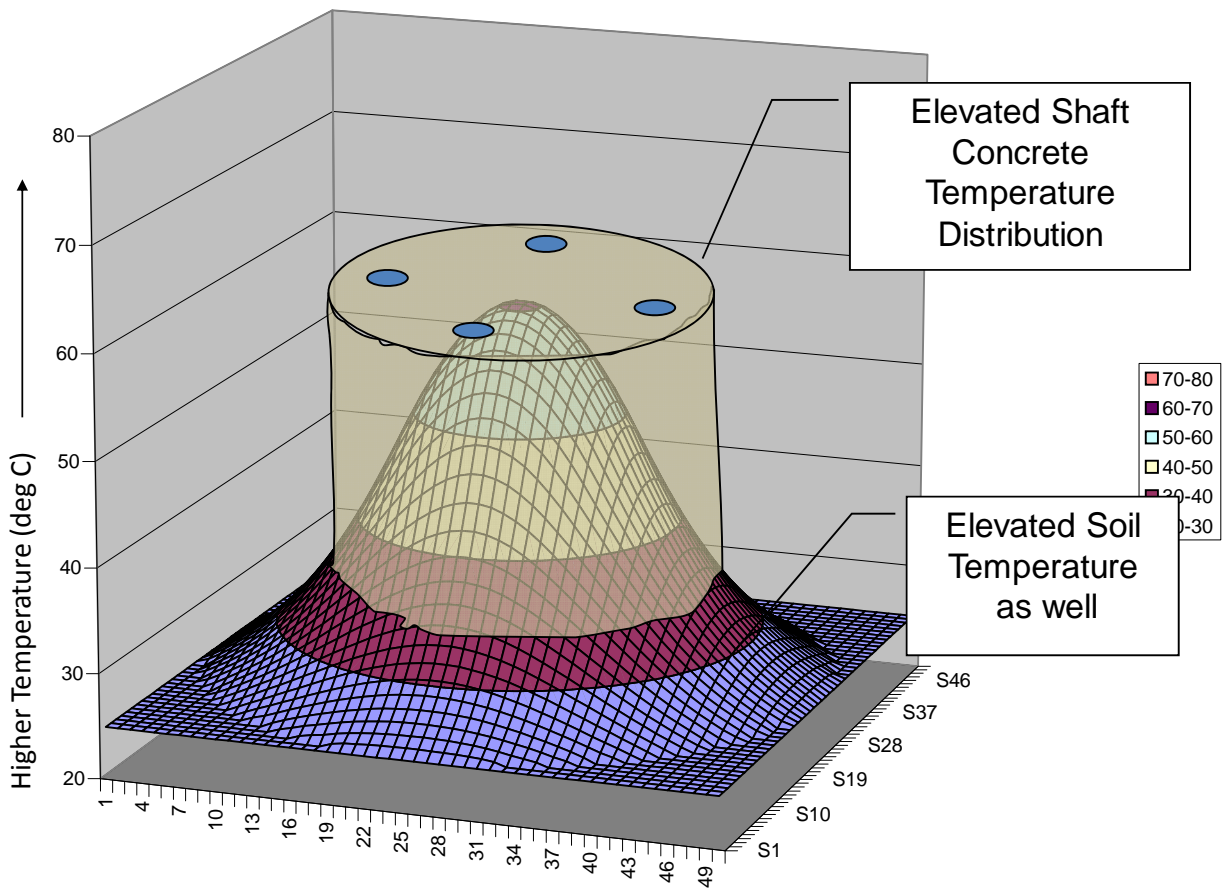
Figure 3.4 Normal temperature distribution within a curing shaft and the surrounding soil.

3.3.1 Cage Alignment

When the cage is shifted from centered, the side of the cage closer to the shaft center becomes warmer and the opposite side becomes cooler (closer to the edge of shaft). Figure 3.5 shows an example this phenomenon where the centered cage temperature is roughly 150ºF; when

the cage moves to the right (in this case 4 inches), opposite side temperature measurements increase or decrease accordingly (again in this case ±10ºF or 2.5ºF/in).

Figure 3.6 shows thermal profiles from two 4 ft diameter shafts (4 access tubes) that exhibited different cage offsets. The average of all tube temperatures (red) corresponds to the centered cage temperature and provides a direct indication of average shaft shape. With the exception of the most obvious cage offsets, temperature between tubes varied no more than 2 or 3ºF from the average at that depth. However, on the left, Tubes 2 and 4 from 22 to 30 ft show roughly equal and opposite variations (up to ±8ºF) from the overall shaft average where the other tubes 1 and 3 stay mostly centered about that axis. On the right, the cage remains mostly centered down to 25 ft where Tubes 3 and 4 become 10ºF cooler than 1 and 2. In this case, the cage pushed upward approximately 3 to 5 ft during concreting and was forced back down.
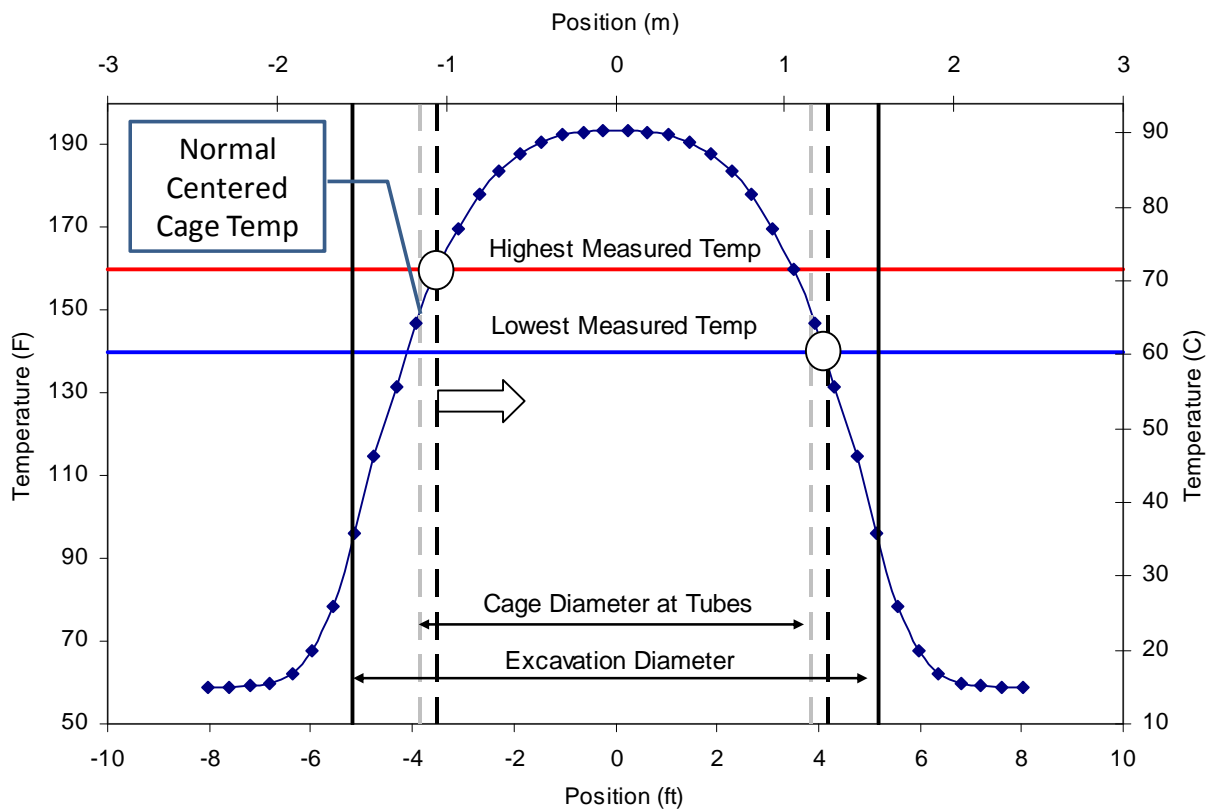
Figure 3.5 Effect of cage eccentricity on measured temperature at the cage.

40
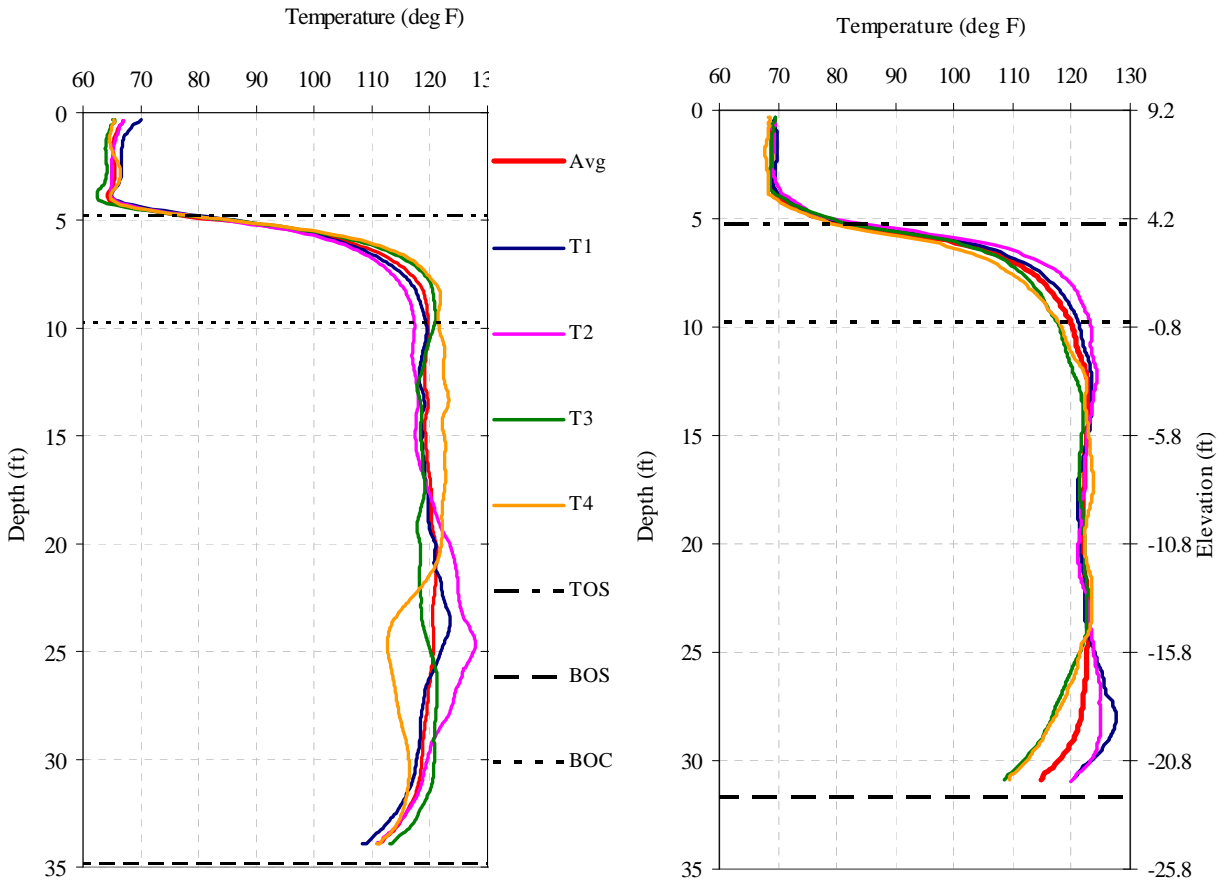
Figure 3.6 Typical cage offset for two different shafts.

3.3.2 End Effects

Typical of thermal profiles is a reduction in temperature as the measurements approach the ends of shaft. This portion of the shaft dissipates temperature in both radial and longitudinal modes whereas the body of the shaft dissipates in a purely radial manner. In this way, a normal shaft should exhibit temperature reduction near the bottom of the reinforcing cage unless the shaft has been over-excavated and/or the cage is hanging high above the shaft bottom. The effect of end conditions can be left in place to help identify normal end effects or can be removed mathematically using known thermal diffusion functions. The latter is useful when converting measured temperature to shaft radius.

41

3.3.3 Temperature to Radius Conversion

Concreting logs (or concrete yield plots) are perhaps the most important shaft inspection tool. Therein, weighted measuring tapes are routinely used to track the rising concrete level as subsequent truck loads of concrete are placed. In some states these are converted to average diameter per truck and in others the concrete level is compared to expected level for that volume and an idealized diameter of shaft. As the measured temperature is dependent on cover and thus the shaft diameter, it has been shown that direct correlations from temperature to shaft diameter (or radius) can be developed using concreting information (Mullins and Winters, 2011). Figure 3.7 shows a case where a significant over-pour was noted by inspection records and the information was converted to shaft diameter per truck. When compared to the average temperature measured from each of 7 access tubes a clear relationship can be established and used to produce a 3-D rendering of the shaft shape.

3.4 Field Testing Equipment

Thermal integrity profiling can be performed using a reusable thermal probe lowered into standard access tubes or by installing thermal wires into the reinforcing cage (in conjunction with or in lieu of access tubes). Figures 3.8 and 3.9 show the basic equipment types used for the two field testing methods. When using the thermal probe, a single set of profiles are taken from each tube at a time near or after the peak temperature. The beginning of the testing window is determined by the concrete mix design and the cement and flyash constituent compositions. The time of testing is usually 1 to 2 days after casting but extends to at least the number of days expressed in feet of shaft diameter (e.g. 4 ft shaft can be tested from 1 to 4 days after concreting). Tubes need not be filled with water for thermal testing, but often are to accommodate all other methods of testing that require it.

42
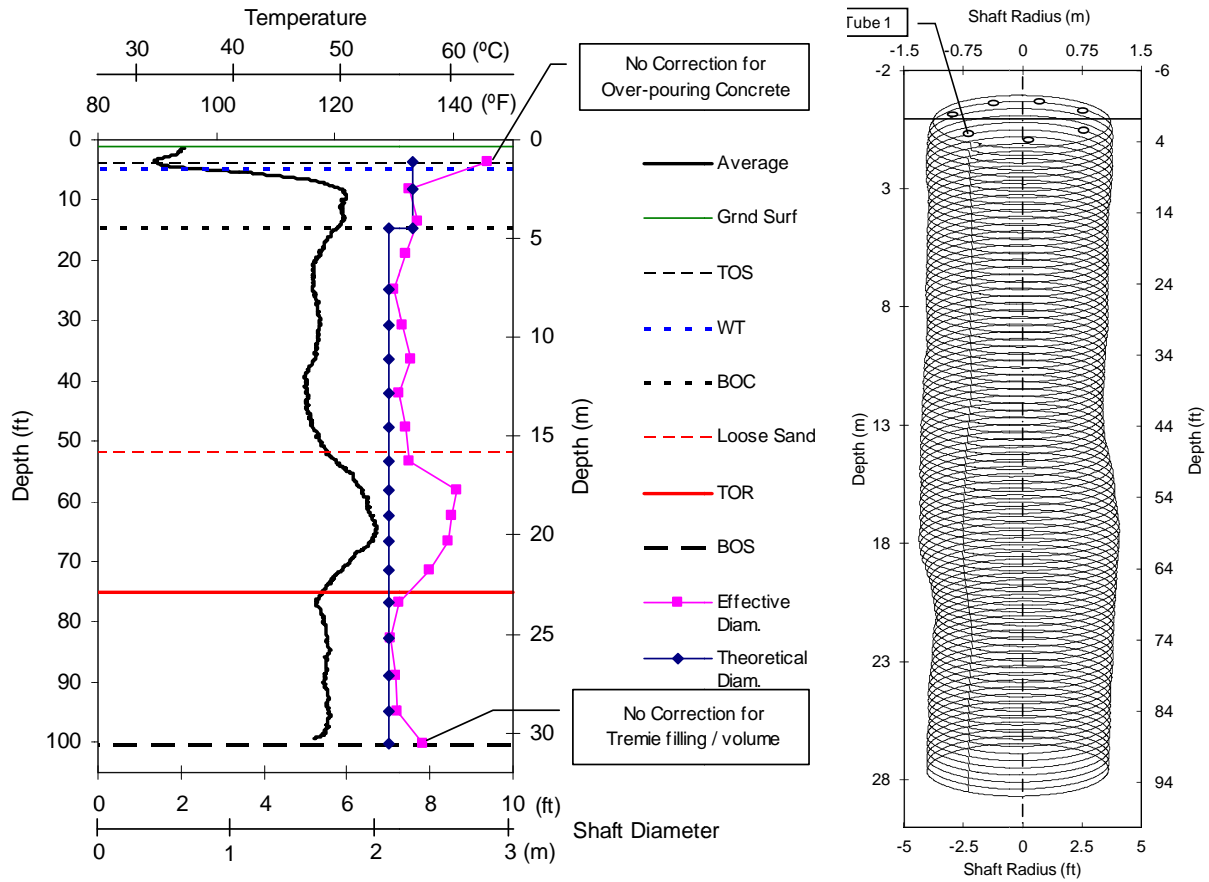
Figure 3.7 Average shaft temperature compared to field recorded average shaft diameter.

Figure 3.8 Thermal profiling using the thermal probe method (probe shown separately).

43

When using the thermal wire method, individual data collectors are attached to the top of each thermal wire shortly after concreting. The data collectors continue to take data at user prescribed intervals (e.g. 15 min.) until retrieved. The peak temperature and hence the optimal time of testing is automatically obtained despite scheduling obstacles. Both methods can provide results of shaft acceptability one to two days after casting.

Figure 3.9 Thermal profiling components using the thermal wire method.

3.5 Case Study

The shaft shown in Figure 3.2 required a supplemental shaft to be installed alongside due to poor concrete quality. The shaft (shown again in Figure 3.10) registered lower than expected temperature throughout the upper 15 ft but did not cross the local 30% wave speed reduction threshold for acoustic testing (CSL). As a result, gamma radiation testing (GGL) was requested to provide further insight and either dispel or confirm the thermal results.

Gamma testing showed increased gamma count rates in the upper portion of the shaft and was denoted as bad to questionable, but no correlation to density was performed making the result only qualitative. Figure 3.11 shows the results from CSL and GGL testing and both indicate anomalous results from elevation 0 to -5 ft; perhaps qualitatively down to -10 ft when looking at the GGL trends. However, as the shaft had already been replaced with an adjacent shaft, the shaft was cut off and cored both above and below the cut location. The location of the cut is shown in Figure 3.10 where the cover was removed by jack hammer to expose the steel.
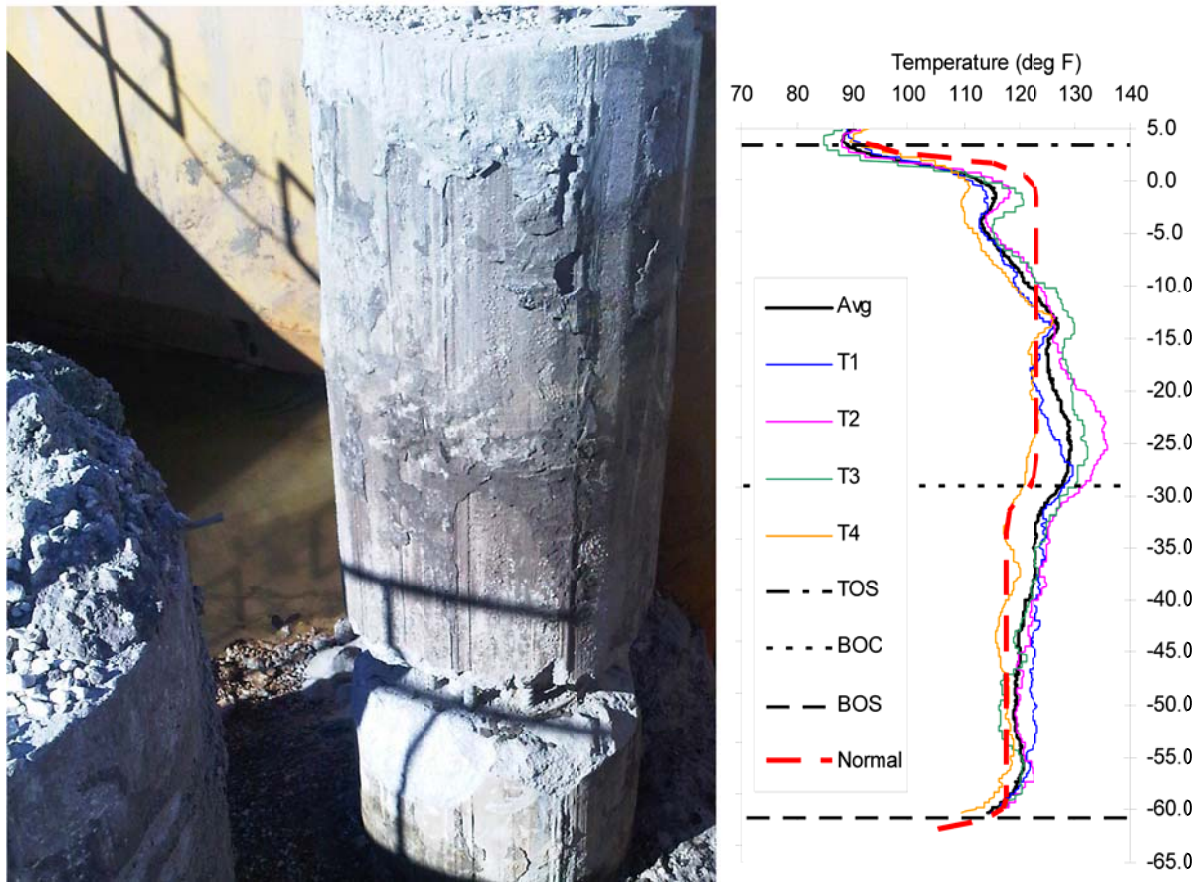
Figure 3.10 Visually intact shaft that was flagged as anomalous by thermal testing.
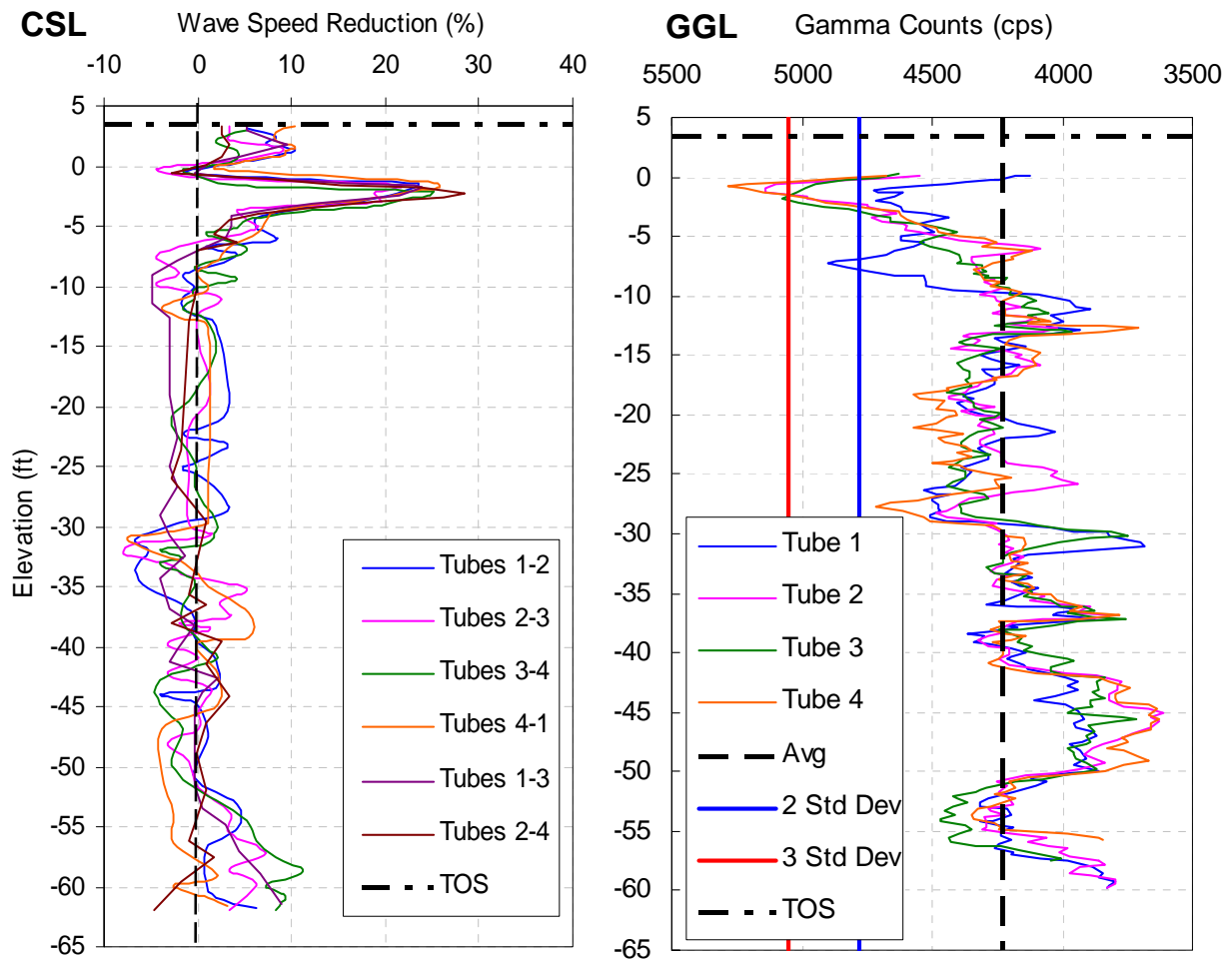
Figure 3.11 Acoustic and gamma radiation test results.

Subsequent compressive strength tests of the cores showed over 50 percent of the cores did not achieve the 4 ksi design strength, over 80 percent did not achieve the 28 day strength, and only two samples reached the 56 day strength; compression tests were performed 182 days after concreting (Likins and Mullins, 2011). Figure 3.12 shows the relative depth of the samples and the measured compression strength for the 42 test specimens. Samples were equally taken from both inside and outside the cage.
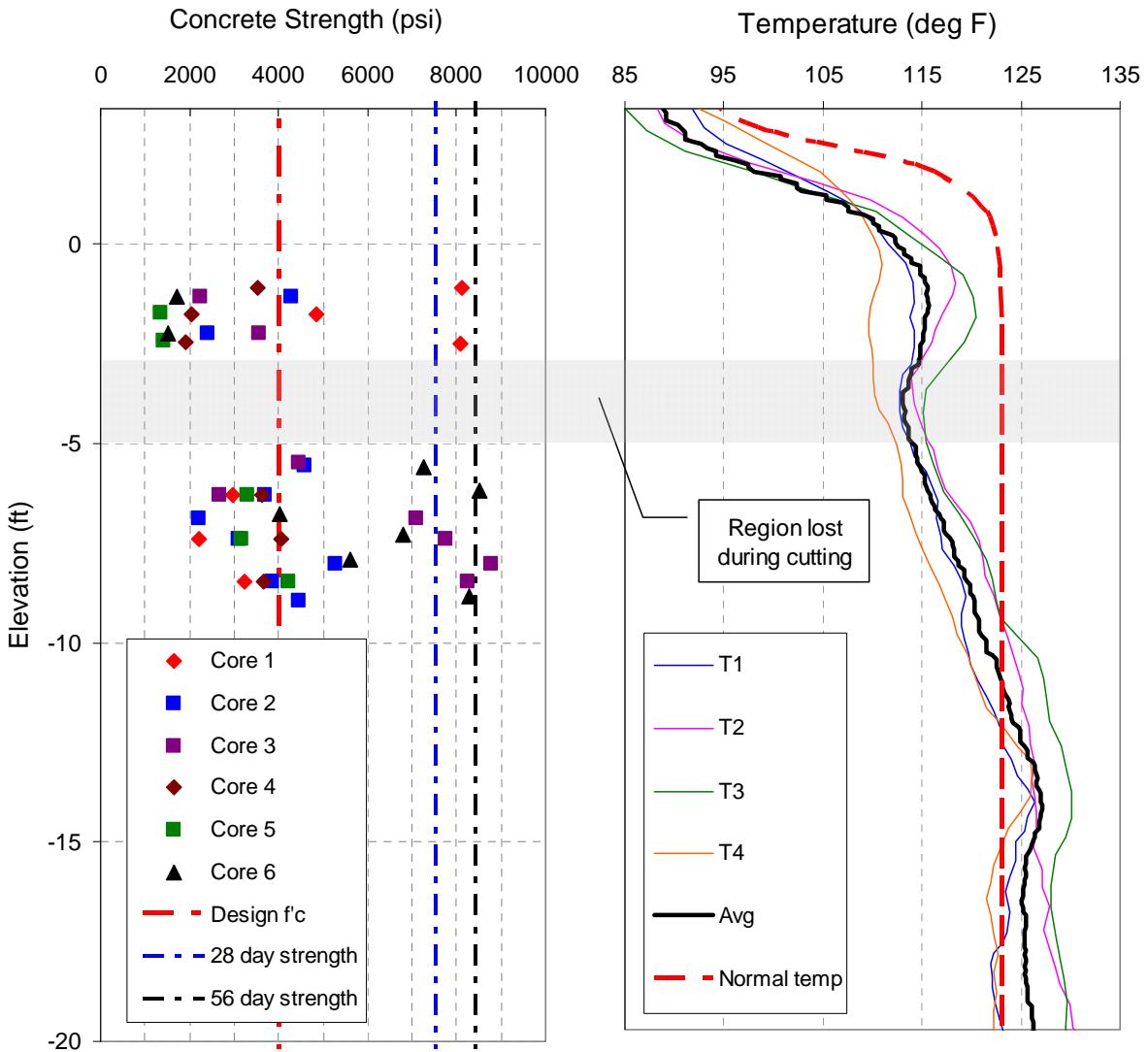
Figure 3.12 Results of compression tests on cored concrete samples.

3.6 Conclusions

The use of thermal integrity profiling adds to the arsenal of testing approaches presently accepted by offering additional insight into the intactness of concrete deep foundations such as drilled shafts. Field testing can use either a thermal probe in access tubes or full length thermal wires tied to the cage and embedded into the concrete. Measurements are sensitive to cage alignment, concrete cover, shaft radius and can detect anomalies both inside and outside the reinforcing cage. The zone of detection is limited only by the size of anomaly. Therein, large

anomalies are detected at multiple tubes (or wires); smaller anomalies are detected by the closest tubes or wires. However, as a reference, a 10% section loss or inclusion will be detected at multiple tubes or wires. The number or access tubes or thermal wires to be used is the same as CSL or GGL but in cases of large diameter shafts, fewer tubes have been shown to be just as effective.

3.7 References

FDOT (2010). "Standard Specifications for Road and Bridge Construction – 2010," Florida Department of Transportation, Tallahassee, FL.

Likins, G. and Mullins G. (2011). "Structural integrity of drilled shaft foundations by thermal measurements" Structural Engineering & Design, www.gostructural.com.

Mullins, G., and Ashmawy, A. (2005). "Factors Affecting Anomaly Formation in Drilled Shafts," Final Report, FDOT Project BC 353-19, March, 293 pp. (original source Dan Brown, P.E., Ph.D.)

Mullins, G. (2010) "Thermal Integrity Profiling of Drilled Shafts," DFI Journal, Deep Foundations Institute, Vol. 4, No. 2, December, pp 54-64.

Mullins, G. and Winters, D. (2011) Infrared Thermal Integrity Testing, Quality Assurance Test Method To Detect Drilled Shaft Defects, WSDOT Project WA-RD 770.1, 175 pp.

Winters, D. and Mullins, G. (2012). "Thermal Integrity Profiling of Concrete Deep Foundations." Geo-Construction Conference Proceedings, San Antonio, TX, pp. 155-165.

CHAPTER 4 COMPARATIVE STUDY OF THERMAL INTEGRITY PROFILING WITH OTHER NON-DESTRUCTIVE INTEGRITY TEST METHODS FOR DRILLED SHAFTS[3]

Integrity testing of drilled shafts and similarly constructed concrete foundations has evolved to combat the blind nature of the construction process and to increase quality assurance. The more popular methods include cross-hole sonic logging (CSL), gamma-gamma logging (GGL), and more recently thermal integrity profiling (TIP) and sonic caliper. Thermal Integrity Profiling, developed at the University of South Florida in the mid-1990s, utilizes the heat of hydration of curing concrete to evaluate the integrity of drilled shaft foundations. Comparing the results of the different test types is difficult due to the varied nature of the different tests. This chapter looks at various shafts constructed across the nation which were tested with thermal and at least one other method. When compared to CSL and GDL test results, TIP agreed with 4 of 6 cases for CSL and 2 of 5 cases for GDL. In the one case were both sonic caliper and inclination data were available, TIP showed good agreement.

4.1 Introduction

With concrete being designed to be stronger and more durable, the anticipated service life of concrete structures is increasing to over 100 years. Not only are structures designed to last longer, but they are also designed to handle more load to accommodate the demands of growing civil infrastructures. As such, this requires the foundations to be just as reliable which includes

---

[3] This chapter is in press with the 2014 Geo-Congress: Geo-Characterization and Modeling for Sustainability (Winters, 2014).

www.manaraa.com

durability and strength both structurally and geotechnically (Figure 4.1). The inherent flaw of drilled shafts is the blind construction of these elements, as well as different construction techniques. Testing methods to assess the integrity of drilled shafts and similarly constructed concrete foundations have been developed to combat the blind nature of the construction process. The more popular methods include cross-hole sonic logging (CSL), gamma-gamma logging (GGL), and more recently thermal integrity profiling (TIP) and sonic caliper.
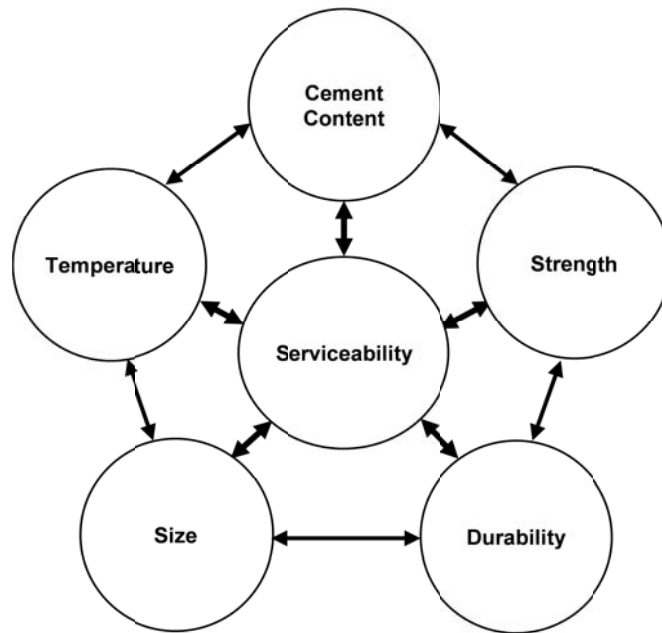
Figure 4.1 Components of drilled shafts to define the serviceability.

4.2 Background

Due to the blind nature of drilled shaft construction and various techniques in construction, multiple tests methods have been developed to evaluate the integrity of the foundation. Non-Destructive Integrity Testing (NDT) of drilled shafts has been around since the early 1970's. NDT is broken into two different techniques: (1) surface and (2) down-hole. Surface techniques rely on stress waves applied to the top of shaft and include the sonic echo test (SET) and the impulse response test (IRT). Both of these methods rely on measuring the

50

reflected response of the stress wave and are analyzed either by time domain or frequency domain. Iskander et al. (2001) points out a number of limitations of these surface techniques which include the inability to determine the size and lateral location of the defect and difficulty of detecting toe anomalies.

Down-hole techniques use access tubes attached to the reinforcement cage to measure the quality of the drilled shaft. These methods include cross-hole sonic logging (CSL), single-hole sonic logging (SSL), cross-hole tomography (CT), gamma density logging (GDL), and thermal integrity profiling (TIP). CSL, SSL, and CT use a transmitter probe and a receiver probe to measure the time an ultrasonic pulse takes to travel from one side to the other. GDL emits gamma rays and measures the backscatter a set distance up from the emitter. The data collected is usually plotted as gamma counts, but can be calibrated and presented as material density.

The most recent development in NDT methods, TIP assesses the presence of intact concrete as well as the alignment of the reinforcement cage. This is accomplished by measuring the heat generated within the shaft during the hydration period. A uniformly-shaped cylinder of uniform concrete mix will produce a temperature signature that is constant with depth (except at the ends) assuming uniform thermal properties of the surrounding soil. When combined with construction and concreting logs, thermal results can be converted into effective radius measurements (Winters and Mullins, 2012). Therein, the effective radius is defined as the amount of intact concrete that would result in the measured temperature. However, an effective radius value less than theoretical can be caused by a complete section loss or a larger radius than predicted with a poorly cemented mixture of concrete and debris. In either case, the absence of heat producing cementitious material can have a detrimental effect on strength and/or durability.

51

The cage alignment can be assessed based on tube temperatures higher and lower than average temperatures and the associated effective radii. As a result tubes on opposite sides of the cage will respond with roughly equal and opposite temperature variations when misaligned. Higher temperatures correspond to tubes closer to the center of concrete while lower temperatures corresponds to tubes closer to wall excavation. Figure 4.2 shows raw temperature measurements, the computed effective shaft radius / effective concrete cover, and cage movement.
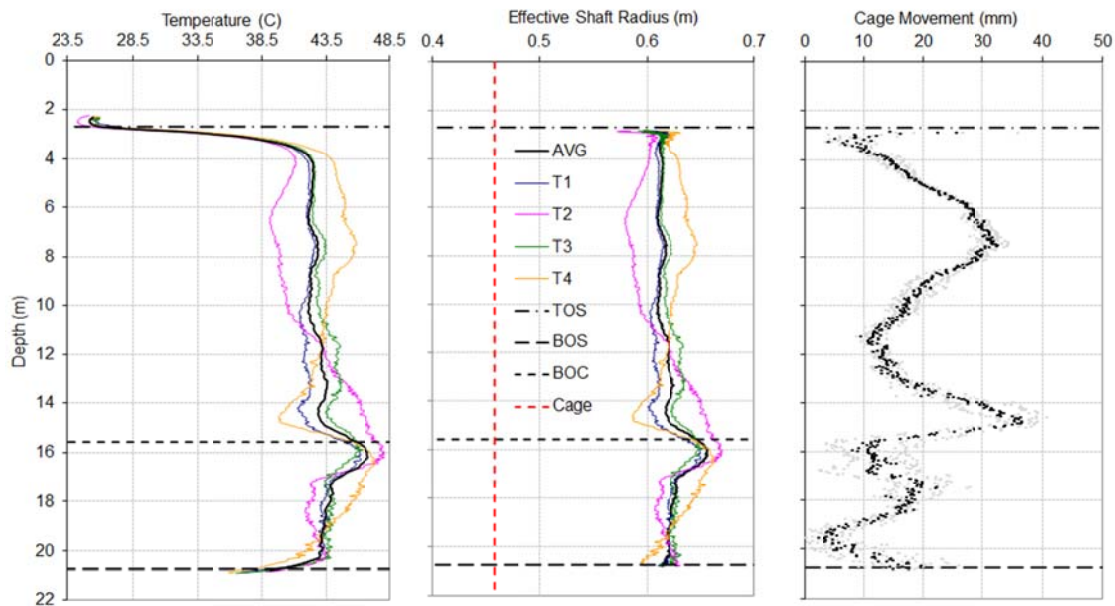
Figure 4.2 TIP results showing measured temp. (left), effective shaft size (center), and cage alignment (right).

Other down-hole methods include the sonic caliper and parallel seismic integrity testing (PSIT). The sonic caliper is a profiling sonar device lowered into the excavation prior to cage placement. PSIT is similar to IRT and SET by using stress waves from the top of the foundation and measuring the arrival times within a borehole adjacent to the shaft. As with any of these methods, the measured values are relative to the overall shaft, except with GDL when calibrated to density. Each NDT method has advantages and limitations (Table 4.1). To overcome some of

52

the limitations of each method, multiple methods can be combined to better define anomalous areas within a drilled shaft (Hertlein, 2001). It is up to the engineer to determine the appropriate NDT method to use based on the information they are trying to obtain (i.e. concrete cover, necks, bulges, concrete durability, etc).

Table 4.1 Non-destructive testing (NDT) methods.

	Length	Diameter	Strength	Durability	Serviceability Score
SET	2	1	2	1	1.50
IRT	2	1	2	1	1.50
CSL	3	1	2	1	1.75
SSL	3	-	1	1	1.25
CT	3	1	2	1	1.75
GDL	3	-	2	2	1.75
TIP	3	2	1	2	2.00
Sonic Caliper*	3	2	-	-	1.25
PSIT	3	-	-	-	0.75

*Note: Measurements made prior to concrete placement, therefore not a direct measure of the as-built shaft.
Code: 3 = Direct Measurement; 2 = Indirect Measurement; 1 = Least Applicable Measurement; - = Not Applicable

Comparing the results of the different test types is difficult due to the varied nature of each test. However, this chapter will look at various shafts constructed across the nation tested with TIP and at least one other method. In keeping with state and federal national security initiatives, the identities of the test sites are not provided.

53

4.3 Case Histories

Very few papers have compared TIP with other NDT methods despite the large number of shafts tested to-date. To compare NDT results, Table 4.2 provides three conditions for TIP, CSL, and GDL. The following is a review of NDT shafts which included TIP testing.

4.3.1 Shaft 1

Likins and Mullins (2011) and Winters and Mullins (2012) discuss probably one of the only shafts that has been tested with multiple NDT methods as well as destructive verification to confirm the quality of the concrete. The shaft was constructed with four steel access tubes with a nominal shaft diameter of 0.9 meters and a length of 19.8 meters.

Table 4.2 Non-destructive testing (NDT) evaluation criteria (after Likins and Mullins, 2011).

Test Method	Good	Questionable	Poor
TIP*	Effective Radius reduction up to 25mm	Effective Radius reduction from 25 to 50mm	Effective Radius reduction 50mm or greater
CSL	Velocity reduction 10% or less	Velocity reduction 11% to 29%	Velocity reduction 30% or greater
GDL	Within 2 standard deviations	Between 2 and 3 standard deviations	Greater than 3 standard deviations

* Note: Cage alignment can cause reduced local effective radius that is not an indication of the overall shaft shape. Therefore, TIP evaluation criteria combines effective radius reduction and cage alignment into the above conditions.

54

The recorded top and bottom elevations for Shaft 1 were +1.02 and -18.99 meters, respectively. Summary of the TIP, CSL, and GDL results are as follows:

TIP concluded the following:

- Tube 1:   Questionable quality from elevation +0.91 to -1.71m

- Tube 2:   Questionable quality from elevation -0.30 to -1.71m

- Tube 3:   Questionable quality from elevation -0.91 to -1.71m

- Tube 4:   Questionable quality from elevation +0.91 to -0.18m

                   Poor quality from elevation -0.18 to -1.52m

                   Questionable quality from elevation -1.52 to -2.47m

CSL concluded the following:

- Tube Pair 1-2:   Questionable quality from elevation -0.32 to -0.99m

- Tube Pair 3-4:   Questionable quality from elevation -0.32 to -0.99m

- Tube Pair 4-1:   Questionable quality from elevation -0.20 to -0.81m

                   Questionable quality from elevation -4.05 to -5.30m

                   Questionable quality from elevation -5.76 to -6.68m

- Tube Pair 2-4:   Questionable quality from elevation 0.53 to 0.26m

                   Questionable quality from elevation -0.26 to -0.93m

                   Questionable quality from elevation -4.18 to -4.69m

                   Questionable quality from elevation -5.21 to -6.28m

                   Questionable quality from elevation -7.96 to -8.87m

                   Questionable quality from elevation -11.16 to -11.43m

GDL concluded the following:

- Tube 1:   Questionable quality from elevation -1.98 to -2.29m

55

- Tube 2:   Questionable quality from elevation 0 to -0.91m

                              Poor quality from elevation -0.15 to -0.46m

- Tube 3:   Questionable quality from elevation 0 to -0.91m

- Tube 4:   Questionable quality from elevation 0 to -0.91m

                              Poor quality from elevation -0.15 to -0.46m

With the results of the three NDT methods, the shaft was rejected and replaced with an adjacent shaft. During excavation for the footing, the shaft in question was visually perfect. This led to the verification of the compressive strength of the concrete within the questionable regions. The shaft was cut-off and concrete cores were taken from both inside and outside the reinforcement cage. Compressive strength tests from the cores showed the following:

- Core 1: Outside the reinforcement cage near Tube 4 from an elevation of -0.33 to -0.76m, the average compressive strength was 48.4MPa with a low of 33.5MPa and a high of 56.0MPa.

- Core 2: Inside the reinforcement cage near Tube 4 from an elevation of -0.33 to -0.75 feet, the average compressive strength was 17.2MPa with a low of 13.1MPa and a high of 24.4MPa.

- Core 3: Inside the reinforcement cage near Tube 3 from an elevation of -0.52 to -0.74m, the average compressive strength was 9.6MPa with a low of 9.2MPa and a high of 9.9MPa.

- Core 4: Outside the reinforcement cage near Tube 4 from an elevation of -1.69 to -2.58m, the average compressive strength was 26.8MPa with a low of 15.2MPa and a high of 36.3MPa.

- Core 5: Inside the reinforcement cage near Tube 4 from an elevation of -1.70 to -2.69m, the average compressive strength was 46.5MPa with a low of 27.7MPa and a high of 58.7MPa.

- Core 6: Inside the reinforcement cage near the center of the shaft from an elevation of -1.67 to -2.58m, the average compressive strength was 44.9MPa with a low of 18.5MPa and a high of 60.6MPa.

Over 50 percent of the cores did not achieve the 27.6MPa design strength with a low of 9.2MPa, over 80 percent did not achieve the 28 day strength, and only two samples reached the 56 day strength; compression tests were performed 182 days after concreting (Likins and Mullins, 2011).

Both GDL and TIP showed this shaft to have areas of poor concrete, while CSL only showed questionable concrete using the above criteria. GDL results were based on raw gamma counts and not correlated densities which are not a recommended practice.

4.3.2 Shaft 2

This shaft was constructed with four steel access tubes with a nominal shaft diameter of 0.91 meters and a length of 27.13 meters. The recorded top and bottom of shaft elevations are +2.13 and -25.05 meters, respectively. Summary of the TIP, CSL, and GDL test results are as follows:

TIP concluded the following:

- All Tubes: Good throughout the length of the shaft.

CSL concluded the following:

- Tube Pair 4-1: Questionable quality from elevation -24.87 to -25.05m

- Tube Pair 1-3: Questionable quality from elevation -24.81 to -25.05m

57

GDL concluded the following:

• Tube 4: Questionable quality from elevation +1.52 to +1.22m

TIP showed this shaft to be good while GDL and CSL found questionable concrete in different areas. GDL results were based on raw gamma counts and not correlated densities.

4.3.3 Shaft 3

This shaft was constructed with four steel access tubes with a nominal shaft diameter of 0.91 meters and a length of 23.47 meters. The recorded top and bottom of shaft elevations are +2.53 and -21.06 meters, respectively. Summary of the TIP, CSL, and GDL test results are as follows:

TIP concluded the following:

• All Tubes: Questionable quality from elevation -20.42 to -21.06m.

CSL concluded the following:

• Tube Pair 1-2: Questionable quality from elevation +2.19 to +1.52m

Questionable quality from elevation -20.73 to -20.79m

• Tube Pair 2-3: Questionable quality from elevation -20.73 to -20.79m

• Tube Pair 3-4: Questionable quality from elevation -20.79 to -20.88m

• Tube Pair 4-1: Questionable quality from elevation -20.73 to -20.79m

• Tube Pair 1-3: Questionable quality from elevation -20.79 to -20.85m

• Tube Pair 2-4: Questionable quality from elevation -20.79 to -20.85m

GDL concluded the following:

• Tube 1: Questionable quality from elevation +2.44 to +1.52m

• Tube 2: Poor quality at elevation -1.22m

• Tube 3: Questionable quality from elevation +2.44 to +1.52m

58

- Tube 4:   Questionable quality at elevation -1.22m

TIP and CSL showed questionable concrete near the bottom of shaft while GDL found questionable to poor areas near the top of shaft. GDL results were based on raw gamma counts and not correlated densities.

4.3.4 Shaft 4

This shaft was constructed with four steel access tubes with a nominal shaft diameter of 0.91 meters and a length of 23.53 meters. The recorded top and bottom of shaft elevations are +3.23 and -20.30 meters, respectively. Summary of the TIP, CSL, and GDL test results are as follows:

TIP concluded the following:

- All Tubes: Good throughout the length of the shaft.

CSL concluded the following:

- All Tube Pairs: Good throughout the length of the shaft.

GDL concluded the following:

- All Tubes: Questionable quality from an elevation of +2.44 to +1.83m

TIP and CSL showed this shaft to be good while GDL found some questionable areas. Again, GDL results were based on raw gamma counts and not correlated densities.

4.3.5 Shaft 5

This shaft was constructed with six steel access tubes with a nominal shaft diameter of 1.52 meters and a length of 32.92 meters. The recorded top and bottom of shaft elevations were +0.61 and -32.43 meters, respectively. Also, this shaft was constructed with an O-cell from an elevation of -22.65 to -23.13 meters. Sonic caliper was performed on this shaft prior to cage

59

placement, as well as inclination measurements of the tubes after concrete placement (Figure 4.3). Summary of the sonic caliper, TIP, GDL, and inclination test results are as follows:

Both sonic caliper and inclination concluded the following:

• Wall encroachment of 226mm at an elevation of -3.66m.

• Wall encroachment of 170mm at an elevation of -23.77m.

• Wall encroachment of 178mm at an elevation of -24.99m.

• Wall encroachment of 175mm at an elevation of -32.31m.

TIP concluded the following:

• Tube 1:   Questionable quality from elevation +0.61 to -7.01m

• Tube 2:   Questionable quality from elevation +0.61 to -5.18m

• Tube 4:   Questionable quality from elevation -15.24 to -20.12m

GDL concluded the following:

• Tube 1:   Questionable quality from elevation +0.61 to -1.07m

                      Probe would not pass elevation -23.16m (O-cell)

• Tube 2:   Questionable quality from elevation +0.61 to -0.15m

                      Poor quality from elevation -0.15 to -0.91m

                      Poor quality from elevation -22.56 to -23.01m (O-cell)

• Tube 3:   Questionable quality from elevation +0.61 to -0.61m

                      Poor quality from elevation -0.61 to -0.91m

                      Probe would not pass elevation -23.16m (O-cell)

• Tube 4:   Poor quality from elevation +0.61 to -1.07m

• Tube 5:   Questionable quality from elevation +0.61 to -0.91m

60

Poor quality from elevation +0.15to -0.15m

-        Tube 6:   Questionable quality from elevation +0.61 to -0.91m

                                             Poor quality from elevation -0.46 to -0.76m

                                             Probe would not pass elevation -23.16m (O-cell)

Both TIP and GDL found common areas of questionable concrete. Sonic caliper and inclination data confirmed TIP predicted cage movement. Again, GDL results were based on raw gamma counts and not correlated densities.
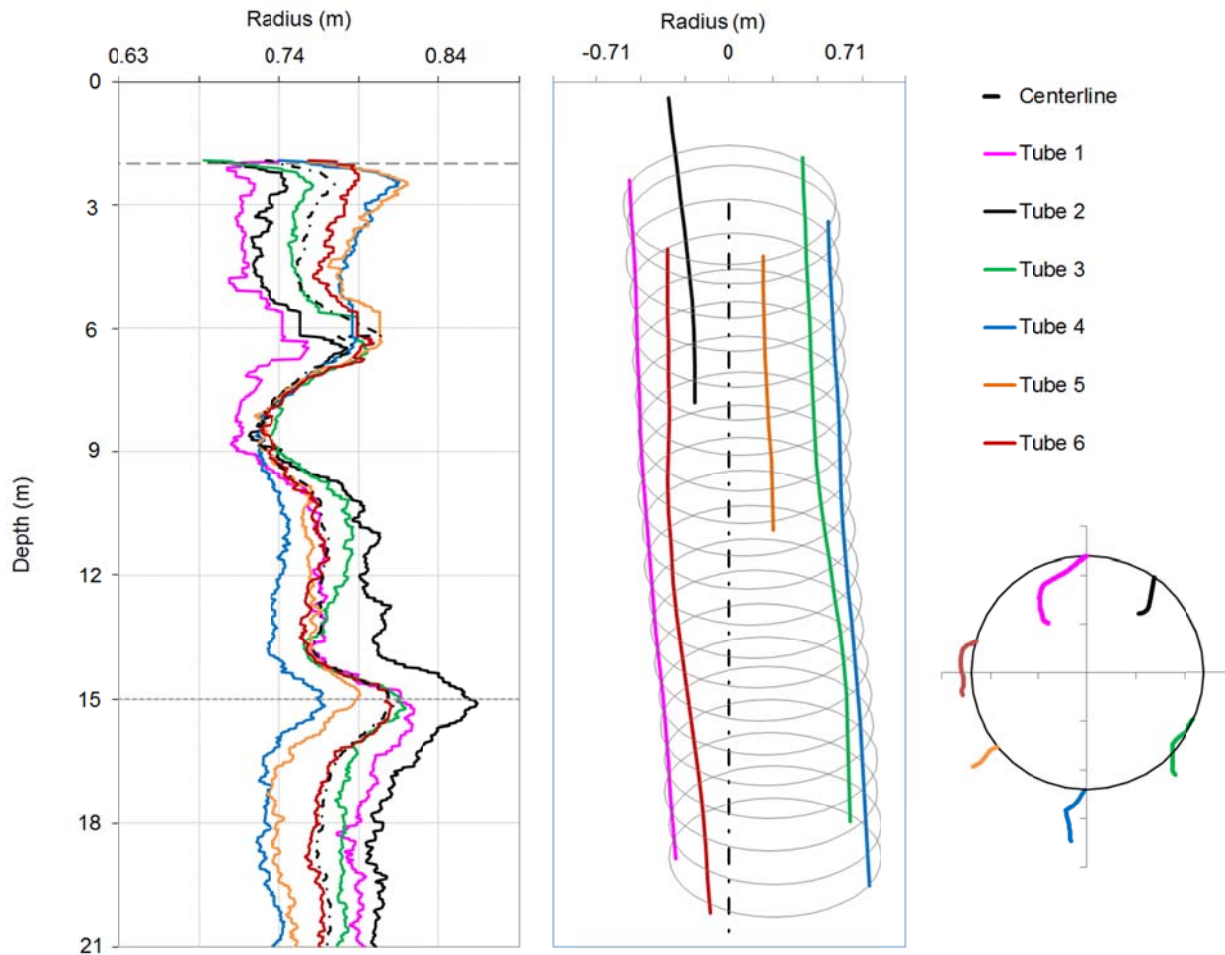
Figure 4.3 Effective radius from TIP (left) compared to inclination data (right) for Shaft 5.

61

4.3.6 Shaft 6

This shaft was constructed with five steel access tubes with a nominal shaft diameter of 1.52 meters and a length of 10.67 meters. The recorded top and bottom of shaft elevations are +5.70 and -5.06 meters, respectively. Summary of the TIP and CSL test results are as follows:

TIP concluded the following:

- Tube 1: Questionable quality from elevation -4.57 to -5.06m

- Tube 2: Poor quality from elevation -4.57 to -5.06m

- Tube 3: Poor quality from elevation -4.27 to -5.06m

- Tube 4: Poor quality from elevation -4.27 to -5.06

- Tube 5: Questionable quality from elevation -4.57 to -5.06m

CSL concluded the following:

- Tube Pair 1-2: Poor quality from elevation -4.75 to -5.06m

- Tube Pair 2-3: Poor quality from elevation -4.57 to -5.06m

- Tube Pair 3-4: Poor quality from elevation -4.57 to -5.06m

- Tube Pair 4-5: Poor quality from elevation -4.57 to -5.06m

- Tube Pair 5-1: Poor quality from elevation -4.75 to -5.06m

- Tube Pair 1-3: Poor quality from elevation -4.57 to -5.06m

- Tube Pair 1-4: Poor quality from elevation -4.75 to -5.06m

- Tube Pair 2-4: Poor quality from elevation -4.57 to -5.06m

- Tube Pair 3-5: Poor quality from elevation -4.57 to -5.06m

- Tube Pair 2-5: Poor quality from elevation -4.57 to -5.06m

Both CSL and TIP found poor concrete mostly near the bottom of the shaft.

62

4.3.7 Shaft 7

This shaft was constructed with nine steel access tubes with a nominal shaft diameter of 2.79 meters and a length of 34.26 meters. Summary of the TIP and CSL test results are as follows:

TIP concluded the following:

•   Tubes 4 - 7:   Questionable quality from depth of 32.00 to 36.58m

•   Cage alignment varies up to 102mm (Figure 4.4).

CSL concluded the following:

•   Tube Pair 4-5:   Questionable quality from depths of 0 to 0.49m

•   Tube Pair 5-6:   Questionable quality from depths of 0 to 0.88m

•   Tube Pair 5-6:   Questionable quality from depths of 1.16 to 2.07m

•   Tube Pair 5-6:   Questionable quality from depths of 3.63 to 3.72m

•   Tube Pair 6-7:   Questionable quality from depths of 0 to 0.88m

•   Tube Pair 6-7:   Questionable quality from depths of 1.16 to 2.07m

•   Tube Pair 6-7:   Questionable quality from depths of 3.66 to 3.72m

While CSL found questionable concrete near the top of shaft, TIP showed questionable concrete near the bottom of shaft and excessive cage movement. Based on the normal temperature profile near the top, CSL results may have been affected by debonding.

4.4 Conclusions

The use of thermal integrity profiling adds to the arsenal of NDT methods presently accepted by offering additional insight into the evaluation of drilled shafts. TIP measurements are sensitive to cage alignment, concrete cover, shaft radius and can detect anomalies both inside and outside the reinforcing cage. When compared to CSL and GDL test results, TIP agreed with

4 of 6 cases for CSL and 2 of 5 cases for GDL. In the one case were both sonic caliper and inclination data were available, TIP showed good agreement. Despite the differences in testing methods for drilled shafts, TIP correlates well with other NDT methods when all methods are testing the same zone of influence.
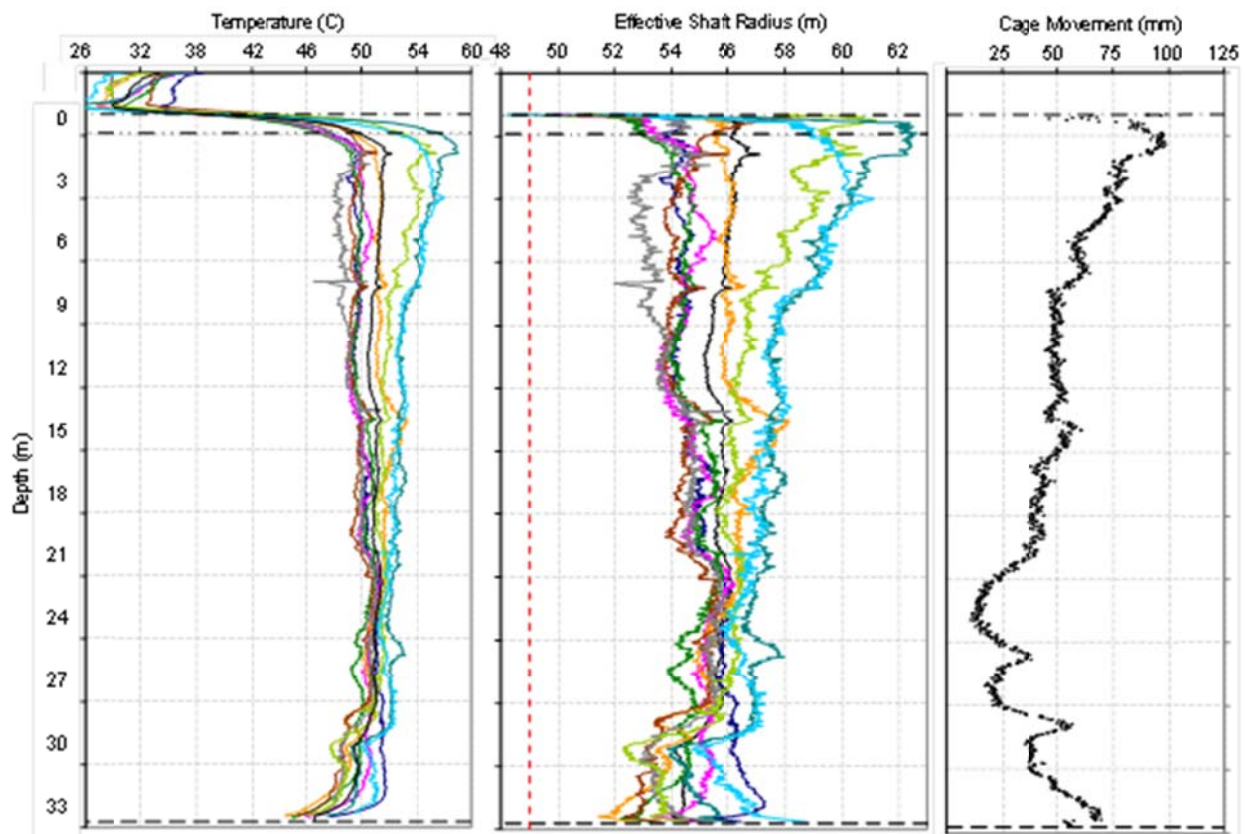
Figure 4.4 TIP results showing measured temperature (left), effective shaft size (center), and cage alignment (right) for shaft 7.

4.5 References

Hertlein, B. (2001). "Are our clients' expectations realistic?" Geo-Strata, Geo-Institute of American Society of Civil Engineers, January, p.11.

Likins, G. and Mullins G. (2011). "Structural integrity of drilled shaft foundations by thermal measurements" Structural Engineering & Design, www.gostructural.com.

Mullins, G. (2010) "Thermal Integrity Profiling of Drilled Shafts," DFI Journal, Deep Foundations Institute, Vol. 4, No. 2, December, pp 54-64.

Winters, D. (2014). "Comparative Study of Thermal Integrity Profiling with Other Non-Destructive Integrity Test Methods for Drilled Shafts," Submitted to *2014 Geo-Congress: Geo-Characterization and Modeling for Sustainability*, Febvruray 23-26, 2014, Atlanta, Georgia.

Winters, D. and Mullins, G. (2012). "Thermal Integrity Profiling of Concrete Deep Foundations." Geo-Construction Conference Proceedings, San Antonio, TX, pp. 155-165.

CHAPTER 5 BOND ENHANCEMENT FOR FRP PILE REPAIR IN TIDAL WATERS[4]

Vacuum bagging and pressure bagging are established techniques used by the composites industry for fabricating components. This chapter discusses the research that explored the adaptation of these techniques for improving the FRP-concrete bond in the repair of partially submerged piles. Prototype vacuum bagging and pressure bagging systems were developed and bond improvement assessed from results of pullout tests on full size piles repaired under simulated tide in the laboratory. Pressure bagging gave better bond and was found to be simpler because it did not require an airtight seal. A field demonstration project was conducted in which pressure bagging was used in combination with two different GFRP systems to repair two corroding piles supporting the Friendship Trails Bridge across Tampa Bay. Inspection of the post-cured wrap showed no evidence of air voids. The study demonstrates that techniques developed by the composites industry may be readily adapted to provide effective and inexpensive means for improving FRP-concrete bond.

5.1 Introduction

Recent advances in resin technology have made it possible to use FRP for the corrosion repair of partially submerged piles (Bazinet et al. 2003, Watson 2003, Mullins et al. 2005, 2006, 2007). In all the applications, the FRP was directly applied over the corroding region in the

---

[4] This chapter was published in ASCE Journal of Composites for Construction (Winters, et al. 2008). Permission is included in Appendix A.

'splash zone' (subjected to diurnal wet/dry cycles) without removal of the chloride-contaminated concrete.

Several investigators, e.g. Sheikh et al. (1997), Bonacci, (2000), Debaiky et al. (2002), Wheat (2002), Wootton et al. (2003), Suh et al. (2007), have independently demonstrated that while FRP cannot stop corrosion it can significantly reduce the corrosion rate. However, the extent of the reduction depends on the integrity of the FRP-concrete bond. Thus, Michigan State University researchers Baiyasi and Harichandran 2001 reported that metal loss was lower where FRP was bonded compared to its unbonded counterpart. Similarly, a study sponsored by Texas DOT found that in locations where the FRP had debonded, there was increased localized corrosion under simulated tidal cycles (Berver et al. 2001). Thus, good FRP-concrete bond over the entire wrapped region is essential for successful performance.

The authors recently conducted on-site pullout tests on FRP repaired piles at both above and below high water locations (Sen and Mullins 2007). Figure 5.1 shows a plot of the residual bond stress obtained for two different systems, a pre-preg and a wet layup. Inspection of Figure 5.1 shows considerable variability in the bond. It ranges from 0.7 to 1 MPa in the dry region of the pile and from 0.4 to 1.8 MPa in the critical wet/dry region. In another demonstration project, the FRP was found to have completely debonded from the concrete (Suh et al. 2005). Research suggests that if the on-site FRP bond were improved by making it less variable, service life of the FRP repair would be extended making it more cost effective.

5.2 Why Bond Is Variable

FRP pile repair typically uses hand lay-up techniques to impregnate the fibers. In this case, the weight of the wet FRP material acting downwards has a tendency to make it slide down

67

the pile surface. Moreover, as the vertical surface is seldom absolutely true, the FRP is not necessarily in continuous contact with the concrete over the entire length as the resin cures.

To counteract these tendencies, a plastic sheet called shrink wrap is tightly wound around the wet FRP over its entire length. Unfortunately, because of buoyancy effects and difficulty in wrapping tightly above shoulder height, the applied pressure is not uniform.

Figure 5.1 Residual bond stress from field study.
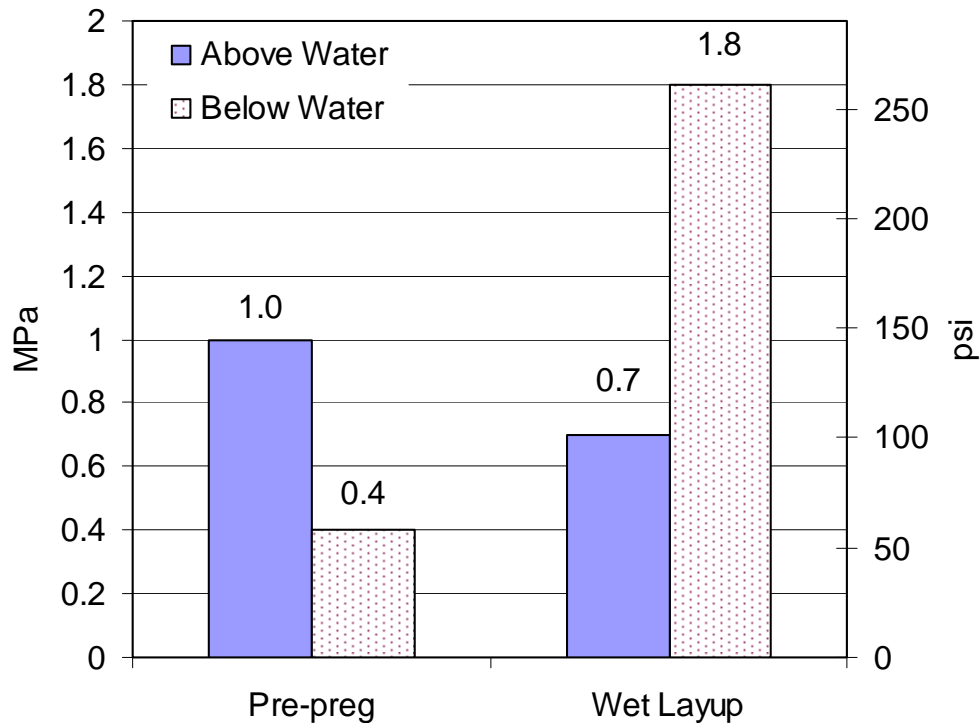
Uniform pressure is widely used to improve adhesion in bonded connections. For example, in segmental construction, a minimum compressive pressure of 276 kPa (40 psi) is applied to join epoxied match-cast units (AASHTO 1999). If uniform (gage) pressure can be maintained on the FRP wrap while the resin cured, the FRP concrete bond may be similarly expected to improve.

68

5.3 Techniques For Applying Uniform Pressure

Uniform pressure, through vacuum or pressure bagging, has long been used by the aerospace and automotive industry for fabricating FRP components. Vacuum bagging has occasionally been used in infrastructure applications, e.g. Stallings et al. (2000), Nazier et al. (2005). However, no similar reference relating to the application of pressure bagging was found in the literature.

5.4 Objectives

The overall goal of the research project was to explore the feasibility of adapting vacuum bagging or pressure bagging for improving FRP-concrete bond in the field repair of corroding piles in tidal waters. In order to meet this objective it was necessary to:

1. To develop prototype vacuum bagging and pressure bagging techniques appropriate for FRP repair of partially submerged piles.

2. To evaluate improvement in bond through pullout testing.

3. To implement the system developed through a field demonstration.

5.5 Background

Vacuum bagging applies pressure by creating a vacuum (limited to a maximum of 1 atmosphere - 760 mm of Hg). The essential components of a vacuum bagging system are (1) a vacuum bag and (2) a vacuum pump capable of creating a significant vacuum. Stallings et al. (2000) used a vacuum pressure of 0.034 MPa during a 6 hr curing period for repairing a bridge girder. Nazier et al. (2005) did not state the vacuum pressure used but their pump had the facility to achieve 25 microns of vacuum (1 atmosphere = 760000 microns Hg).

Since vacuum is only sustained with an airtight seal around the perimeter of the wrapped region, surface smoothness at the perimeter is a critical consideration. Additionally, there needs

69

to be a method for soaking up expelled resin and its subsequent removal after the FRP has cured so that its external appearance is not marred.

Figure 5.2 shows a schematic of the vacuum bagging system used in the study. In this figure, a porous, thin, non-stick film is referred to as the "release" and a thicker layer of absorbent material, called a "breather".
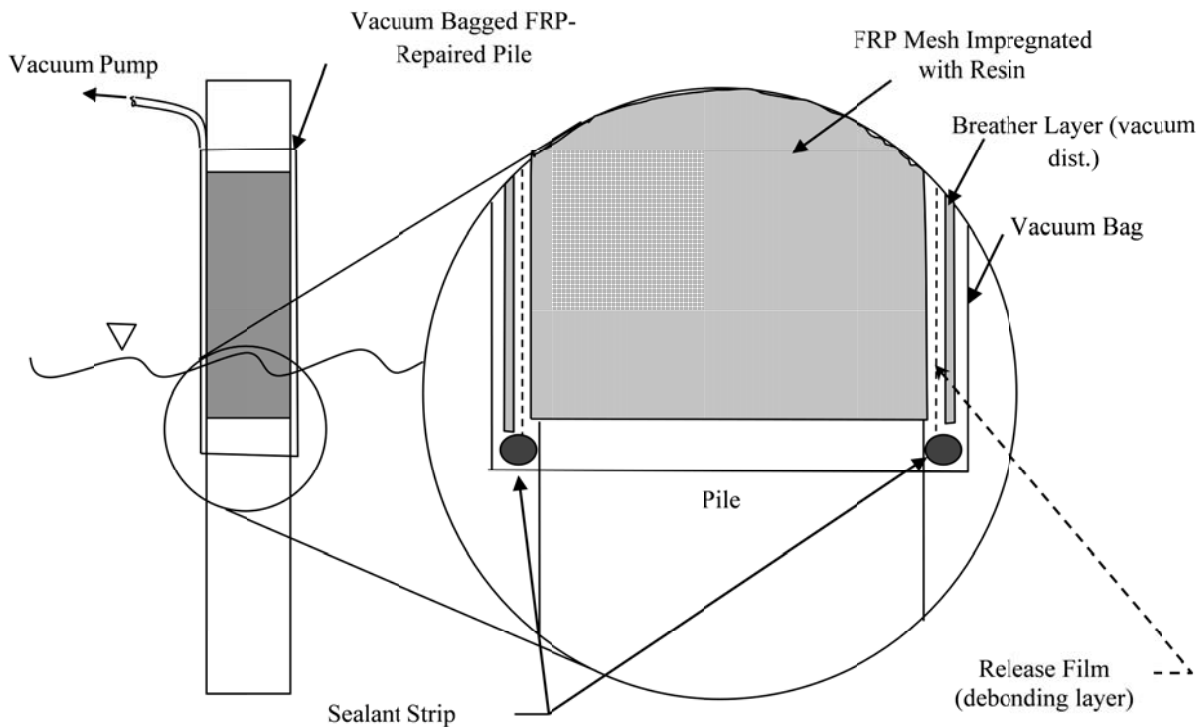
Figure 5.2 Vacuum bagging schematic.

The release is a non-stick plastic stretch wrap material. The breather material was a thick burlap cloth which allows air to be extracted from inside the bag. The bag is sealed at its ends so that there are no leaks.

Pressure bagging makes use of a pressure bladder that surrounds a pile (or a column in above water applications) similar to a blood pressure cuff. In essence it incorporates an air-tight

bladder inside an outer restraining structure which can be rigid or flexible. Flexible restraints are more suitable as they can be fitted and adapted as necessary to accommodate different pile sizes.

Figure 5.3 shows a schematic of the pressure bag system developed. It secures to itself using a set of 21 toggles. The air bladder is inside this bag and is connected to a source of compressed air. The material of the bladder needs to be able to withstand tensile stresses that develop as it is inflated. Figure 5.4 shows the components of the prototype used in the laboratory testing.
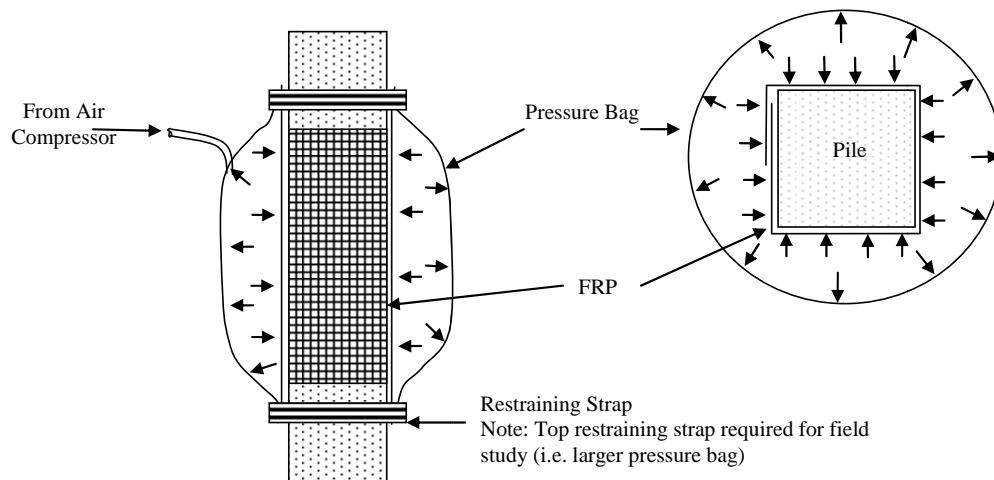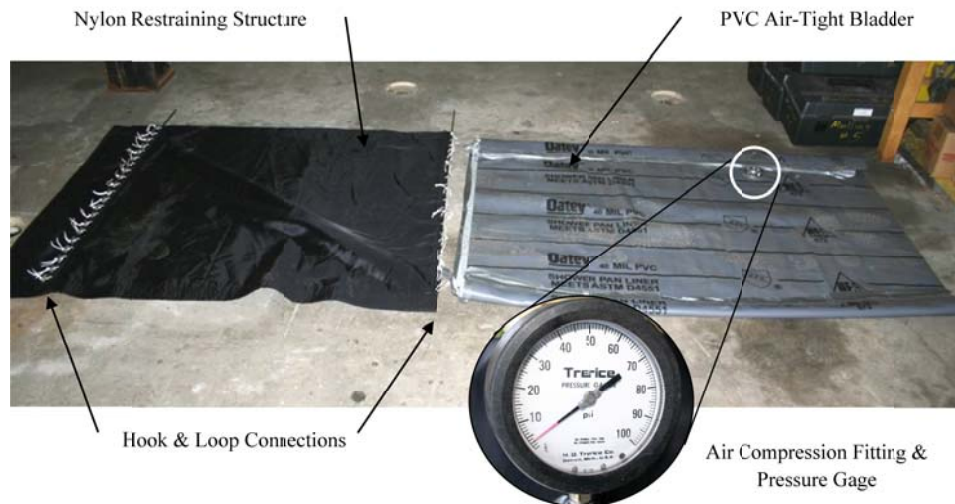

Figure 5.3 Pressure bagging schematic.

Figure 5.4 Pressure bagging components.

71

5.6 Experimental Program

The intent of the laboratory testing was to develop and evaluate a prototype system that could be used in a field demonstration study. Since the literature was dismissive regarding the suitability of pressure bagging, e.g. Nazier et al. (2005), only vacuum bagging was considered initially. However, because of problems encountered in establishing a vacuum, pressure bagging was included and the original test program modified. In the text, tests relating to vacuum bagging are referred to as the 'first series' while those for pressure bagging as the 'second series'.

5.6.1 Material Properties

The FRP systems selected for the laboratory study were identical to that used in previous demonstration studies (Mullins et al. 2005, 2006, 2007). These were a pre-preg system developed by Air Logistics and a wet layup system developed by Fyfe. Since the goal of the study was to improve bond, only the lower cost fiberglass was tested.

The pre-preg system uses a unique water-activated urethane resin in conjunction with a custom woven fabric. Because it is water-activated, the FRP material is pre-impregnated with resin and sent to the site in hermetically sealed foil pouches. The pouches are opened just prior to application to prevent premature curing from moisture present in the atmosphere. The properties of the uni-directional fibers as provided by the manufacturer are summarized in Table 5.1.

Fyfe's Tyfo® SEH-51A was the wet layup system used. It is a custom weave, uni-directional glass fabric that is usually used with Tyfo-S Epoxy. However, for underwater application, Tyfo® SW-1 underwater epoxy is used instead. The FRP fabric must be impregnated on-site just prior to use. Properties of the materials as provided by the manufacturer are summarized in Table 5.2.

72

Table 5.1 Properties of Aquawrap® fabrics[1].

Fibers	Tensile Strength (MPa)	Tensile Modulus (GPa)	Load per Ply (kN/m)
Uni-directional (GFRP)	590	36	420
Bi-directional (GFRP)	320	21	210
Uni-directional (CFRP)	830	76	596
Bi-directional (CFRP)	590	22	420

[1]Data derived from coupons prepared and tested in accordance with ASTM D3039

Table 5.2 Dry fiber properties of Tyfo® SEH-51A (Fyfe 2002).

Properties	Quantities
Tensile Strength	3.24 GPa
Tensile Modulus	72.4 GPa
Ultimate Elongation	4.5 %
Weight	915 g/m^2

5.6.2 Specimen Details

A total of eight, 1.52 m (5 ft) long x 0.305 m (12 in) wide square prestressed piles were used in the study. These were obtained by cutting two 6.1 m (20 ft) length piles donated by a local precaster. The piles were prestressed by eight 12.7 mm (0.5 in) diameter Grade 270 (1861 MPa) strands. The average compressive strength was estimated to be 27.6 MPa (4,000 psi) using a Schmidt hammer.

73

The eight specimens were originally labeled A1 to A4 or F1 to F4 depending on whether the pre-preg or the wet layup systems was used. However, because of changes made to incorporate pressure bagging, one of the originally designated wet layup specimens, F4, was used with the pre-preg system (re-labeled A5). Thus, five pre-preg specimens (A1-A5) and three wet layup specimens (F1-F3) were tested.

5.6.3 Underwater Set Up

Wrapping was conducted inside a 3.05 m x 1.83 m x 1.22 m deep tank filled with fresh water to a depth of 0.914 m (3 ft) to simulate field repair conditions (Figure 5.5). This ensured that exactly half the wrapped length (0.457 m) was under water and half above. To encourage marine type growth on the pile surface, specimens were left in standing water for 3 months prior to wrapping.

5.6.4 Surface Preparation

The corners of the piles were rounded to a 12.7 mm (½ in.) radius and all surface irregularities in the region to be wrapped were patched and filled with hydraulic cement. Water pressure was used to clean the pile surface. In the first test series, a 20.7 MPa (3 ksi) water pressure was used (vacuum bagging). A higher pressure, 68.9 MPa (10 ksi) was used in the second series (pressure bagging) for which equipment had to be rented. This is the pressure recommended by the ACI Guide for Underwater Repair (ACI 546.2R-98). Figure 5.6 shows pressure washing of the test piles at 68.9 MPa (10 ksi).

5.6.5 Test Program

As mentioned earlier, four piles were originally designated for testing using vacuum bagging for each of the two FRP systems. In each set, there was one control, i.e. external pressure applied using a shrink wrap, and three other piles in which the pressure was kept at -

74

14.5 kPa (-2.1 psi), -34.5 kPa (-5 psi) and -68.9 kPa (-10 psi). These pressures were selected because they could be readily provided by ordinary vacuum pumps.

Figure 5.5 View of partially submerged full-size test piles.

Figure 5.6 Pressure washing test piles with 68.9 MPa water pressure.

Vacuum bagging posed problems not only because of the difficulty in maintaining an airtight seal along the perimeter of the wrap, but more importantly air could infiltrate through cracks in the concrete outside the wrapped region. For this reason, vacuum bagging was abandoned after initial tests and pressure bagging evaluated with the remaining specimens. In

75

all, two piles, A3 and A4 (both pre-preg) were tested under vacuum pressure of -68.9 kPa (-10 psi). Three others, F1, F2 (both wet layup) and A5 (pre-preg originally labeled F4) were tested using pressure bagging. These were tested under three different pressures of 14.5 kPa (2.1 psi), 34.5 kPa (5 psi) and 68.9 kPa (10 psi). One specimen, A2 could not be tested because an experimental surface coating peeled off. Table 5.3 summarizes the revised test matrix.

Table 5.3 Test matrix.

Test Pile	Wrapping System	Confinement System	Applied Pressure (kPa)
A1	Air Logistics	Control (stretch wrap)	0
A2[1]	1 longitudinal layer, 4	N/A	N/A
A3	pieces – 0.914 m x	Vacuum Bag	68.9
A4	0.305 m	Vacuum Bag	68.9
A5	2 transverse layers, 1 piece – 0.203 m x 15.8 m	Pressure Bag	68.9
F1	Tyfo SEH-51A	Pressure Bag	34.5
F2	1 longitudinal layer, 4	Pressure Bag	14.5
F3	pieces – 0.914 m x 0.305 m 2 transverse layers, 2 pieces – 0.914 m x 1.27 m	Control (stretch wrap)	0

[1]Pile A2 was abandoned and not used for pressure bag tests

The FRP wrapped region extending 0.457 m (18 in.) above and 0.457 m (18 in.) below the water-line is shown in Figure 5.7. As stated earlier, the pressure provided by the hand-applied stretch film (deemed as zero applied pressure) was taken as the control. The pre-preg piles were tested using both the vacuum bag and pressure bag systems, while the wet layup piles were only tested with the pressure bag system.
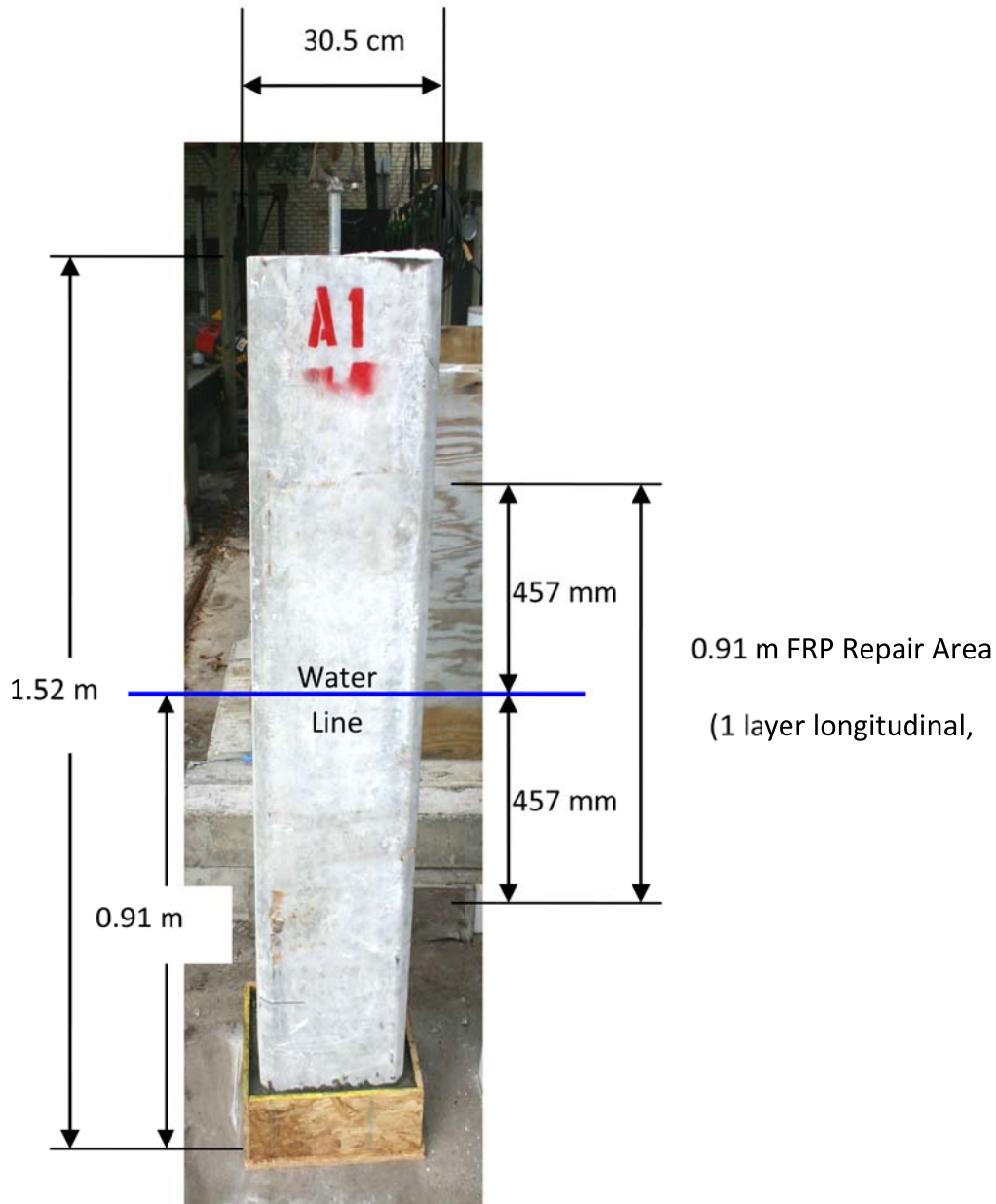

Figure 5.7 Test pile repair schematic.

5.6.6 FRP Wrapping

The wrapping scheme used by both systems consisted of three glass layers - one unidirectional layer in the longitudinal direction and two unidirectional layers in the transverse direction. The pre-preg system had an additional veil layer. This was consistent with layouts used in earlier demonstration studies.

The longitudinal layer consisted of four 0.914 m x 0.305 m wide individual pieces. The dimensions of the transverse pieces differed for the two systems: for the pre-preg it was a single 0.203 m x 15.85 m long piece whereas for the wet layup it consisted of two 0.305 m x 1.27 m pieces.

5.6.7 Vacuum Bagging

In the pre-preg system, a base resin coating is applied to the concrete surface prior to wrapping to improve the FRP-concrete bond. The opportunity was taken to evaluate two different resins (1) Aquawrap Base Primer #4 and (2) Bio-Dur 563, a heavy-duty epoxy. These were each applied to two of the four pile surfaces.

Test piles A1 and A4 were wrapped on the first day with A1 as the control pile and A4 with vacuum pressure (-68.9 kPa). Test pile A4 encountered problems with the sealing of the vacuum bag to the concrete surface above and below the FRP area. Extensive cracking above the FRP repair area allowed air to breach the vacuum bag, not allowing formation of an airtight seal. The air leaks were contained by filling in the cracks with epoxy, and a vacuum seal was obtained 45 minutes after the FRP was applied (Figure 5.8).

Test piles A2 and A3 were repaired next with the base resin applied to the entire pile beyond the repair areas so as to seal the cracked concrete surface. As before, two surfaces used Aquawrap Base Primer #4 resin and the other two used Bio-Dur 563 epoxy.

78

The FRP material was immediately installed on pile A3 following the application of the base resin. Again, the vacuum bag had difficulties sealing despite the coating of the uncured resin on the pile. Once an airtight seal was obtained, a -68.9 kPa (-10 psi) vacuum pressure was readily achieved.

The base resin applied to Pile A2 was allowed to cure 24 hours prior to the application of the FRP material. After 24 hours the resin pre-coat was inspected and it was found that no significant bond was achieved below the waterline between the resin base layer and the concrete substrate. As a result, no FRP was subsequently applied to the pile.

The researchers concluded that vacuum bagging was only effective for undamaged piles where an air-tight seal could be obtained. There was no similar need for air-tight seals if only an external pressure had to be maintained. As piles in need of repair were likely to be cracked, vacuum bagging was likely to be problematic in field repairs.

5.6.8 Pressure Bagging

Unlike vacuum bagging where a vacuum pump was needed, pressure bagging only needed compressed air. However, a suitable pressure bag had to be designed and fabricated for the testing. Consideration had to be given to the material used for the bladder so that it could withstand tensile hoop stresses that developed from pressurization.

The two components of the pressure bag are the inner bladder and the restraining bag (Figure 5.4). The inner bladder was constructed of PVC shower liner material and the restraining bag made out of nylon rip-stop material. The nylon rip-stop material was selected to withstand the tensile hoop stresses.

The pressure bag was designed to resist the maximum 68.9 kPa (10 psi) pressure applied to the FRP repair area during curing. Pile A5 was repaired using the pressure bag system. Figure

79

5.9 shows the inflated pressure bag around the test pile. No major difficulties were encountered. However, gas bubbles generated during the curing phase of the urethane resin were seen escaping from between the pile and bag below the waterline.
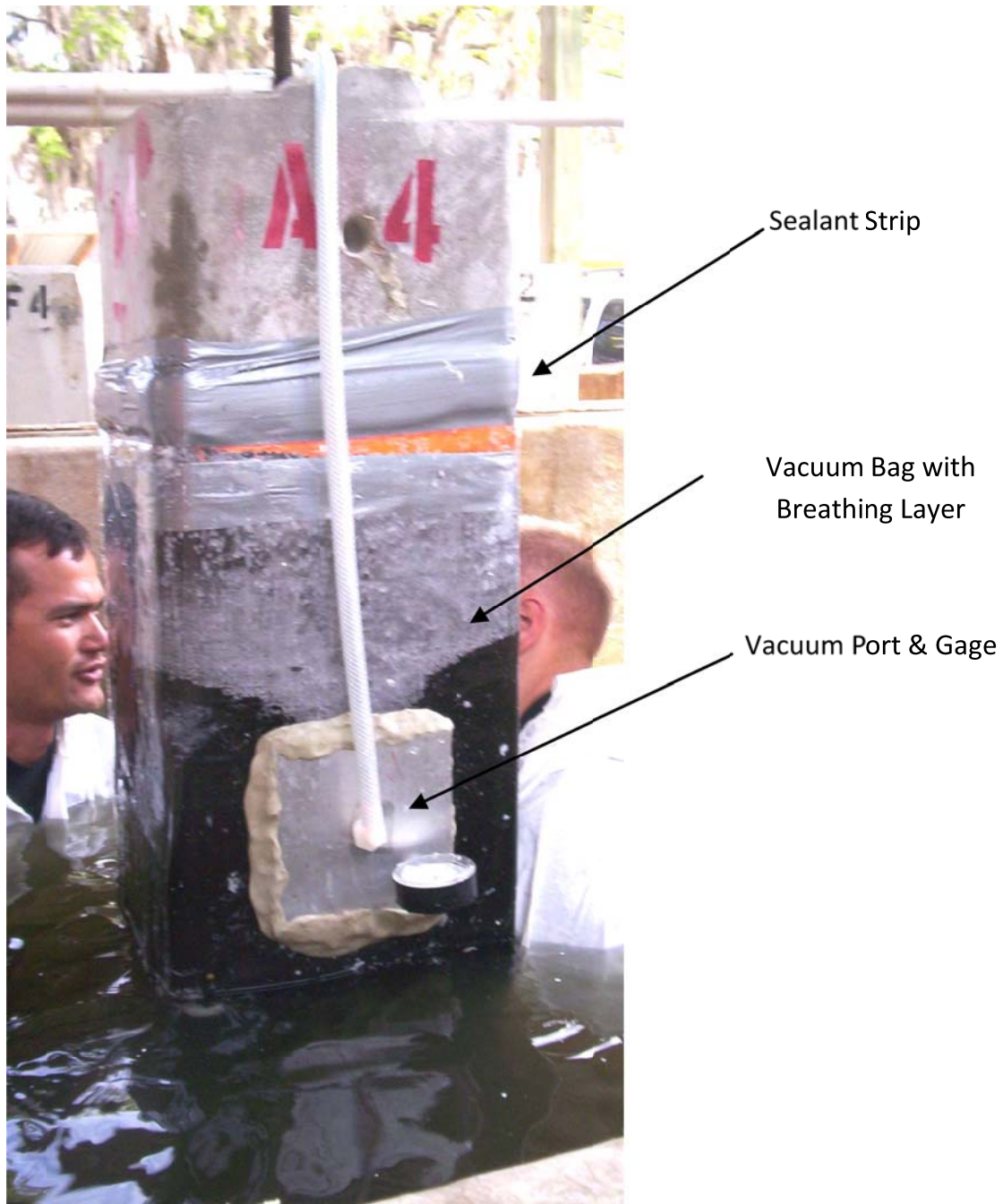

Figure 5.8 Vacuum bag applied to pre-preg system.

Figure 5.9 Pressure bag applied to pre-preg system.

The wet layup system was only tested using the pressure bag system on piles F1 and F2 with F3 serving as a control pile. The applied pressure was 34.5 kPa (5 psi) and 14.5 kPa (2.1 psi) on test piles F1 and F2, respectively.

5.7 Results

The FRP-concrete bond was evaluated both non-destructively via acoustic and thermal imaging tests and destructively from pullout tests. Only the results of the destructive testing are reported here. Results of the non-destructive testing may be found elsewhere (Mullins et al. 2007, Schrader 2007).

The bond between FRP and concrete was determined from pull-out tests carried out in accordance with ASTM D 4541 using an Elcometer 106 Adhesion Tester. The tester used 3.6 cm (1.456 in.) diameter aluminum dollies. A 0.1 m x 0.1 m grid was drawn on all four wrapped surfaces and destructive tests conducted at selected intersections in all the test specimens. A total

81

of 151 pullout tests were conducted. Of these, 83 were conducted above the waterline and 68 below the waterline. Fewer tests were conducted below the original waterline because regions where the bond was poor were not smooth (Schrader 2007).

A summary of relevant results is shown in Figure 5.10. The 'above water' and 'below water' results are shown separately. These compare the average bond for both the pre-preg and the wet layup systems.

Inspection of Figure 5.10 shows that vacuum bagging (used only with the pre-preg system) did not lead to any improvement in bond. Pressure bagging on the other hand led to significant improvement in bond both above (from 0.94 to 1.57 MPa) and below the waterline (from 0.26 to 1.17 MPa). In contrast, the results for the wet layup system were mixed. It reduced marginally from 2.01 MPa to 1.95 MPa above water but increased from 1.65 MPa to 1.77 MPa below water.

FRP pile repair is part bond-critical, part contact critical since the wrap must withstand expansive forces due to corrosion. For bond-critical applications, ACI 440 guidelines specify 1.38 MPa (200 psi) as a minimum pull-off strength if FRP is to be used. This limit was used as a filter to distinguish between satisfactory and unsatisfactory bond.

Figure 5.11 plots the percentage of pullout results that exceeded the ACI 1.38 MPa threshold from all the tests. Inspection of this figure shows that pressure bagging benefited both the wet layup and the pre-preg systems. In case of wet layup, the increase in satisfactory bond ranged from around 83% to 89% above water and from around 63% to over 72% below water. For the pre-preg system, the corresponding increase was from 19% to about 67% (above water) and from 0.5% to over 30% below water. The percentage improvement was more noticeable for the pre-preg system due to low initial baseline values (see Figure 5.1).
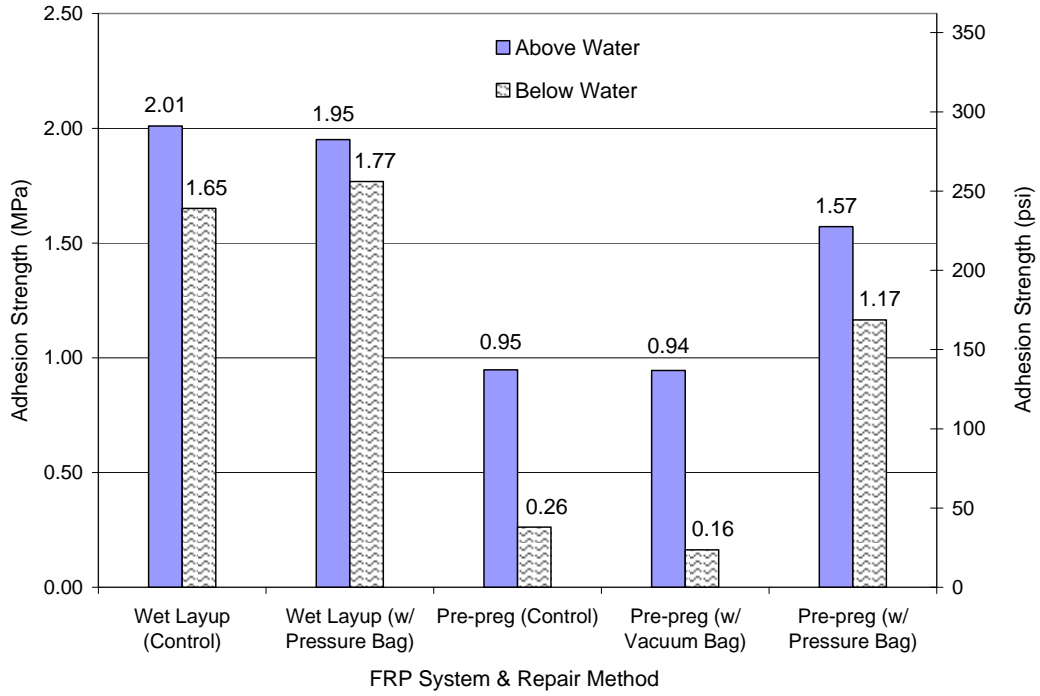
82

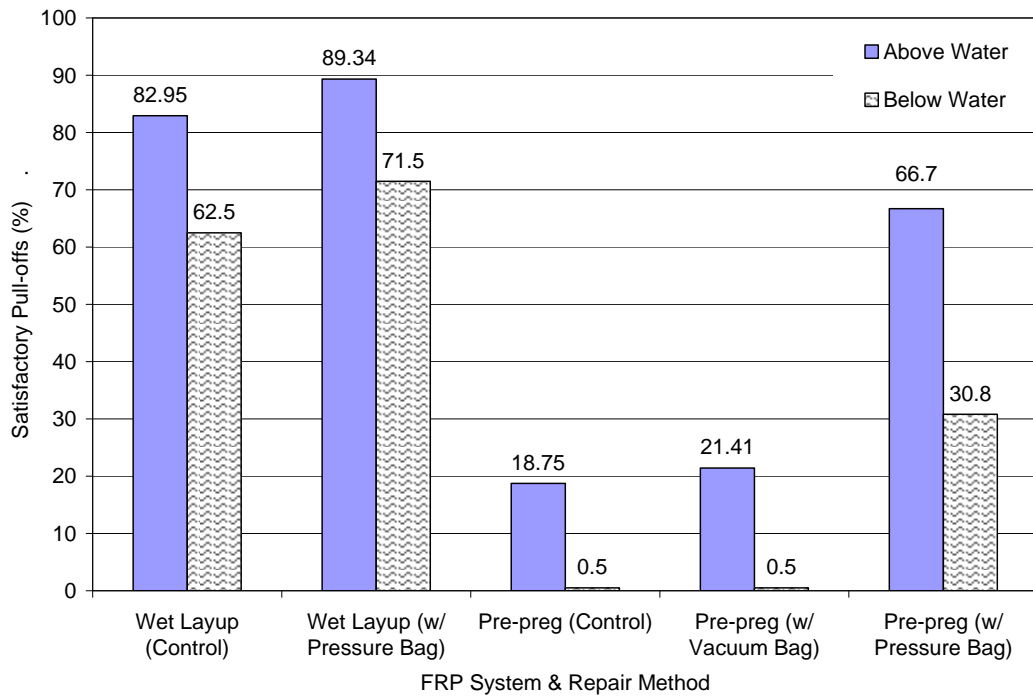Figure 5.10 Pullout test results for two systems.

Figure 5.11 Percentage of satisfactory pullout results using 1.38 MPa cut-off.

83

5.8 Field Study

A demonstration project was conducted to implement the pressure bag system developed. The site for the repair was the Tampa side of the Friendship Trails Bridge that is under the jurisdiction of Hillsborough County.

The Friendship Trails Bridge no longer carries vehicular traffic but is now the world's longest over-the-water recreation trail. The 4.18 km (2.6 mile) bridge is supported on 254 piers and 22 columns numbered 1-276 extending east from St. Petersburg to Tampa. Seventy seven percent of the 254 piers have needed to be repaired indicating that the environment is very aggressive.

In a previous study (Mullins et. al 2006), piers 99-101 on the Tampa side of the Friendship Trails Bridge were considered to be the most suitable because all the piles were in a similar state of disrepair. For this reason, two remaining unwrapped reinforced concrete piles in Pier 101 were selected for the field demonstration in this study. The 0.508 m x 0.508 m (20 in. x 20 in.) piles were reinforced by eight #8 (25.4 mm dia) bars.

Details of the two piles selected are summarized in Table 5.4. The table also includes information on the two instrumented controls in pier 99 from the previous study. The relative positions of the test piles in the pier are shown in Figure 5.12. Instrumentation consisting of rebar probes developed by the Florida Department of Transportation was the same as used in the earlier study. As before they were installed at two different depths along a pile to allow measurement of the corrosion current between the probes after the system had stabilized.

84

Table 5.4 Test pile details.

Pier Number	Repair System	Specimen Type	Pile Name	Instrumentation
Pier 99	N/A	Control	99-N	Yes
	N/A	Control	99-S	Yes
Pier 101	Pre-preg	Glass 1 + 1 layers[1]	101-I.N.	Yes
	Wet Layup	Glass 1 + 1 layers[1]	101-I.S.	Yes

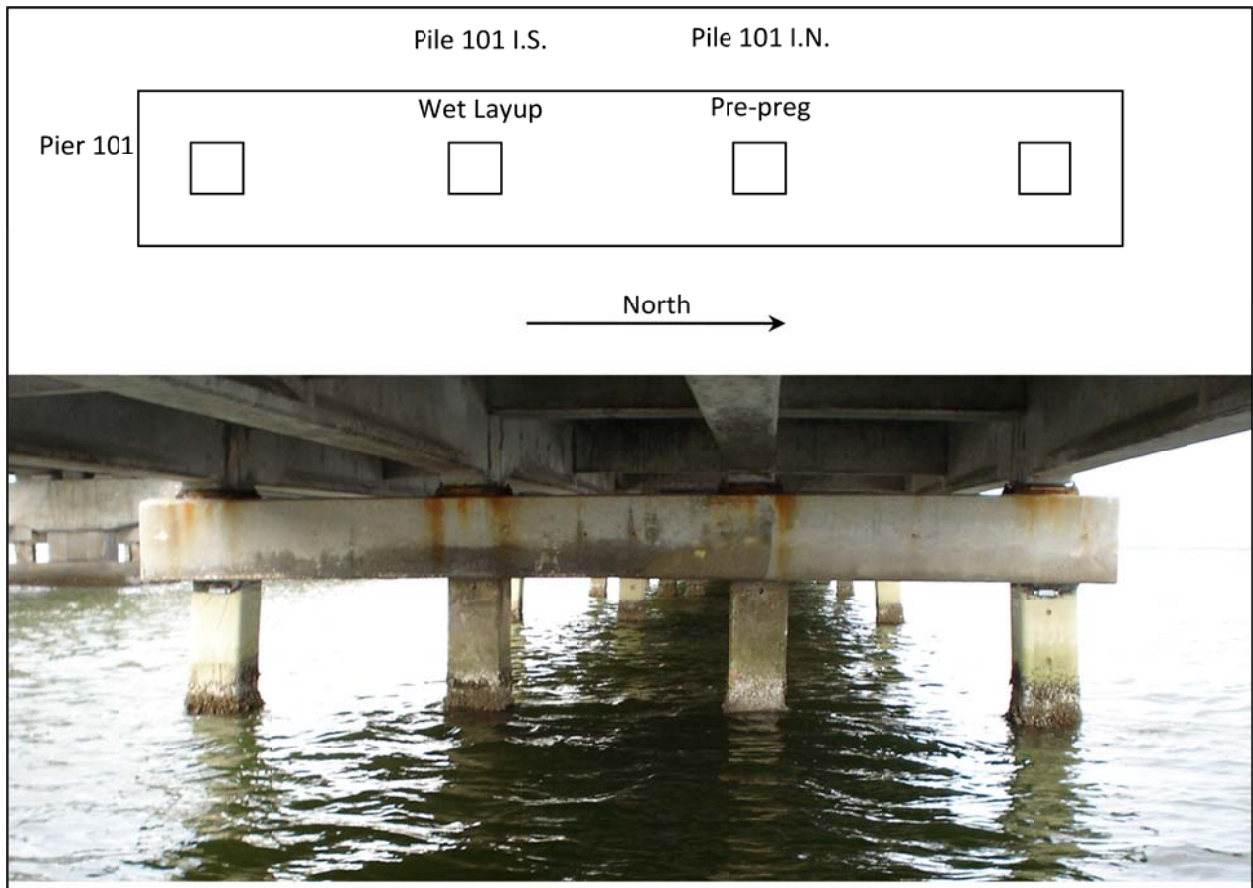[1] signifies number of layers in the longitudinal and transverse direction respectively

Figure 5.12 Pier 101 layout.

5.8.1 Pressure Bag

The prototype built for the laboratory testing was scaled up to match the dimensions of the larger field piles. However, some changes were made to the original design, namely (1) a cinch strap was introduced to tie the bag at the top to prevent upward movement (due to buoyancy effects) after the bladder had been inflated, (2) the toggle connections of the two ends (Figure 5.4) were replaced by snap-on hooks. In addition, a burlap breather layer was added to the pre-preg system to allow gases generated during curing to exit. It was believed bond had been adversely affected for the pre-preg system by the outward pressures exerted by escaping gases that formed during curing.

5.8.2 Surface Preparation

Previous procedures were followed excepting for a change in the water pressure used for the final cleaning. A scraper was used to remove all marine growth from the region to be wrapped. Projecting parts of the concrete surface were chipped using a hammer and chisel. All four corners were chamfered and were ground to a 19 mm (¾ in) radius using a grinder. Finally, all surfaces were ground and pressure washed using freshwater to remove all dust, debris, and remaining marine growth just prior to wrapping.

Figure 5.13 shows the test piles prior to FRP application. Pressure washing was attempted with the same 68.9 MPa (10 ksi) unit used in the laboratory study. However, because of the large water supply demand and lack of ready availability of freshwater at the site, the 20.7 MPa (3 ksi) pressure washer was used instead.

5.8.3 Wrapping: Pre-preg

The pre-preg system was used to wrap the interior north pile in Pier 101. It was wrapped using one unidirectional glass fiber layer in both the longitudinal and transverse directions.

86

Wrapping commenced from the pile top 0.3048 m (12 in.) below the underside of the pile cap to accommodate the presence of the junction box used for corrosion measurements. The procedure for applying the glass fiber used earlier was followed (Mullins et. al. 2006). However, a new device (resembling a miniature bed of nails) was used to puncture the entire surface of the stretch wrap with tiny holes to allow curing gases to escape.

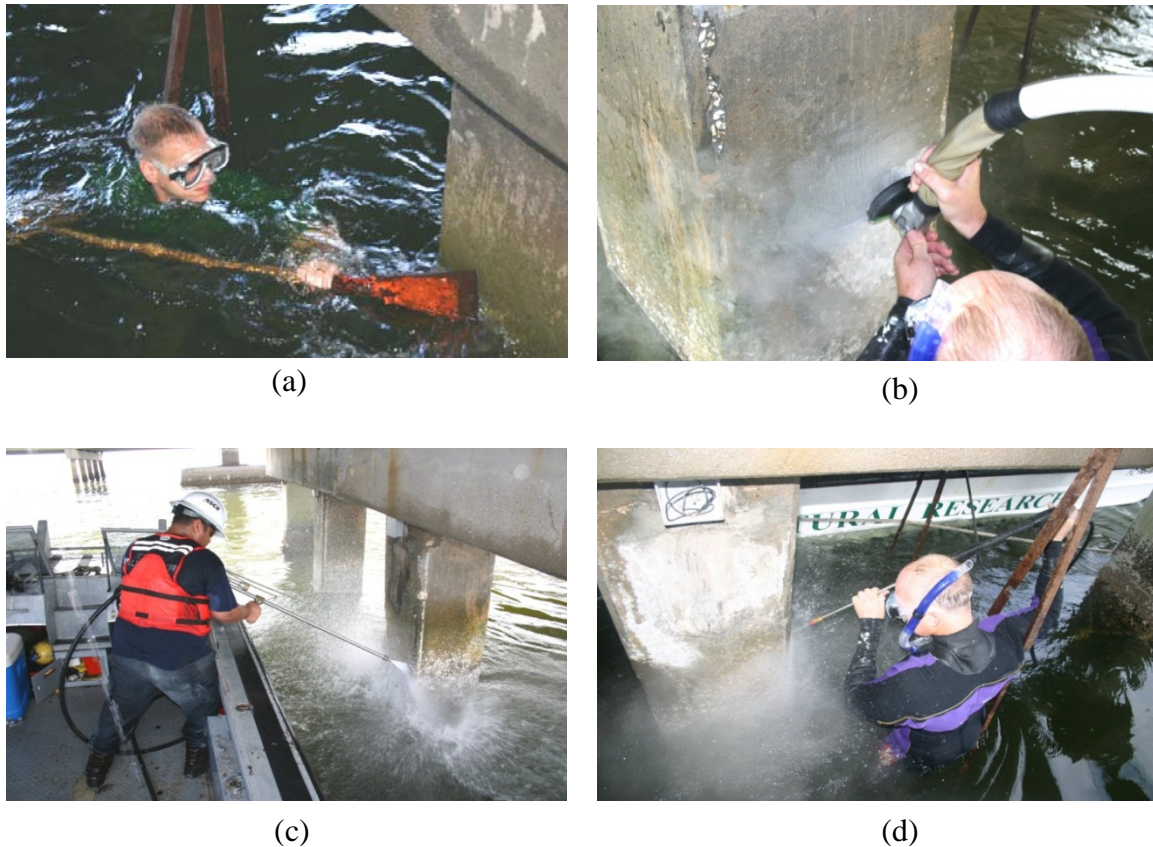(a)　　　　　　　　　　　　　　　　(b)

(c)　　　　　　　　　　　　　　　　(d)

Figure 5.13 (a) Scraping large deposits off the surface of the piles; (b) Grinding the surface and corners; (c) Pressure washing with 68.9 MPa water pressure; (d) Pressure washing with 20.7 MPa water pressure

A burlap breathing layer was now placed over the punctured stretch wrap. This ensured that gases generated during curing of the urethane resin could escape without compromising bond. Next the pressure bag was carefully positioned so that the two ends were joined over the middle of the pile. The cinch straps were tightened at the top and bottom to prevent the bag from

moving upwards once the bladder inside the bag had been inflated. A constant pressure of 14.5 kPa (2.1 psi) was applied to the wrap during curing for a period of 3 hours (initial set). The pressure bag was then removed. The wrap was subsequently allowed to cure for one week. After removing the plastic stretch film, the pile was painted with the same base primer for UV protection.

5.8.4 Wet Layup System

The interior south pile in Pier 101 was wrapped using the wet layup system. The fibers were impregnated with resin on-site by hand using a roller to distribute the epoxy evenly over the fabric. The usual procedure for wrapping was followed (Mullins et al. 2006). Since no gases are given off during curing, the burlap breathing layer was not required. The pressure bag was placed directly placed over the plastic stretch film that covered the entire wrapped region. As before the ends of the pressure bag were positioned over the middle face of the pile and cinch straps at the top and bottom tightened to prevent the bag from moving when it was inflated. A constant pressure of 14.5 kPa (2.1 psi) was applied to the wrap during curing for a period of 16 hours. This was significantly longer than the time used for the pre-preg system because the initial set time was longer. Figure 5.14 shows the pressure bag applied to the wet layup pile. Figure 5.15 shows the FRP repaired piles with the UV protection applied.

5.9 Discussion

This study described the adaptation of techniques widely used by the composite industry to improve FRP-concrete bond. Both vacuum bagging and pressure bagging were successfully implemented.

The advantage of the vacuum bag system is that there are no strength requirements since pressure is applied by evacuating air. However, it requires air tight seals around the perimeter

that may be difficult to achieve especially if the pile is cracked. The pressure bag system does not require air tight seals but the material of the air bladder must be strong enough to withstand tensile hoop stresses that develop.

Figure 5.14 Pressure bag applied to the wet layup pile at 14.5 kPa.

Figure 5.15 Piles after FRP repair with UV coating.

In the study, vacuum bagging was only tested for the pre-preg system where it was found to be ineffective possibly because of the short setting time of the urethane resin. The time taken to resolve leaks in the seal coupled with gases generated during curing may have been responsible for this unanticipated result. However, as the chemistry for epoxy resin is different, it would be unwise to extrapolate the findings for the urethane resin. Unfortunately, tight deadlines did not permit further investigation.

Destructive pullout tests showed that pressure bagging led to improved bond. This is most probably because uniform pressure ensured the FRP was in continuous contact with the concrete surface as it cured. This automatically enhanced the chemical adhesion between concrete surface and FRP. Additionally, bond was enhanced by forcing resin into the concrete pore structure. Pressure also made the FRP denser by squeezing out excess resin, thereby improving the mechanical and corrosion resistant properties of the system.

5.10 Conclusions

This study was undertaken to improve the integrity of the FRP-concrete bonding that was achievable under water. Previous tests had found this to be variable (Figure 5.1). It was believed that if constant pressure were maintained as the resin cured, bond would be improved because of increased frictional resistance.

Two disparate approaches were tested in the laboratory – vacuum bagging and pressure bagging. Both systems were made to work. However, inherent sealing problems associated with vacuum bagging made it a less attractive solution particularly for repairs of damaged piles. Pressure bagging had no similar requirement and was found to be more effective, particularly for the wet layup system.

90

The pressure bagging system developed was implemented without incident in the repair of two piles on pier 101 of the Friendship Trails Bridge. Visual and tactile inspection indicated that the FRP-concrete bond obtained was better than in earlier projects.

The study is indicative of the relative ease with which technologies developed by the composites industry can be used in infrastructure applications. While the application focused on pile repair, the systems developed are versatile and can also be used for repairs of columns and bents under dry conditions.

5.11 References

AASHTO (1999) Guide Specifications for Design and Construction of Segmental Concrete Bridges, Section 28.3.2, Washington, DC.

ACI 440.2R-02 (2002). "Guide for the Design and Construction of Externally Bonded FRP Systems for Strengthening Concrete Structures". ACI, Farmington Hills, MI.

ACI 546.2R-98 (1998). "Guide to Underwater Repair of Concrete", ACI, Farmington Hills, MI.

Air Logistics Corporation, (2002). Aquawrap Repair System, Pasadena, CA.

ASTM D4541 (2002). Test Method for Pull off Strength of Coatings Using Portable Adhesive Tester.

Baiyasi, M. & Harichandran, R. (2001). Corrosion and Wrap Strains in Concrete Bridge Columns Repaired with FRP Wraps. Paper No 01-2609, 80th Annual Meeting, Transportation Research Board, Washington, DC.

Bazinet, S., Cereone, L. and Worth, F. (2003). "Composite FRP Moves into Underwater Application", SAMPE Journal, Vol. 39, No. 3, pp. 8-16.

Berver, E., Jirsa, J., Fowler, D., Wheat, H. and Moon, T. (2001). "Effects of Wrapping Chloride Contaminated Concrete with Fiber Reinforced Plastics", FHWA/TX-03/1774-2, University of Texas, Austin, October.

Bonacci, J. (2000). Rehabilitation of Corrosion-Damaged RC Infrastructure Using Externally Bonded FRP. Proceedings of ACMBS 2000, CSCE, Montreal, P.Q. 561-568.

Debaiky, A., Green, M. and Hope, B. (2002). "Carbon Fiber-Reinforced Polymer Wraps for Corrosion Control and Rehabilitation of Reinforced Concrete Columns". ACI Materials Journal, 2002, Vol. 99, No. 2, pp. 129-137.

Fyfe Co. LLC (2002). "Tyfo® SEH-51A Composite Using Tyfo® S Epoxy." <http://www.fyfeco.com/products/compositesystems/pdf/seh-51a.pdf> (Aug. 24, 2007).

Mullins, G., Sen, R., Suh, K and Winters, D. (2005). "Underwater FRP Repair of Prestressed Piles in the Allen Creek Bridge". ASCE, Journal of Composites for Construction, Vol. 9, Issue 2, pp. 136-146.

Mullins, G., Sen, R., Suh, K. and Winters, D. (2006). "A Demonstration of Underwater FRP Repair" Concrete International, Vol 28, No 1, pp.1-4.

Mullins, G., Sen, R., Winters, D. and Schrader, A. (2007). Innovative Pile Repair. Final Report submitted to Hillsborough County, FL, Jan., 40 pp.

Nazier, M., Giancaspro, J. and Balaguru, P. (2005). "Composite Jackets for Rehabilitation of Damaged Reinforced Concrete Pier Caps". SAMPE '05 Proceedings, Long Beach, CA, Vol. 50, pp. 1011-1024.

Schrader, A. (2007). "Methods to Improve Bond on FRP Wrapped Piles", MSCE thesis submitted to Department of Civil and Environmental Engineering, USF, Tampa, FL. April.

Sen, R. and Mullins, G. (2007). "Application of FRP for Underwater Pile Repair". Composites Part B, Vol. 38, No. 5-6, 751-758.

Sheikh, S., Pantazoupoulou, S., Bonacci, J., Thomas, M. & Hearn. N. (1997). Repair of Delaminated Circular Pier Columns with Advanced Composite Materials, Ontario Joint Transportation Research Report No 31902, Ministry of Transportation of Ontario, Aug.

Stallings, J., Tedesco, J., El-Mihilmy, M. and McCauley, M. (2000). "Field Performance of FRP Bridge Repairs", ASCE, Journal of Bridge Engineering, Vol. 5, No. 2, pp. 107-113.

Suh, K.S., Mullins, G., Sen, R., and Winters, D. (2005). Use of FRP for Corrosion Strengthening Applications in a Marine Environment. Final Report submitted to Florida / US Department of Transportation, Tallahassee, FL Oct., 406 pp.

Suh, K.S., Mullins, G., Sen, R. and Winters, D (2007). "Effectiveness of FRP in Reducing Corrosion in a Marine Environment". ACI Structural Journal, Vol. 104, No. 1, 76-83.

Watson, R.J. (2003). "The Use of Composites in the Rehabilitation of Civil Engineering Structures", in ACI SP-215 (eds. S. Rizkalla and A. Nanni), Farmington Hills, MI, pp. 291-302.

Wheat, H.G. (2002). Using Polymers to Minimize Corrosion of Steel in Concrete, Cement and Concrete Composites, Vol. 24, 119-126.

Winters, D., Mullins, G., Sen, R., Schrader, A. and Stokes, M. (2008). "Bond Enhancement for FRP Pile Repair in Tidal Waters". ASCE, *Journal of Composites for Construction*, Vol. 12, No. 3, pp. 334-343.

Wootton, I., Spainhour, L. and Yazdani, N. (2003). Corrosion of Steel Reinforcement in CFRP Wrapped Concrete Cylinders", Journal of Composites for Construction, Vol. 7, No 4, pp. 339-347.

CHAPTER 6 CONCLUSIONS AND RECOMMENDATIONS

Advancements in foundation design, quality assurance, and remediation are intended to increase the service life of new structures to 100+ years and extend the life of existing structures. This dissertation focuses on methodologies that further the performance of concrete foundation elements such as drilled shafts and driven piles. A brief overview of these advancements and recommendations are discussed in the following sections.

6.1 Design Advancements

Design of drilled shaft end bearing capacity has been limited due to poor construction techniques and large shaft displacements required to develop capacity. Pressure grouting the bottom of the drilled shaft densifies the soils beneath the shaft eliminating construction soft toe problems and reducing the anticipated displacement. However, pressure grouting can also provide higher end bearing capacities than a conventional ungrouted drilled shaft tipped in sands due to the increased relative density of loose soils. In this way, denser soils show less improvement when compared to medium dense to loose sands.

Further developments in post grouting since the publication of this portion of the dissertation include the development of software to aid in the design process of pressure grouted shafts. This design software (called *Shaft 1-2-3*) incorporates the design procedure presented herein and is available for download from http://geotech.eng.usf.edu/Shaft123.html. Shaft 1-2-3 is a macro-driven Excel spreadsheet which utilizes VBA programming for calculating ungrouted and grouted drilled shaft capacities. It includes different analysis methods for sand, clay, silt, and

94

limestone. Shaft 1-2-3 was developed to help quickly determine the feasibility of post grouting drilled shafts in various soil types.

6.2 Quality Assurance Advancements

Thermal integrity profiling aids in the evaluation of drilled shaft integrity by measuring the temperature caused by the hydrating / curing concrete. TIP measurements are sensitive to cage alignment, concrete cover, shaft radius and can detect anomalies both inside and outside the reinforcing cage. Despite the differences in testing methods for drilled shafts, TIP correlates well with other NDT methods when all methods are testing the same zone of influence. TIP compared well with CSL in 4 of 6 cases and 2 of 5 cases with GDL. In the one case where both sonic caliper and inclination data were available, TIP showed good agreement in cage movement and shaft size.

6.3 Rehabilitation / Repair Advancements

Vacuum bagging and pressure bagging are established techniques used by the composites industry for fabricating components. Applying these techniques to improve the FRP-concrete bond for the repair of partially submerged piles provides increased corrosion protection and overall increased durability to the repair while also increasing the life of the foundation element and bridge. Vacuum bagging and pressure bagging systems were developed and tested on full size piles within the laboratory to demonstrate bond improvement. Pressure bagging produced better bond and was found to be more reliable because it did not require the airtight seal required by vacuum bagging (cracked piles tend to leak air around the cracks into the vacuum bag). Field demonstrations were conducted using pressure bagging on two different FRP systems used to repair corroding piles supporting the Friendship Trails Bridge across Tampa Bay. Performance monitoring after the repairs showed reduced corrosion rates and improved FRP-concrete bond.

95

6.4 Future Needs

6.4.1 Design

While post grouting has great potential to improve shaft capacity and reduce costs, it can be problematic to implement effectively and ensure that the intended outcome is obtained. Therein, the grout pressure is intended to be applied to the entire base area as demonstrated in the numerous instrumented case studies used to develop the design process. Today, routine grouting procedures monitor grout pressure, grout volume and survey shaft uplift whereby each parameter must achieve or stay below a given threshold (e.g. pressure>threshold; volume>threshold; uplift<threshold). However, satisfying these thresholds does not in itself define effectiveness. It is therefore conceivable to meet all criteria and yet not properly grout the end bearing soils. It is in vain that new field standards are recommended to ensure that proper grouting has taken place. The recommended standards require the grout pressure, volume, and shaft displacement be monitored during grouting and concurrently plotted using the concept tri-axis graphs shown in Figure 6.1. In short, all graphs should demonstrate a diagonal trend away from the center. If any one of the graphs demonstrates a horizontal or vertical trend, the post grouting process has become ineffective for one of the reasons shown.

6.4.2 Quality Assurance

Thermal testing of drilled shafts subjected to extreme changes in the surroundings (i.e. soil to air, soil to water, or water to air) requires time consuming modeling and data analysis to properly interpret. Further development in data regression techniques may help minimize time needed for data regression allowing for timely reporting. Similar to Shaft 1-2-3, a macro-driven Excel workbook was created to aid in the regression process. This software is still in beta testing, but has been used extensively in production testing to further develop the software.

96

Advantages of the software include the ability to compare temperature profiles quickly and analyze data from shafts cast in relatively uniform surroundings (e.g. all in soil). Again, the limitation to the software currently lies with the inability to input external constraints or changes in boundary conditions.
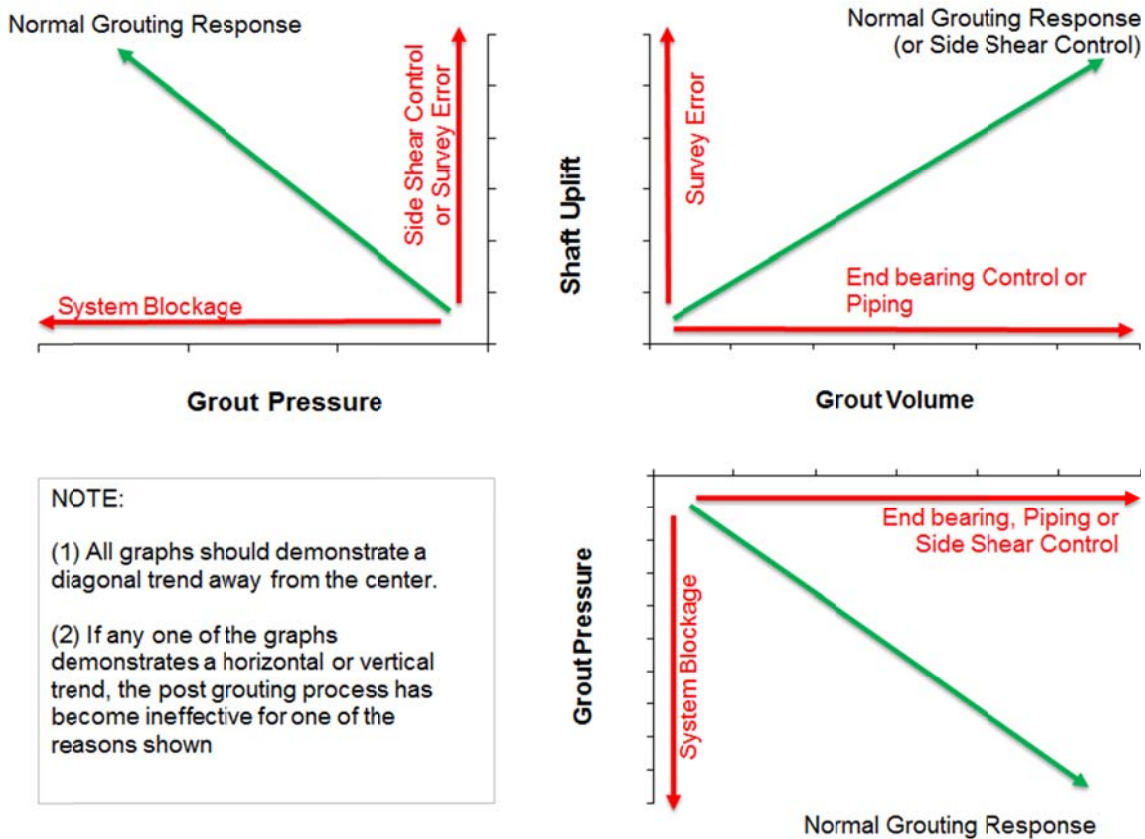

Figure 6.1 Quality assurance plots for post grouting drilled shafts.

6.4.3 Remediation

Further developments may be possible to make vacuum bagging systems more viable. The advantage of vacuum bagging is the versatility of adapting to any shape/surface and the reduced cost of vacuum bags relative to pressure bags. The largest hurdle with this system is providing an airtight seal across irregular surfaces. By overcoming this limitation, vacuum bagging has the potential to be a more cost effective technique than pressure bagging.

97

APPENDICES

Appendix A Copyright Permissions

The following are Copyright permissions for use of materials in Chapters 2, 3, and 5, respectively.

Winters, Danny

From: BD Smith <bdsmith@ADSC-IAFD.COM>
Sent: Wednesday, February 12, 2014 2:38 PM
To: Winters, Danny
Subject: ADSC Article

Danny, please move forward with whatever is needed. The ADSC has no issue with you utilizing your contribution to the 2012 GeoCongress Proceedings.

B. D. Smith, CPCU
Administrative Services
ADSC: The International Association of Foundation Drilling
8445 Freeport Parkway, Suite 325
Irving, TX 75063
Office: 469/359.6000
Fax: 469/359.6007
Website: www.adsc-iafd.com

1

100

www.manaraa.com

Copyright Clearance Center

RightsLink®

Home | Create Account | Help

ASCE
AMERICAN SOCIETY OF CIVIL ENGINEERS

Title: Bond Enhancement for FRP Pile Repair in Tidal Waters

Author: Danny Winters; Gray Mullins; Rajan Sen; Andy Schrader; Michael Stokes

Publication: Journal of Composites for Construction

Publisher: American Society of Civil Engineers

Date: 2008-06-00

Copyright © 2008, ASCE. All rights reserved.

User ID

Password

☐ Enable Auto Login

LOGIN

Forgot Password/User ID?

If you're a copyright.com user, you can login to RightsLink using your copyright.com credentials. Already **a RightsLink user** or want to learn more?

Permissions Request

As an ASCE author, you are permitted to reuse you own content for another ASCE or non-ASCE publication.

Please add the full credit line "With permission from ASCE" to your source citation. Please print this page for your records.

Type of use: Dissertation/Thesis

Portion: full article

Format: print

Use of this content will make up more than 25% of the new work: no

Author of this ASCE work or ASCE will publish the new work: yes

BACK | CLOSE WINDOW